Satellite-based monitoring of pasture degradation on the Tibetan Plateau: A multi-scale approach

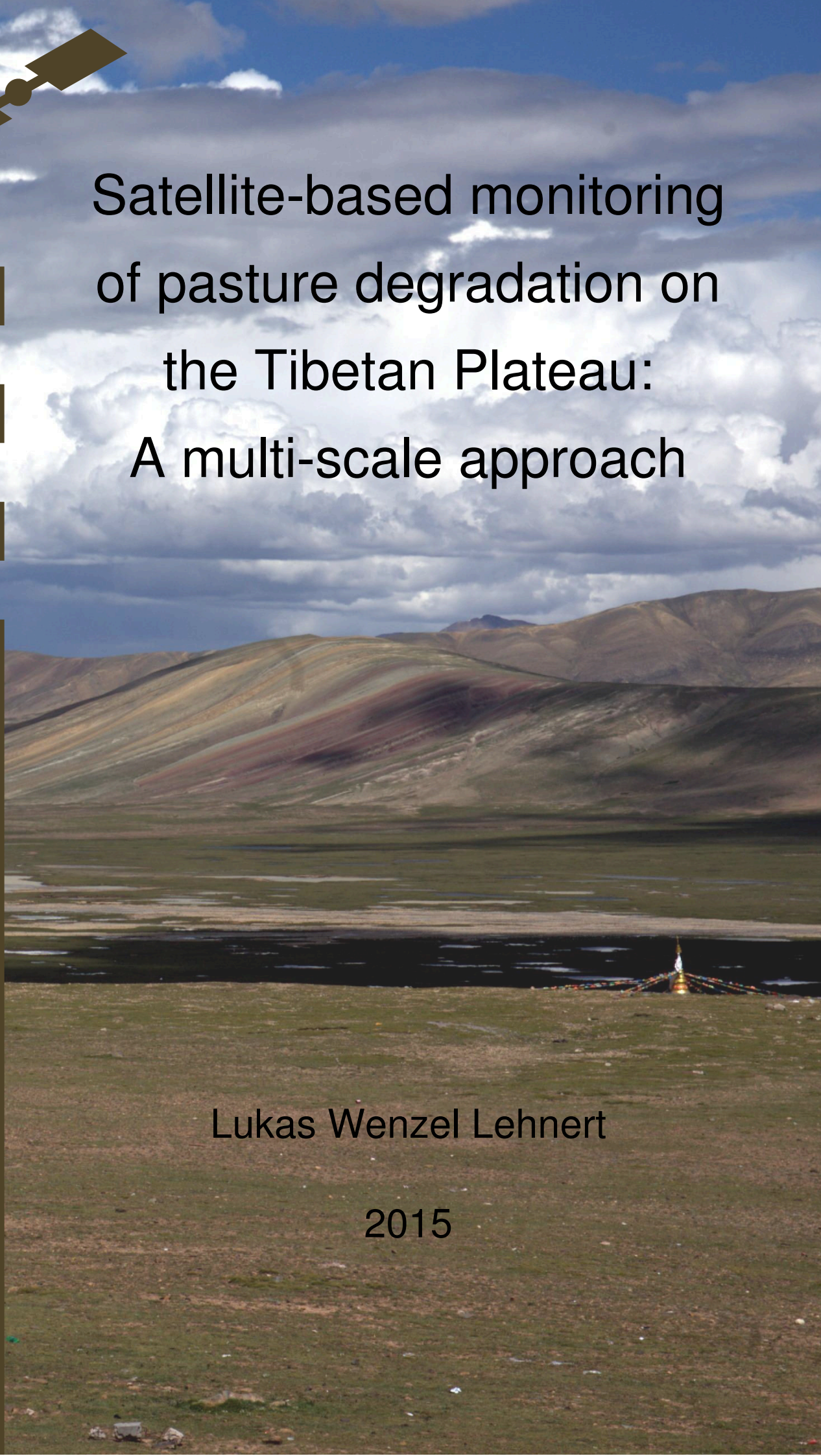

Lukas Wenzel Lehnert

2015

Titleimage: Tibetan pastures north of the Tanggula Pass at approx. 5,000 m (taken 2013 by Lukas Lehnert)

Satellite-based monitoring of pasture degradation on the Tibetan Plateau: A multi-scale approach

kumulative Dissertation
zur
Erlangung des Doktorgrades der
Naturwissenschaften
(Dr. rer. nat.)

dem Fachbereich Geographie
der Philipps-Universität Marburg
vorgelegt von

Lukas Wenzel Lehnert

aus Nürnberg

Marburg / Lahn, Mai 2015

Vom Fachbereich Geographie
der Philipps-Universität Marburg als Dissertation
am 20.05.2015 angenommen.

Erstgutachter: Prof. Dr. Jörg Bendix
Zweitgutachter: Prof. Dr. Georg Miehe
Drittgutachter: Prof. Dr. Stefan Dech

Tag der mündlichen Prüfung: 03.11.2015

Table of contents

List of Figures

List of Tables

Summary

The Tibetan Plateau has been entitled “Third-Pole-Environment” because of its outstanding importance for the global climate and the hydrological system of East and Southeast Asia. Its climatological and hydrological influences are strongly affected by the local vegetation which is supposed to be subject to ongoing degradation. The degradation of the Tibetan pastures was investigated on the local scale by numerous studies. However, because methods and scales substantially differed among the previous studies, the overall pattern of degradation on the Tibetan Plateau is hitherto unknown. Consequently, the aims of this thesis are to monitor recent changes in the grassland degradation on the Tibetan Plateau and to detect the underlying driving forces of the observed changes. Therefore, a comprehensive remote sensing based approach is developed. The new approach consists of three parts and incorporates different spatial and temporal scales: (i) the development and testing of an indicator system for pasture degradation on the local scale, (ii) the development of a MODIS-based product usable for degradation monitoring from the local to the plateau scale, and (iii) the application of the new product to delineate recent changes in the degradation status of the pastures on the Tibetan Plateau.

The first part of the new approach comprised the test of the suitability of a new two-indicator system and its transferability to spaceborne data. The indicators were land-cover fractions (e.g., green vegetation, bare soil) derived from linear spectral unmixing and chlorophyll content. The latter was incorporated as a proxy for nutrient and water availability. It was estimated combining hyperspectral vegetation indices as predictors in partial least squares regression. The indicator system was established and tested on the local scale using a transect design and *in situ* measured data. The promising results revealed clear spatial patterns attributed to degradation, indicating that the combination of vegetation cover and chlorophyll content is a suitable indicator system for the detection of pasture degradation on local scales on the Tibetan Plateau.

To delineate patterns of degradation changes on the plateau scale, the green plant

coverage of the Tibetan pastures was derived in the second part. Therefore, an upscaling approach was developed. It is based on satellite data from high spatial resolution sensors on the local scale (WorldView-type) via medium resolution data (Landsat) to low resolution data on the plateau scale (MODIS). The different spatial resolutions involved in the methodology were incorporated to enable the cross-validation of the estimations in the new product against field observations (over 600 plots across the entire Tibetan Plateau). Four methods (linear spectral unmixing, spectral angle mapper, partial least squares regression, and support vector machine regression) were tested on their predictive performance for the estimation of plant cover and the method with the highest accuracy (support vector machine regression) was applied to 14 years of MODIS data to generate a new vegetation coverage product.

In the third part, the changes in vegetation cover between the years 2000 and 2013 and their driving forces were investigated by comparing the trends in the new vegetation coverage product against climate variables (precipitation from tropical rainfall measuring mission and 2 m air temperature from ERA-Interim reanalysis data) on the entire Tibetan Plateau. Large areas in southern Qinghai were identified where vegetation cover increased as a result of positive precipitation trends. Thus, degradation did not proceed in these regions. Contrasting with this, large areas in the central and western parts of the Tibetan Autonomous Region were subject to an ongoing degradation. This degradation can be attributed to the coincidence of rising temperatures and anthropogenic induced increases in livestock numbers as a consequence of local land-use change. In those areas, the ongoing degradation influenced local precipitation patterns because sensible heat fluxes were accelerated above degraded pastures. In combination with advected moist air masses at higher atmospheric levels, the accelerated heat fluxes led to an intensification of local convective rainfall.

The ongoing degradation detected by the new remote sensing approach in this thesis is alarming. The affected regions encompass the river systems of the Indus and Brahmaputra Rivers, where the ongoing degradation negatively affects the water storage capacities of the soils and enhances erosion. In combination with the feed-back mechanisms between plant coverage and the changed precipitation on the Tibetan Plateau, the reduced water storage capacity will exacerbate runoff extremes in the middle and lower reaches of those important river systems.

Zusammenfassung

Das Tibetische Plateau wird häufig aufgrund seiner herausragenden Bedeutung für das globale Klima sowie die Hydrologie in Ost- und Südostasien als „Dritter Pol“ bezeichnet. Die klimatischen und hydrologischen Einflüsse des Plateaus werden unter anderem von der Vegetation gesteuert. Bereits durchgeführte Studien haben Hinweise geliefert, dass die Vegetationsdecke in den letzten Jahren zunehmende Degradation erfährt. Der genaue Status und Einfluss dieser Degradation konnten bisher jedoch noch nicht umfassend quantifiziert werden, da den bisherigen Studien unterschiedliche Methoden und Skalen zugrunde lagen. Dies führt dazu, dass der gegenwärtige Zustand der plateauweiten Vegetation unbekannt ist. Daher sind das Monitoring der Graslanddegradation und die Untersuchung der zugrundeliegenden Treiber die zentralen Gegenstände dieser Untersuchung. Hierfür wurde ein neuer fernerkundungsbasierter Ansatz entwickelt, der aus drei Teilen besteht und verschiedene räumliche und zeitliche Skalen umfasst. Der erste Teil beinhaltet die Entwicklung eines Indikatorsystems für Weidedegradation auf der lokalen Skala. Im zweiten Teil wird ein MODIS-basiertes Produkt entwickelt, das zum Monitoring der Degradation von der lokalen zur plateauweiten Skala verwendet werden kann. Im dritten Teil wird dieses neue Produkt mit dem Ziel angewendet, kürzlich stattgefundene Veränderungen der Degradation auf dem Tibetischen Plateau aufzuzeigen.

Der erste Teil des neuen Ansatzes umfasst den Test auf die Verwendbarkeit eines neuen Indikatorsystems und dessen Übertragbarkeit auf Satellitendaten. Das System besteht aus zwei Indikatoren: den Anteilen verschiedener Landbedeckungsklassen (z.B. grüne Vegetation, offener Boden), die mittels linearer spektraler Entmischung berechnet werden, und dem Chlorophyllgehalt der Blätter, der mit Hilfe von hyperspektralen Vegetationsindices und Partial Least Squares Regression geschätzt wird. Das Indikatorsystem wurde auf der lokalen Skala basierend auf einem Transektdesign und *in situ* gemessenen Daten aufgebaut und getestet. Da die Methode gute Ergebnisse erzielte und klare räumliche Muster detektiert wurden, die nur durch Degradationsunterschiede erklärbar waren, wur-

de das neue Zwei-Indikatorsystem als geeignet eingestuft, um auf der lokalen Skala die Degradation der Weiden des Tibetischen Plateaus abzuschätzen.

Im zweiten Teil des neuen Ansatzes wurde der Deckungsgrad der grünen Vegetation der tibetischen Weiden entlang einer Kaskade von Satellitendaten mit absteigender räumlicher Auflösung beginnend mit der lokalen Skala (WorldView-Typ) über die regionale Skala (Landsat-Typ) zur plateauweiten Skala (MODIS) abgeleitet. Das Konzept der aufeinander aufbauenden räumlichen Auflösungen wurde angewendet, da es eine direkte Validierung der Schätzwerte des Deckungsgrades mit Feldmessungen ermöglicht (über 600 Messpunkte, verteilt auf das gesamte Plateau). Zur Ableitung des Deckungsgrades wurden vier Methoden getestet (lineare spektrale Entmischung, Spectral Angle Mapper, Partial Least Squares Regression und Support Vector Machine Regression). Mit Hilfe der Methode mit der größten Genauigkeit (Support Vector Machine Regression) wurde schließlich eine 14 Jahre umfassende Zeitreihe des plateauweiten Deckungsgrades aus den MODIS Daten berechnet.

Die Veränderungen des Deckungsgrads zwischen 2000 und 2014 und deren Steuergrößen wurden im dritten Teil der Arbeit analysiert, indem plateauweit die Trends des Deckungsgrades mit den Trends der Klimavariablen (Niederschlag aus Daten der Tropical Rainfall Measuring Mission und 2 m Lufttemperaturdaten aus den Reanalysen von ERA-Interim) verglichen wurden. Dabei wurde festgestellt, dass der Deckungsgrad in großen Gebieten im Süden Qinghais zunahm, was durch positive Trends im Niederschlag erklärt werden kann. Die Degradation schritt in diesen Gebieten folglich nicht fort. Im Gegensatz hierzu waren große Gebiete im zentralen und westlichen Bereich der Autonomen Region Tibet von einem Rückgang im Deckungsgrad betroffen, der auf die Koinzidenz eines Temperaturanstiegs und steigender Viehzahlen als Konsequenz des Landnutzungswandels zurückzuführen ist. In diesen Gebieten hat die fortschreitende Degradation die lokalen Niederschlagsmuster beeinflusst, da es über degradierten Flächen zu einem Anstieg der fühlbaren Wärmeflüsse kommt, die bei advektiv herangeführten feuchten Luftmassen in hohen Atmosphärenschichten zu einer Verstärkung der Konvektion führen.

Die fortschreitende Degradation, wie sie von dem neuen Fernerkundungsansatz detektiert wurde, ist alarmierend, da die betroffenen Regionen die Oberläufe der wichtigen Flusssysteme des Brahmaputra und Indus betreffen. In diesen Gebieten sinkt durch die Degradation die Wasserhaltekapazität der Böden und die Erosion wird verstärkt. Durch

das Zusammenspiel mit den Rückkopplungen zwischen fortschreitender Degradation und zunehmendem Niederschlag kann somit eine Verstärkung von extremen Hochwasserereignissen in den Unterläufen beider Flüsse verursacht werden.

1 Introduction

Grasslands are among the most wide-spread vegetation types on Earth as they occupy approx. 26% of the ice-free land surface of the Earth (FOLEY et al., 2011). The usage of grasslands as meadows or pastures provide income for over 1.3 billion people on the Earth (HERRERO et al., 2013). However, the ecosystem services provided by grasslands are not restricted to the usage of biomass for livestock production but encompass their ability to protect soils against erosion (LIU & DIAMOND, 2005), to provide water (FOLEY et al., 2005) and to serve as large carbon dioxide sinks if they are managed sustainably (SCURLOCK & HALL, 1998). Worldwide, these functions are thought to become more and more threatened as the stability of the grassland ecosystems is reduced by global climate change (HOOPER et al., 2005) and land use change (FOLEY et al., 2005).

High mountain ecosystems are generally more vulnerable to climate change than ecosystems in non-mountainous areas (BENISTON, 2003). Reasons for this vulnerability are the generally high adaption of organisms to the abiotic conditions prevailing at high mountains and the sharp transitions at small spatial distances between different vegetation communities leading to isolated ecosystems. Additionally, the magnitude of climate change is increasing with altitude as shown by QIN et al. (2009) for the Tibetan Plateau.

The Tibetan Plateau has been recently called "third pole environment" because of its outstanding global importance (QIU, 2008). It is undisputed that the Tibetan Plateau influences the monsoon generation (DUAN & WU, 2005). Additionally, as all major rivers of East and Southeast Asia originate on the Tibetan Plateau, the Tibetan Plateau plays a key role for the hydrology and the fresh water supply of East Asia (IMMERZEEL et al., 2010). Situated at the interface between atmosphere and hydrosphere, the vegetation plays a crucial role. On the one hand it actively effects hydrology and climate by affecting the vertical transport of moisture and heat (CUI et al., 2006). On the other hand the vegetation depends on water and temperature that are again determined by climate and hydrology. Regarding its hydrological services, the vegetation cover reduces run-off

through transpiration, protects the soils against erosion and, thus, maintains the water storage capacity of the soils (ZHANG et al., 2011). Thus, the ecosystem services are of outmost importance for 1.4 billion people in Asia living at the lower reaches of the large river systems originating on the Tibetan Plateau (IMMERZEEL et al., 2010).

1.1 Motivation

The Tibetan Plateau is a long term grazed ecosystem and the current vegetation is mainly the result of human land-use with the first grazing indication dated 8,800 BP (MIEHE et al., 2009). Thus, the grazing tolerance of the present vegetation cover is generally high, which is indicated by high proportions of poisonous and tiny species throughout the plateau's vegetation (MIEHE et al., 2011a,b, 2008). However, the society on the Tibetan Plateau is recently undergoing significant changes during the ongoing transformation of the traditional nomadic land-use. The intended effects of the transition are an increase in agricultural production (GOLDSTEIN & BEALL, 2002), sedentarisation of the nomads (BAUER, 2005) and shifts in herd compositions and livestock densities (SHEEDY et al., 2006). It is still under discussion if transition policies positively or negatively influence the livelihood and the ecosystem stability (CAO et al., 2013; LI et al., 2009; XU et al., 2008; YAMAGUCHI, 2011; ZHAOLI et al., 2005). However, regardless of whether the stocking numbers are carefully chosen and monitored, it is clear that the sedentarisation leads to a high stress for the vegetation nearby the newly established permanent settlements (DORJI et al., 2013; HARRIS, 2010).

Beside these anthropogenic effects, climate change progressively affects the Tibetan environment. For instance, it is undisputed based on long term climatological data that climate on the Tibetan Plateau is becoming warmer, glaciers are melting (MÖLG et al., 2014; YAO et al., 2012), and extreme events in China are becoming more frequent (PIAO et al., 2010). Considering precipitation, the current trend over the Tibetan Plateau is unclear because long term area-wide observations are lacking (QIN et al., 2009). This highlighs the general knowledge gaps as identified by the Intergovernmental Panel on Climate Change (IPCC). In the eastern and northern part of the plateau, where field measurements are available, the precipitation is increasing (IPCC, 2014).

The changing environmental conditions and the changing land-use systems contribute to the concern that the Tibetan ecosystems could increasingly become degraded with

negative effects on the stability of the fragile ecosystems (LI et al., 2010; NAN, 2005; WEN et al., 2013). For China, a frequently reported number is that up to 90% of the grasslands are degraded (LIU & DIAMOND, 2005). However, this number is uncertain as large parts of the grasslands are located on the Tibetan Plateau where the degradation estimates are varying severely, depending on the region and methods applied (HARRIS, 2010). If degradation would proceed on the plateau, the reduced water storage capacity of the soils in degraded areas in combination with the higher frequency of precipitation extremes as predicted under global climate change in the headwater regions of the large rivers of East and Southeast Asia will accelerate catastrophic flooding events (ZHANG et al., 2011). There are already examples for the far reaching economic consequences of such scenarios. One of them is the large flooding event in 1998 at the Yangtze causing an economic loss of over US $20 billion (ZONG & CHEN, 2000).

The concern about the degradation is even more emphasized as the economy and the infrastructure on the Tibetan Plateau is subject to sharp changes. The construction of the new railway from Golmud to Lhasa and its extension to Shigatze directly impacted the fragile ecosystems along the track (QIN & ZHENG, 2010). Even more problematic is that the railway has the purpose to serve for enhanced exploitation and mining of the - presumed - rich natural resources in the southern and western part of the plateau. The mining activities impact the ecosystems in a dramatic way, as demonstrated in the Muli mining area in northern Qinghai. For this region, Greenpeace estimated that an area 14 times larger than the city of London has been converted to an opencast coal mine (GREENPEACE EAST ASIA, 2014). This led to a severe enhancement of the permafrost degradation and negatively affected ecosystem stability in the surroundings of the mining area (CAO et al., 2011).

Many previous studies focused on the investigation of pasture degradation on the Tibetan Plateau (e.g., LI et al., 2010; NAN, 2005; NIU et al., 2010; WEN et al., 2013; ZHOU et al., 2005) and its consequences for instance on the carbon pool (HAFNER et al., 2012; LI et al., 2013; WANG et al., 2009) or the plant available nutrients (WANG et al., 2006, 2012). However, most of these studies were conducted on small scales whereas only few studies aimed to investigate degradation patterns on large scales. Among the few studies performed on larger scales, YANG et al. (2006) investigated changes in vegetation cover in the upper reaches of the Yangtze and Yellow River between 1982 and 2001, SUN et al. (2013) analyzed time series of normalized difference vegetation

index (NDVI) data, and GAO et al. (2010) provided a grassland degradation index for the northern part of the Tibet Autonomous Region (TAR) based on a change detection analysis. Unfortunately, all of these studies have their specific drawbacks because their findings are either restricted to the investigated time span and geographical extent (GAO et al., 2010; YANG et al., 2006) or the validity of the results cannot be assessed because no or only few ground truth data were incorporated into the analysis (GAO et al., 2010; SUN et al., 2013).

These drawbacks underline that the investigation of grassland degradation is scale-dependent, because data sets to investigate the specific research questions are only available on certain scales and resolutions. On small and local scales, remote sensing data with very high spatial resolutions are available. However, these data sets have a coarse spectral and temporal resolution. Thus, they cannot be used for time series analysis or the delineation of plant chemistry parameters. One possibility to overcome the deficit of the spectral resolution is to acquire *in situ* hyperspectral reflectance data by using a hyperspectral camera or a spectrometer. On larger spatial scales, there are no reliable hyperspectral data sets available, because the only hyperspectral satellite, Hyperion, suffers from a low signal to noise ratio (e.g., PENGRA et al., 2007) and provides only data featuring small spatial coverages. However, the temporal resolution of the available multispectral satellite sensors is much higher, which allows to investigate changes over time. Subsequently, this scale-dependence of the degradation monitoring requires the usage of different concepts and indicators at different spatial scales. This fortifies the general requirement to incorporate different spatial scales into the analysis of degradation patterns, which has not been conducted for the entire plateau yet.

1.2 Objectives of the thesis

The aims of this thesis are to assess recent changes in the degradation status of the pastures on the Tibetan Plateau and to identify their drivers. As there are no suitable large scale data sets of degradation status, the basic requirement for the investigation of pasture degradation is the development of a satellite-based pasture degradation monitoring system. Since the area of investigation is extremely large and complex in terms of the spectral properties of the vegetation (SHEN et al., 2008), the indicators for pasture degradation to be monitored in the newly developed degradation product must be carefully chosen.

The general need for a proper selection of degradation indicators has been recently outlined by REEVES & BAGGETT (2014). They conclude that a reliable remote sensing based indicator system can only be developed if spatially explicit data containing site conditions, such as biotic and abiotic factors, are incorporated.

Therefore, the first key question to be answered in this thesis is whether the local grassland degradation can be delineated by developing a specific indicator system using multi- and hyperspectral remote sensing data. It has to be tested if plant coverage is a reliable indicator for grassland degradation on the Tibetan Plateau. Additionally, a second indicator will be incorporated which allows to account for site conditions. This second indicator will be chlorophyll content, which has been proven to be a suitable indicator for nitrogen (CLEVERS & KOOISTRA, 2012; OPPELT & MAUSER, 2004; YODER & PETTIGREW-CROSBY, 1995), phosphorus (LOPEZ-CANTARERO et al., 1994) and water content (FILELLA & PEÑUELAS, 1994) in the vegetation.

Given that plant coverage will be a reliable indicator for grassland degradation on the Tibetan Plateau, it has to be tested, how plant coverage can be derived for the entire Tibetan Plateau using remote sensing technologies. Therefore, a specific approach has to be developed which allows to validate the satellite derived plant coverage values against field measurements to assess the order of uncertainty across the large spatial extent of the product's coverage.

After a reliable plant coverage product has been developed for the Tibetan Plateau, the changes in plant coverage on the Tibetan Plateau during the last decade must be outlined. If significant trends of this variable can be observed, the underlying drivers of the change must be identified to separate abiotic and biotic factors on the plant coverage change.

To answer these questions, the following hypothesis will be tested in the present thesis:

H 1 The degradation of the pastures on the Tibetan Plateau is accompanied by a reduction in plant coverage, which can be derived on the local scale from multi- and hyperspectral datasets.

H 2 The combination of plant coverage and chlorophyll content provides a useful indicator system to distinguish between effects of grazing pressure and effects of other environmental factors on the local scale.

H 3 Plant coverage of the Tibetan Plateau can be derived along a cascade of multispectral satellite data with increasing spatial resolution from the local to the plateau scale.

H 4 On the plateau scale, effects of climate and anthropogenic land-use on degradation status can be separated by comparing the trends in the new plant coverage product to the trends in climate datasets.

1.3 Study outline

The main part of the present thesis consists of three scientific articles which are either published, accepted or currently under review at internationally renown journals. The general structure is presented in Fig. 1.1.

For the thesis, the three articles are embedded into the scientific context summarizing the state of research in **chapter 2** which is divided into a brief overview of the vegetation on the Tibetan Plateau (**chapter 2.1**) followed by a description of the assumed degradation processes and the previous attempts to measure grassland degradation on the Tibetan Plateau (**chapter 2.2**). Finally, the conception of the working packages will be outlined in **chapter 2.3**.

In the first article in **chapter 3**, a new indicator system based on plant coverage and chlorophyll content will be developed and tested in a case study at two locations on the Tibetan Plateau. The indicators will be retrieved from hyperspectral data sampled in the field. For the plant coverage indicator, the derivation is tested for hyperspectral and simulated multispectral data (**chapter 3.4.1**, **H 1**). The chlorophyll content indicator is derived from hyperspectral data using partial least squares regression (**chapter 3.4.2**, **H 1**). Afterward, the suitability of the combination of both indicators within a pasture degradation indicator system for the local scale is tested (**chapter 3.4.3**, **H 2**).

In the second article (**chapter 4**), different methods to retrieve plant coverage on the Tibetan Plateau are presented in **chapter 4.3**. **Chapter 4.4** describes the results of the comparison of the accuracies yielded with the methods applied and presents the final plant coverage product (**H 3**).

The third article (**chapter 5**) will present the trends in plant coverage as observed by the new coverage product (**chapter 5.3**) and will discuss the drivers of the coverage

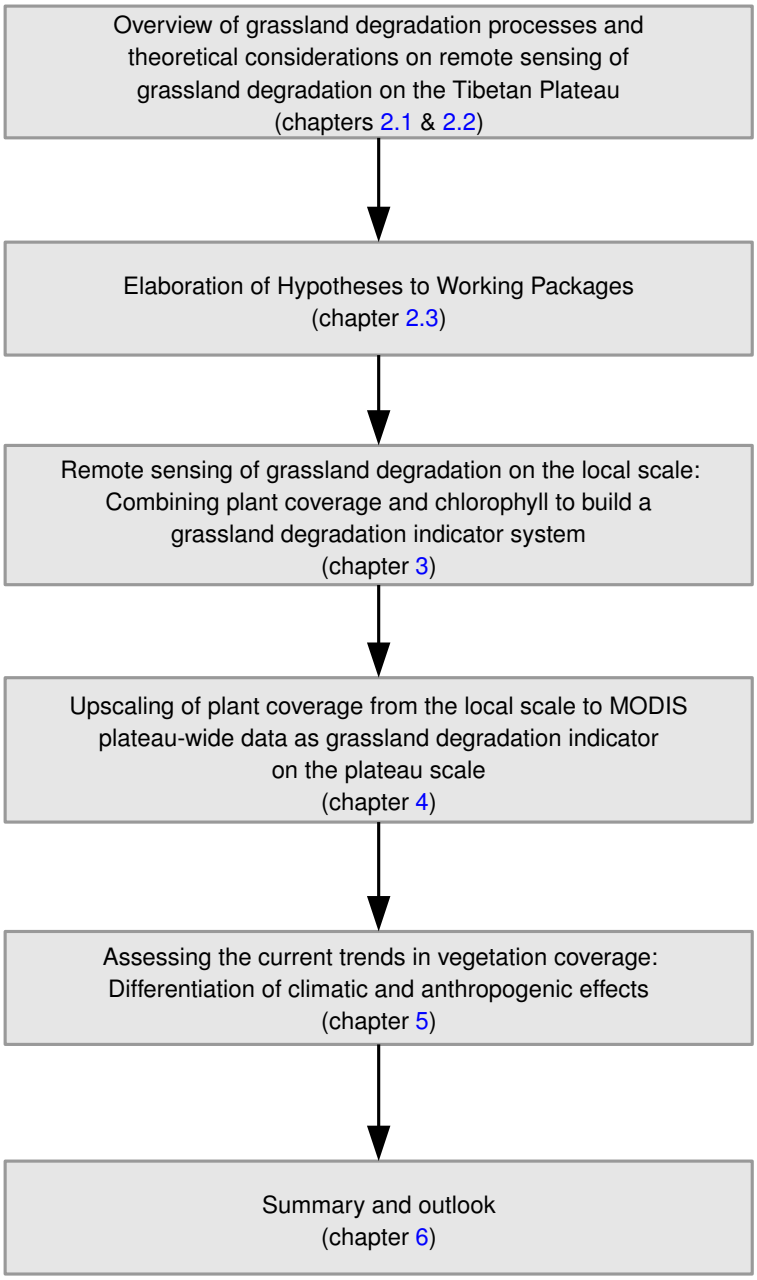

Figure 1.1: Outline of the thesis

changes (**chapter 5.4**, **H 4**).

Finally, the thesis will close summarizing the important new contributions of the presented work to the scientific discussions of pasture degradation and its effects on climate and hydrology in East and Southeast Asia (**chapter 6**).

References

BAUER, K. (2005): Development and the enclosure movement in pastoral Tibet since the 1980s. *Nomadic Peoples*, 9, 1-2, 53–81.

BENISTON, M. (2003): Climatic change in mountain regions: A review of possible impacts. *Climatic Change*, 59, 1-2, 5–31.

CAO, J.J., YEH, E.T., HOLDEN, N.M., YANG, Y.Y., & DU, G.Z. (2013): The effects of enclosures and land-use contracts on rangeland degradation on the Qinghai-Tibetan Plateau. *Journal of Arid Environments*, 97, 3–8.

CAO, W., SHENG, Y., QIN, Y., LI, J., & WU, J. (2011): An application of a new method in permafrost environment assessment of Muli mining area in Qinghai-Tibet Plateau, China. *Environmental Earth Sciences*, 63, 3, 609–616.

CLEVERS, J.G.P.W. & KOOISTRA, L. (2012): Using hyperspectral remote sensing data for retrieving canopy chlorophyll and nitrogen content. *Ieee Journal of Selected Topics In Applied Earth Observations and Remote Sensing*, 5, 2, 574–583.

CUI, X., GRAF, H.F., LANGMANN, B., CHEN, W., & HUANG, R. (2006): Climate impacts of anthropogenic land use changes on the Tibetan Plateau. *Global and Planetary Change*, 54, 1-2, 33 – 56.

DORJI, T., TOTLAND, Ø., & MOE, S.R. (2013): Are droppings, distance from pastoralist camps, and pika burrows good proxies for local grazing pressure? *Rangeland Ecology and Management*, 66, 1, 26–33.

DUAN, A. & WU, G. (2005): Role of the Tibetan Plateau thermal forcing in the summer climate patterns over subtropical Asia. *Climate Dynamics*, 24, 7-8, 793–807.

FILELLA, I. & PEÑUELAS, J. (1994): The red edge position and shape as indicators of plant chlorophyll content, biomass and hydric status. *International Journal of Remote Sensing*, 15, 7, 1459–1470.

FOLEY, J.A., DEFRIES, R., ASNER, G.P., BARFORD, C., BONAN, G., CARPENTER, S.R., CHAPIN, F.S., COE, M.T., DAILY, G.C., GIBBS, H.K., HELKOWSKI, J.H.,

HOLLOWAY, T., HOWARD, E.A., KUCHARIK, C.J., MONFREDA, C., PATZ, J.A., PRENTICE, I.C., RAMANKUTTY, N., & SNYDER, P.K. (2005): Global consequences of land use. *Science*, 309, 5734, 570–574.

FOLEY, J.A., RAMANKUTTY, N., BRAUMAN, K.A., CASSIDY, E.S., GERBER, J.S., JOHNSTON, M., MUELLER, N.D., O'CONNELL, C., RAY, D.K., WEST, P.C., BALZER, C., BENNETT, E.M., CARPENTER, S.R., HILL, J., MONFREDA, C., POLASKY, S., ROCKSTRÖM, J., SHEEHAN, J., SIEBERT, S., TILMAN, D., & ZAKS, D.P.M. (2011): Solutions for a cultivated planet. *Nature*, 478, 7369, 337–342.

GAO, Q.Z., WAN, Y.F., XU, H.M., LI, Y., JIANGCUN, W.Z., & BORJIGIDAI, A. (2010): Alpine grassland degradation index and its response to recent climate variability in northern Tibet, China. *Quaternary International*, 226, 143–150.

GOLDSTEIN, M. & BEALL, C. (2002): Changing patterns of Tibetan nomadic pastoralism. In: W. LEONARD & M. CRAWFORD (Eds.), Human Biology of Pastoral Populations. Cambridge University Press, pp. 131–150.

GREENPEACE EAST ASIA (2014): Giant coal mine in violation of laws uncovered at the source of China's mother river. (last access 18.12.2014).
URL http://www.greenpeace.org/eastasia/press/releases/climate-energy/2014/red-wall-palace-in-qinghai/

HAFNER, S., UNTEREGELSBACHER, S., SEEBER, E., LENA, B., XU, X., LI, X., GUGGENBERGER, G., MIEHE, G., & KUZYAKOV, Y. (2012): Effect of grazing on carbon stocks and assimilate partitioning in a Tibetan montane pasture revealed by $^{13}CO_2$ pulse labeling. *Global Change Biology*, 18, 2, 528–538.

HARRIS, R.B. (2010): Rangeland degradation on the Qinghai-Tibetan Plateau: A review of the evidence of its magnitude and causes. *Journal of Arid Environments*, 74, 1, 1–12.

HERRERO, M., HAVLÍK, P., VALIN, H., NOTENBAERT, A., RUFINO, M.C., THORNTON, P.K., BLÜMMEL, M., WEISS, F., GRACE, D., & OBERSTEINER, M. (2013): Biomass use, production, feed efficiencies, and greenhouse gas emissions from global livestock systems. *Proceedings of the National Academy of Sciences*, 110, 52, 20 888–20 893.

HOOPER, D.U., CHAPIN, F.S., EWEL, J.J., HECTOR, A., INCHAUSTI, P., LAVOREL, S., LAWTON, J.H., LODGE, D.M., LOREAU, M., NAEEM, S., SCHMID, B., SETALA, H., SYMSTAD, A.J., VANDERMEER, J., & WARDLE, D.A. (2005): Effects of biodiversity on ecosystem functioning: A consensus of current knowledge. *Ecological Monographs*, 75, 1, 3–35.

IMMERZEEL, W.W., VAN BEEK, L.P.H., & BIERKENS, M.F.P. (2010): Climate change will affect the Asian water towers. *Science*, 328, 5984, 1382–1385.

IPCC (2014): Climate Change 2014: Impacts, Adaptation, and Vulnerability. Part B: Regional Aspects. Contribution of Working Group II to the Fifth Assessment Report of the Intergovernmental Panel on Climate Change. Cambridge University Press, Cambridge.

LI, J., WANG, W., HU, G., & WEI, Z. (2010): Changes in ecosystem service values in Zoige Plateau, China. *Agriculture Ecosystems & Environment*, 139, 4, 766–770.

LI, X.Y., MA, Y.J., XU, H.Y., WANG, J.H., & ZHANG, D.S. (2009): Impact of land use and land cover change on environmental degradation in Lake Qinghai watershed, northeast Qinghai-Tibet Plateau. *Land Degradation & Development*, 20, 1, 69–83.

LI, Y.Y., DONG, S.K., WEN, L., WANG, X.X., & WU, Y. (2013): The effects of fencing on carbon stocks in the degraded alpine grasslands of the Qinghai-Tibetan Plateau. *Journal of Environmental Management*, 128, 393–399.

LIU, J. & DIAMOND, J. (2005): China's environment in a globalizing world. *Nature*, 435, 7046, 1179–1186.

LOPEZ-CANTARERO, I., LORENTE, F.A., & ROMERO, L. (1994): Are chlorophylls good indicators of nitrogen and phosphorus levels? *Journal of Plant Nutrition*, 17, 6, 979–990.

MIEHE, G., MIEHE, S., BACH, K., NÖLLING, J., HANSPACH, J., REUDENBACH, C., KAISER, K., WESCHE, K., MOSBRUGGER, V., YANG, Y.P., & MA, Y.M. (2011a): Plant communities of central Tibetan pastures in the Alpine Steppe/*Kobresia pygmaea* ecotone. *Journal of Arid Environments*, 75, 8, 711–723.

MIEHE, G., BACH, K., MIEHE, S., KLUGE, J., YONGPING, Y., DUO, L., CO, S., & WESCHE, K. (2011b): Alpine steppe plant communities of the Tibetan highlands. *Applied Vegetation Science*, 14, 4, 547–560.

MIEHE, G., MIEHE, S., KAISER, K., JIANQUAN, L., & ZHAO, X. (2008): Status and dynamics of *Kobresia pygmaea* ecosystem on the Tibetan Plateau. *Ambio*, 37, 4, 272–279.

MIEHE, G., MIEHE, S., KAISER, K., REUDENBACH, C., BEHRENDES, L., DUO, L., & SCHLÜTZ, F. (2009): How old is pastoralism in Tibet? An ecological approach to the making of a Tibetan landscape. *Palaeogeography, Palaeoclimatology, Palaeoecology*, 276, 130–147.

MÖLG, T., MAUSSION, F., & SCHERER, D. (2014): Mid-latitude westerlies as a driver of glacier variability in monsoonal High Asia. *Nature Climate Change*, 4, 1, 68–73.

NAN, Z. (2005): The grassland farming system and sustainable agricultural development in China. *Grassland Science*, 51, 1, 15–19.

NIU, K., ZHANG, S., ZHAO, B., & DU, G. (2010): Linking grazing response of species abundance to functional traits in the Tibetan alpine meadow. *Plant and Soil*, 330, 1-2, 215–223.

OPPELT, N. & MAUSER, W. (2004): Hyperspectral monitoring of physiological parameters of wheat during a vegetation period using AVIS data. *International Journal of Remote Sensing*, 25, 1, 145–159.

PENGRA, B.W., JOHNSTON, C.A., & LOVELAND, T.R. (2007): Mapping an invasive plant, *Phragmites australis*, in coastal wetlands using the EO-1 Hyperion hyperspectral sensor. *Remote Sensing of Environment*, 108, 1, 74–81.

PIAO, S., CIAIS, P., HUANG, Y., SHEN, Z., PENG, S., LI, J., ZHOU, L., LIU, H., MA, Y., DING, Y., FRIEDLINGSTEIN, P., LIU, C., TAN, K., YU, Y., ZHANG, T., & FANG, J. (2010): The impacts of climate change on water resources and agriculture in China. *Nature*, 467, 7311, 43–51.

QIN, J., YANG, K., LIANG, S., & GUO, X. (2009): The altitudinal dependence of recent rapid warming over the Tibetan Plateau. *Climatic Change*, 97, 1-2, 321–327.

QIN, Y. & ZHENG, B. (2010): The Qinghai-Tibet Railway: A landmark project and its subsequent environmental challenges. *Environment, Development and Sustainability*, 12, 5, 859–873.

QIU, J. (2008): The third pole. *Nature*, 454, 7203, 393–396.

REEVES, M.C. & BAGGETT, L.S. (2014): A remote sensing protocol for identifying rangelands with degraded productive capacity. *Ecological Indicators*, 43, 172–182.

SCURLOCK, J.M.O. & HALL, D.O. (1998): The global carbon sink: A grassland perspective. *Global Change Biology*, 4, 2, 229–233.

SHEEDY, D.P., MILLER, D., & JOHNSON, D.A. (2006): Transformation of traditional pastoral livestock systems on the Tibetan steppe. *Secheresse*, 17, 1-2, 142–151.

SHEN, M., TANG, Y., KLEIN, J., ZHANG, P., GU, S., SHIMONO, A., & CHEN, J. (2008): Estimation of aboveground biomass using *in situ* hyperspectral measurements in five major grassland ecosystems on the Tibetan Plateau. *Journal of Plant Ecology*, 1, 4, 247–257.

SUN, J., CHENG, G.W., LI, W.P., SHA, Y.K., & YANG, Y.C. (2013): On the variation of NDVI with the principal climatic elements in the Tibetan Plateau. *Remote Sensing*, 5, 4, 1894–1911.

WANG, C.T., LONG, R.J., WANG, Q.L., JING, Z.C., & SHI, J.J. (2009): Changes in plant diversity, biomass and soil C, in alpine meadows at different degradation stages in the headwater region of Three Rivers, China. *Land Degradation & Development*, 20, 2, 187–198.

WANG, G., WANG, Y., QIAN, J., & WU, Q. (2006): Land cover change and its impacts on soil C and N in two watersheds in the center of the Qinghai-Tibetan Plateau. *Mountain Research and Development*, 26, 2, 153–162.

WANG, S., DUAN, J., XU, G., WANG, Y., ZHANG, Z., RUI, Y., LUO, C., XU, B., ZHU, X., CHANG, X., CUI, X., NIU, H., ZHAO, X., & WANG, W. (2012): Effects of warming and grazing on soil N availability, species composition, and ANPP in an alpine meadow. *Ecology*, 93, 11, 2365–2376.

WEN, L., DONG, S.K., LI, Y.Y., LI, X.Y., SHI, J.J., WANG, Y.L., LIU, D.M., & MA, Y.S. (2013): Effect of degradation intensity on grassland ecosystem services in the alpine region of Qinghai-Tibetan Plateau, China. *Plos One*, 8, 3, e58 432.

XU, J., YANG, Y., LI, Z., TASHI, N., SHARMA, R., & FANG, J. (2008): Understanding land use, livelihoods, and health transitions among Tibetan nomads: A case from Gangga Township, Dingri County, Tibetan Autonomous Region of China. *Ecohealth*, 5, 2, 104–114.

YAMAGUCHI, T. (2011): Transition of mountain pastoralism: An agrodiversity analysis of the livestock population and herding strategies in southeast Tibet, China. *Human Ecology*, 39, 2, 141–154.

YANG, J.P., DING, Y.J., & CHEN, R.S. (2006): Spatial and temporal of variations of alpine vegetation cover in the source regions of the Yangtze and Yellow Rivers of the Tibetan Plateau from 1982 to 2001. *Environmental Geology*, 50, 3, 313–322.

YAO, T., THOMPSON, L., YANG, W., YU, W., GAO, Y., GUO, X., YANG, X., DUAN, K., ZHAO, H., XU, B., PU, J., LU, A., XIANG, Y., KATTEL, D.B., & JOSWIAK, D. (2012): Different glacier status with atmospheric circulations in Tibetan Plateau and surroundings. *Nature Climate Change*, 2, 9, 663–667.

YODER, B.J. & PETTIGREW-CROSBY, R.E. (1995): Predicting nitrogen and chlorophyll content and concentrations from reflectance spectra (400-2500 nm) at leaf and canopy scales. *Remote Sensing of Environment*, 53, 3, 199–211.

ZHANG, W., AN, S., XU, Z., CUI, J., & XU, Q. (2011): The impact of vegetation and soil on runoff regulation in headwater streams on the east Qinghai-Tibet Plateau, China. *Catena*, 87, 2, 182–189.

ZHAOLI, Y., NING, W., DORJI, Y., & JIA, R. (2005): A review of rangeland privatisation and its implications in the Tibetan Plateau, China. *Nomadic Peoples*, 9, 1-2, 31–51.

ZHOU, H., ZHAO, X., TANG, Y., GU, S., & ZHOU, L. (2005): Alpine grassland degradation and its control in the source region of the Yangtze and Yellow Rivers, China. *Grassland Science*, 51, 3, 191–203.

ZONG, Y. & CHEN, X. (2000): The 1998 flood on the Yangtze, China. *Natural Hazards*, 22, 2, 165–184.

2 Conceptual design

2.1 Vegetation on the Tibetan Plateau – A brief overview

The present study aims to assess recent changes in the degradation status of the pastures on the Tibetan Plateau and to identify their drivers. Thus, in advance of describing the major causes for pasture degradation, a short overview of the vegetation on the Tibetan Plateau will be given. For a general overview of the spatial configuration of vegetation types see Fig. 2.1 and for a detailed map of grassland vegetation types see Fig. 4.1.

The vegetation on the Tibetan Plateau is mainly comprised of herbaceous species. Only at the eastern declivity, forests of larger extent occur up to 4800 m (MIEHE et al., 2007) and vegetation types dominated by (dwarf-)scrubs are found between 1000 and 4200 m (HOU, 1983). Areas with dominant crop production can be found around Lhasa and in the Yarlung River valley. The major part of the Tibetan Plateau is covered by grasslands which have been classified into five types in this study: *Kobresia humilis*, Montane Steppes, *K. pygmaea*, *K. schoenoides* swamps and Alpine Steppe.

K. humilis pastures occur in the eastern and north-eastern part of the Tibetan Plateau at elevations from 3300 to 3600 m. They are characterized by a high plant cover of over 80%. Montane Steppes cover the north-eastern part of the plateau at lower elevations and in areas with lower precipitation than *K. humilis* pastures (MIEHE et al., 2008a). A large band spanning from south-west to north-east is covered by *K. pygmaea* pastures, which have their core range at elevations between 3000 and 4000 m. Their highest occurrences featuring only small spatial extents are at 5960 m on the slopes of Mt. Everest (MIEHE et al., 2008b). This vegetation type is dominated by the small sedge *K. pygmaea* (2 - 4 cm tall) forming a relatively stable turf layer (up to 20 cm thickness) usually covered by lichens (KAISER et al., 2008; MIEHE et al., 2008b). In areas where the turf layer is destroyed, e.g., by trampling of cattle, *K. pygmaea* is replaced by a sparse vegetation comprised by annual species. It is questioned if the *K. pygmaea* pastures are the natural

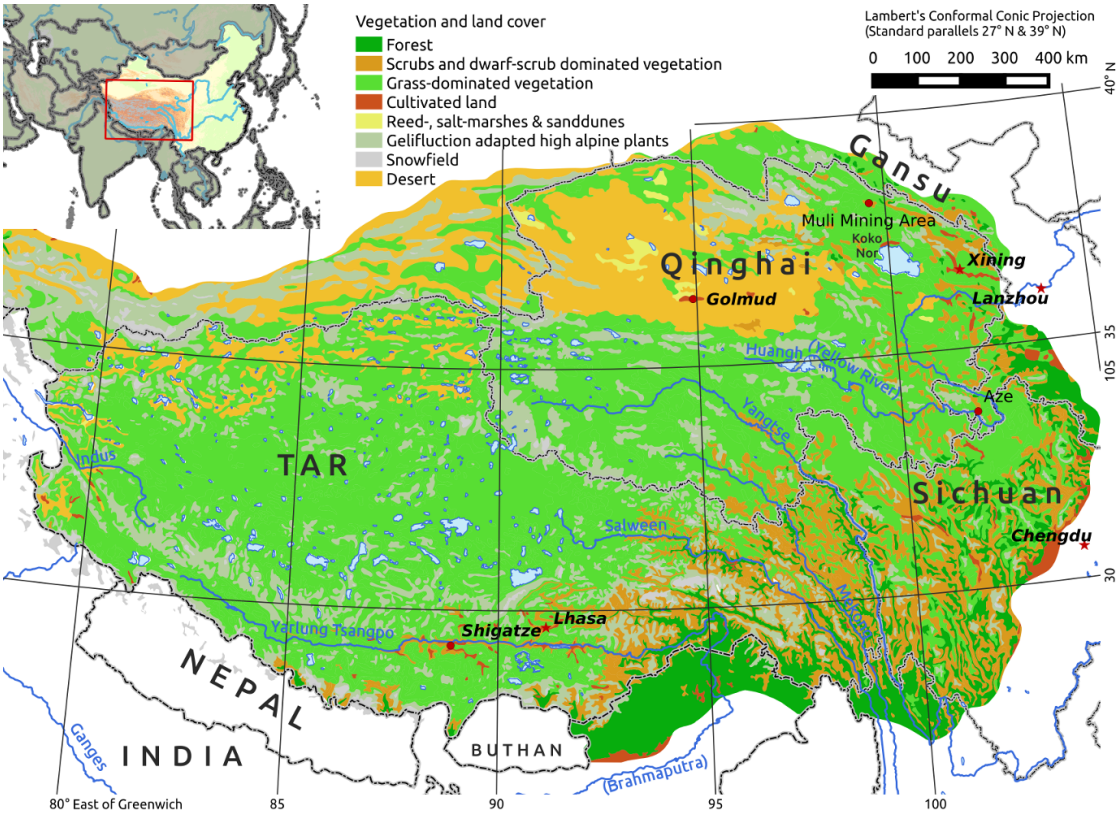

Figure 2.1: Vegetation on the Tibetan Plateau. For further details on subdivision into grassland vegetation types see Fig. 4.1. All geographical names mentioned in chapter 1 & 2 were included in the map. Data source of vegetation types: HOU (2001).

vegetation or if they are the consequence of the current anthropogenic usage. In areas at lower elevations where annual precipitation is above 200 - 300 mm this grassland vegetation type replaced forests as suggested by charcoal finds. In grazing exclosure experiments, a higher vegetation emerges within short periods confirming the hypothesis that *K. pygmaea* pastures are a secondary vegetation type (MIEHE et al., 2008b). The arid parts in the western Tibetan Plateau are covered by the largest grassland vegetation type, the Alpine Steppe vegetation, which is characterized by a low vegetation coverage of below 30% (MIEHE et al., 2011b). For the local pastoral economy the swamps are extremely important because they are traditionally used as winter pastures. Thus, their productivity is one of the most restrictive factors for livestock sizes (LONG et al., 2008). If the swamps are overexploited, *K. schoenoides* is replaced by several *Carex* species and coverage is considerably reduced (MIEHE et al., 2011a).

2.2 Degradation of grasslands on the Tibetan Plateau – The state of research

The investigation of grassland degradation its causes and its current status on the Tibetan Plateau was the aim of numerous studies. Unfortunately, the methods and the scales of the investigations are not consistent making a comparison impossible. Reviews summarizing the state of research in the pasture degradation on the Tibetan Plateau are provided by HARRIS (2010) and CHEN et al. (2013). In the following the state of research with respect to the causes of the – presumed – ongoing degradation will be outlined with a special focus on the recent advances in this field.

2.2.1 Possible causes of degradation

Three main causes of degradation on the Tibetan Plateau are currently under discussion: (1) the changing climate including melting permafrost soils, (2) damage by small mammals and (3) unsustainable rangeland management practices. These will be briefly outlined in the following.

2.2.1.1 Global climate change

The analysis of different data sources revealed that air temperatures are rising on the Tibetan Plateau (PIAO et al., 2010). During the last decades, the slope of this increase was between 0.016 °C/year (LIU & CHEN, 2000) and 0.04 °C/year (DU et al., 2004). In contrast to the temperatures which evinced homogeneous and verified trends, the precipitation trends on the Tibetan Plateau are generally difficult to assess because meteorological stations are rare and restricted to valleys of the eastern part at lower altitudes (QIN et al., 2009). Thus, previous analysis are either restricted to the area where meteorological data sets are available (e.g., PIAO et al., 2010; SHEN et al., 2014a,b) or forced to use data sets from remote sensing (e.g., IMMERZEEL et al., 2009) or numerical models (e.g., TURNER & ANNAMALAI, 2012). As a consequence of the differing data sources, the results of the studies are often inconsistent. A comprehensive pattern, however, is that precipitation is increasing in the more humid eastern part of the plateau (IPCC, 2014). For the drier western part, on the other hand, some data sources are

indicating negative trends (XU et al., 2008). The sign and magnitude of the latter trends differs between seasons as shown by XU et al. (2008). They found dominating negative trends for summer precipitation in the northern part of the TAR while strong positive trends were observed in the same region during winter season. For Qinghai slightly positive precipitation trends are reported (LIU et al., 2014; PIAO & FANG, 2002).

It is unclear if rising temperature values have a generally positive or negative effect on the productivity of the grasslands on the Tibetan Plateau. One reason is that the differences in temperature values are extremely high as a consequence of the large altitudinal gradient. Since the vegetation is highly adapted to local conditions, it is highly probable that the vegetation in the dryer western part will respond in a different way to rising temperatures than the vegetation at the more humid eastern declivity. Therefore, no conclusive and widely accepted relationship between positive temperature trends and vegetation growth on the Tibetan Plateau has been published, yet. On the one hand, studies analyzing remote sensing time series conclude that rising temperatures on the Tibetan Plateau would accelerate plant growth (CHEN et al., 2013; LIU et al., 2014; PIAO et al., 2006; SHEN et al., 2014b). On the other hand, some plot based studies indicate that an increase in temperature values will lead to a less suitable environment for plant growth (KLEIN et al., 2007; LUO et al., 2010). In general, rising temperatures accelerate evapotranspiration. If precipitation is not changing, this acceleration enhances water stress of the vegetation at least in the arid western part of the plateau (YOU et al., 2014). Consequently, the enhanced water stress will cause the plants to reduce their aboveground biomass to counterbalance the increasing water losses.

The effect of changes in precipitation on vegetation is better understood and a positive correlation between precipitation and vegetation growth is widely accepted (FANG et al., 2001). For the eastern Tibetan Plateau, SHI et al. (2014) demonstrated along a large transect that the net primary production of the grasslands is positively correlated to precipitation amounts. Additionally, the authors showed that the net primary production of the grasslands is more strongly influenced by precipitation than temperature.

2.2.1.2 Damage by small mammals

Like in other Eurasian steppes, pikas (*Ochotona curzoniae*) and other small ground-dwelling mammals are frequent on the Tibetan Plateau (YU et al., 2012) and considered

keystone species in those ecosystems (SMITH & FOGGIN, 1999). The diet of the small mammals is comprised by roots and above-ground biomass. Besides that, pikas create burrows and thus, open the vegetation cover. Therefore, they compete with livestock for forage, giving rise to attempts to control them by poisoning campaigns. The effect of the poisoning campaigns on the population sizes of pikas is still disputed. For instance, PECH et al. (2007) showed that the control programs have only small effects as pika populations can recover within one growing season. In contrast, LAI & SMITH (2003) reported that the poisoning campaigns reduced the population sizes of pikas by 95% as compared to the pre-campaign size.

It is undoubted that highest frequencies of pikas are found on degraded grasslands (e.g., DORJI et al., 2014; MIEHE et al., 2008b). Even though, the frequencies are considered unreliable indicators of pasture degradation (GAO et al., 2013) because it is still under discussion if pikas prefer already degraded pastures (HOLZNER & KRIECHBAUM, 2001; WANGDWEI et al., 2013) or if they actively contribute to degradation (LI et al., 2013).

2.2.1.3 Unsustainable land use practices

The land use practices on the Tibetan Plateau have undergone various changes during the last 50 years. A presumed cause of degradation was identified in the collective usage of the pastures in the traditional system (BAUER, 2005) ('tragedy of the commons'; HARDIN, 1968). Several programs were initiated to increase production, to change traditional trading systems and to encourage sedentarisation (MIEHE et al., 2009). It is generally accepted that these programs had enhancing effects on the degradation at least locally (HARRIS, 2010). For instance, MIEHE et al. (2011a) found that the sedentarisation programs led to an enhancement of degradation on winter pastures caused by a reduction in mobility of the herders in the northern part of the TAR. CAO et al. (2011, 2013) reported that degradation is lower on pastures which are used by multiple households (close to the traditional system) compared to the newly introduced single household usage.

The increasing livestock numbers are considered to enhance long-term degradation (ZHOU et al., 2005). A major increase occurred between 1960 and 1980, followed, at least locally, by a reduction after 1990 (XUE et al., 2009). However, data from statistical

yearbooks suggest that, on provincial scale, the livestock numbers increased steadily until present (MA et al., 2013).

2.2.2 Assessment techniques and assumed extent of pasture degradation on the Tibetan Plateau

The assessment of pasture degradation on the Tibetan Plateau was the objective of various studies working on different scales and applying different methods. On a plot scale, long term fencing experiments were conducted for example near Aze, by the University of Lanzhou (NIU et al., 2012; WU et al., 2010; **?**). Here, it was found that aboveground vegetation productivity was significantly higher in fenced areas as compared to the control plots (**?**), resulting in an increase in soil organic carbon content (WU et al., 2010). However, long-term grazing exclosure meanwhile reduced species diversity. This effect was attributed to a shift in the balance between competition between plant species and reproduction towards the long-term occupation of sites at high abundances (NIU et al., 2012). Thus, the studies conclude that high diversity is only maintained within moderately grazed grasslands.

Other plot-based studies measured degradation using various sets of indicators such as plant functional traits (e.g., NIU et al., 2010) and plant functional types (e.g., MIEHE et al., 2011b; ZHU et al., 2012). The impact of grazing on the composition of vegetation communities was investigated by comparing the grazing tolerance of plant species at fenced and grazed sites in Qinghai (MIEHE et al., 2008a). In the northern part of the TAR most of the coverage of the grasslands is comprised by grazing tolerant species (MIEHE et al., 2011a).

The results from grazing exclosure experiments indicate that vegetation coverage and species composition is rapidly changing ($<$ 10 years) (HAFNER et al., 2012; MIEHE et al., 2009). Thus, for monitoring purposes of pasture degradation, an investigated time series of 10 to 15 years would be enough to capture the recent changes.

However, the results of all of these plot based studies are restricted to small areas. Since most of the studies were conducted in the north-eastern and eastern part of the plateau, almost nothing is known about grassland degradation in the western part of the Tibetan Plateau (HARRIS, 2010). These knowledge gaps are aggravated by the fact that degradation estimations are highly subjective and not comparable. The available surveys

are conducted by local grassland bureaus without proper documentation or common criteria among the different institutions (HARRIS, 2010).

On larger scales, remote sensing techniques have been recently conducted to investigate changes in the vegetation on the Tibetan Plateau (e.g., GAO et al., 2010; SHEN et al., 2014b; SUN et al., 2013; TIAN et al., 2014; WAN et al., 2014) which are related to pasture degradation. A prerequisite to achieve valid results about degradation by remote sensing is the careful choice of indicator(s). These must be retrievable from the remote sensing data and must have a strong connection to degradation. Therefore, GAO et al. (2013) compared three indicators (soil moisture content, vegetation coverage and the density of pika burrows) in central Qinghai and found that the best performing indicator was the vegetation coverage.

Remote sensing technologies have been successfully used to retrieve plant coverage in grasslands (e.g., SMITH et al., 1990). The methods to derive plant coverage encompass simple correlations between plant coverage and vegetation indices such as NDVI (HILKER et al., 2014) or spectral angle mapper (YANG & EVERITT, 2012), linear spectral unmixing (GÖTTLICHER et al., 2009; SMITH et al., 1990; SOHN & MCCOY, 1997), and more advanced statistical techniques such as support vector machines, random forest regression, artificial neural networks, and partial least squares regression (BACOUR et al., 2006; HANSEN et al., 2002; SCHWIEDER et al., 2014). Accurate estimations of low plant coverage values are generally difficult because the albedo values at sites with low vegetation coverage are more sensitive to soil moisture than vegetation coverage (HUETE et al., 1997; SMITH et al., 1990).

Based on the assumption that plant coverage is a valid indicator for pasture degradation, a number of studies investigated changes in vegetation indices across Tibet. These investigations were either based on change detection analysis (GAO et al., 2010; LI et al., 2009) or time series analysis. The parameter under consideration of most of the previous studies is the NDVI (e.g., JIANG et al., 2015; SUN et al., 2013; TIAN et al., 2014; WAN et al., 2014). This is problematic in areas with low vegetation cover as soil moisture content significantly influences NDVI values (e.g., MYNENI & WILLIAMS, 1994; TODD & HOFFER, 1998). The general finding of long term time series analysis across the entire Tibetan Plateau is that the areas with increasing vegetation coverage and primary production are larger than those with decreasing trends (PIAO et al., 2006; SUN et al., 2013). However, there are severe differences among different regions (SUN et al., 2013;

TIAN et al., 2014) which are neither completely understood (SHEN et al., 2014b) nor consistent across the different studies. The latter may at least partly be explained by the different data sources and temporal coverages.

2.3 Conception and technical preparation of the working packages

The detection of recent changes of pasture degradation on the Tibetan Plateau in this work will be based on changes in plant coverage which is the most frequently used indicator for remote detection of pasture degradation in previous studies. A general issue of this indicator is that plant coverage is not only constrained by grazing but also by water and nutrient amounts as well as temperature. Especially the effects of water stress on the vegetation in Tibet is problematic as water availability changes within small distances. This results in a generally patchy vegetation mosaic consisting of densely vegetated areas within swamps surrounded by sparser vegetation. Therefore, a second indicator has to be included into the degradation assessment/monitoring to partition the effects into those of the site/climate and those of anthropogenically induced overgrazing.

On the local scale, for which hyperspectral data sets can be acquired *in situ*, a suitable second indicator would be the chlorophyll content of the vegetation as this parameter is correlated to foliage chemistry. It has been shown by several studies that chlorophyll content of single species can be derived by hyperspectral imaging (e.g., MAIN et al., 2011; MALENOVSKY et al., 2013; USTIN et al., 2009). Therefore, chlorophyll content must be derived from hyperspectral data to test if the combination of plant coverage and chlorophyll content provides a reliable indicator system for pasture degradation on a local scale (Fig. 2.2).

On larger scales, the analysis must rely on multispectral data because no hyperspectral data sets are available for the Tibetan Plateau. Unfortunately, the derivation of chlorophyll content from multispectral data is almost impossible. Only in the case of a simple vegetation structure and single dominant species, the retrieval may be successful as demonstrated by GUERSCHMAN et al. (2009) in *Eucalyptus* forests in Australia. Since the vegetation structure and plant composition is highly heterogeneous on the Tibetan Plateau, it is unlikely that the derivation of chlorophyll content is possible for that area

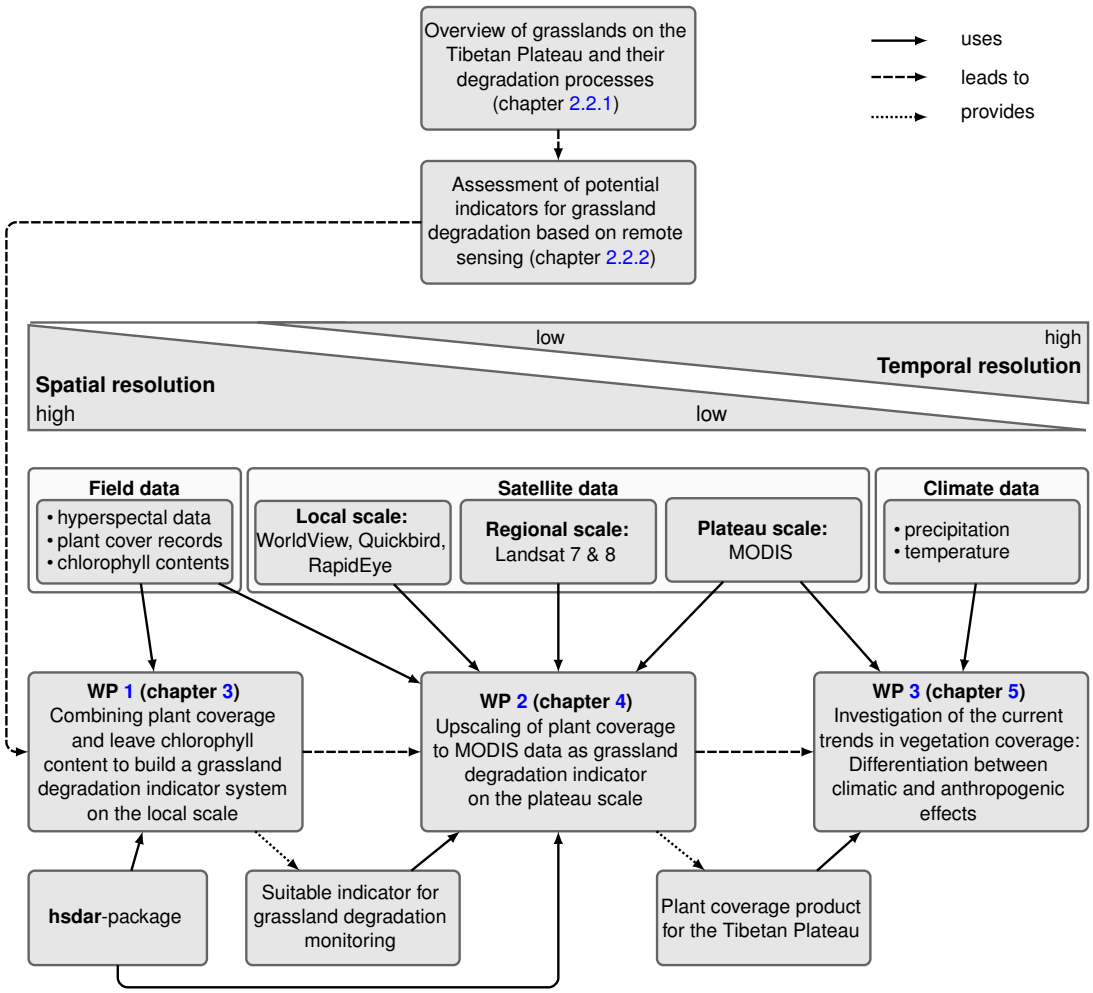

Figure 2.2: Workflow through **WP 1** to **WP 3**.

using multispectral satellite data. Thus, the chlorophyll indicator cannot be derived on larger scales. However, this constraint in the spectral resolution of the available data sets most probably does not affect the plant cover indicator. This will be derived for entire plateau by the development of an upscaling approach which allows to validate the estimates of plant cover values against field measurements. Therefore, satellite data of three spatial resolutions will be used. For each of the field measurement sites, a comprehensive set of cloud-free satellite data from WorldView-type (2 m nominal spatial resolution) via Landsat ETM+/OLI (30 m) to MODIS (500 m) must be available and processed.

To derive the degradation status and changes in the degradation of the pastures across

the large scales of the Tibetan Plateau, an approach without chlorophyll as indicator must be chosen. Here, time series analysis provides an alternative because changes in plant coverage are either dominantly linked to changes in grazing or changes in climate or by any combination of both groups (HARRIS, 2010). If the trends of climate variables are compared to the trends observed in the plant coverage and livestock numbers across the same time span, it can be tested if the separation between climate induced and anthropogenic caused degradation is possible. If consistent pattern will be found, the driver of the changes in the degradation status can be identified.

Thus, to test the mentioned hypotheses, the following three working packages (WP) will build the framework of the present thesis:

WP 1 On the local scale, plant coverage must be derived from multi- and hyperspectral data sets. Additionally, chlorophyll content of the grassland vegetation must be estimated using hyperspectral data (**H 1**). Finally, it must be tested, if the combination of plant coverage and chlorophyll content provides a useful indicator system to separate effects of grazing pressure from other environmental factors (**H 2**).

WP 2 Plant coverage will be derived along a cascade of multispectral satellite data from the local to the plateau scale. To achieve a valuable plant coverage product for the entire Tibetan Plateau, several methods to derive plant coverage will be applied and tested for their predictive accuracy (**H 3**).

WP 3 On the plateau scale, time series in the new plant coverage product, as well as in precipitation and temperature data sets will be compared in order to analyze the potential drivers of vegetation changes between 2000 and 2013 (**H 4**). Using the information of all three time series, the suitability of the new plant coverage data set as degradation monitoring product will be assessed.

The investigation of the indicators at the local scale (**WP 1**) and the upscaling approach of plant coverage (**WP 2**) require a comprehensive field database. To build this database, three field surveys were conducted to investigate all important grassland types on the Tibetan Plateau. One important aspect of the field work was to cover all stages of degradation which are present at the different locations. A time-effective approach to achieve this is to use a transect design, because previous investigations indicate that grazing

pressure and the associated degradation is depending on the distance to settlements in semi-arid ecosystems such as the Tibetan Plateau (e.g., ANDREW, 1988; DORJI et al., 2013; HARRIS & ASNER, 2003; HOSHINO et al., 2009; PICKUP & CHEWINGS, 1994; SASAKI et al., 2007). The transects started at the villages or camp sites. Their length were set according to the local environmental setting and the pasture usage rights of the village at the starting point. Along the transects, small plots were systematically chosen at which plant cover was recorded and hyperspectral measurements were conducted using a spectrometer. Due to time constraints, chlorophyll content was only measured at selected plots.

Many of the basic methods which are presumably useful in the framework of the development of a satellite-based pasture degradation monitoring approach are already implemented in R statistical language. This holds especially true for machine learning and other statistical algorithms. However, there is a great lack of R's functionality regarding the basic processing functions for hyperspectral remote sensing. Therefore, the functionality of R was extended by hyperspectral methods, which were combined in a new R-package entitled "Hyperspectral Data Analysis in R" (hsdar). This package was a prerequisite for **WP 1** and **WP 2** and has been published on the Comprehensive R Archive Network (CRAN) from which it can be downloaded free of charge (LEHNERT et al., 2015).

The structure of this thesis is illustrated in Fig. 2.2. In **chapter 3**, an indicator system to detect pasture degradation on the local scale will be developed. This indicator system consists of two separate indicators, the plant coverage and the chlorophyll content of grasses. The first indicator is derived using linear spectral unmixing. To estimate the chlorophyll content, a partial least squares regression model based on hyperspectral vegetation indices is fitted and tested (**WP 1**). Afterward, the methodology to derive plant coverage and the final plant coverage product are described (**chapter 4**, **WP 2**). Therefore, several methods to derive plant coverage across a cascade of multispectral satellite data with spatial resolutions from 2 m to 500 m are tested on their predictive accuracy. Finally, the spatio-temporal changes in plant coverage according to the novel product are discussed regarding the effects of changes in precipitation, temperature and livestock numbers on the Tibetan Plateau between 2000 and 2013 (**chapter 5**, **WP 3**).

References

ANDREW, M. (1988): Grazing impact in relation to livestock watering points. *Trends in Ecology & Evolution*, 3, 12, 336 – 339.

BACOUR, C., BARET, F., BÉAL, D., WEISS, M., & PAVAGEAU, K. (2006): Neural network estimation of LAI, fAPAR, fCover and LAIxC_{ab}, from top of canopy MERIS reflectance data: Principles and validation. *Remote Sensing of Environment*, 105, 4, 313–325.

BAUER, K. (2005): Development and the enclosure movement in pastoral Tibet since the 1980s. *Nomadic Peoples*, 9, 1-2, 53–81.

CAO, J., HOLDEN, N.M., LUE, X..T., & DU, G. (2011): The effect of grazing management on plant species richness on the Qinghai-Tibetan Plateau. *Grass and Forage Science*, 66, 3, 333–336.

CAO, J.J., YEH, E.T., HOLDEN, N.M., YANG, Y.Y., & DU, G.Z. (2013): The effects of enclosures and land-use contracts on rangeland degradation on the Qinghai-Tibetan Plateau. *Journal of Arid Environments*, 97, 3–8.

CHEN, H., ZHU, Q., PENG, C., WU, N., WANG, Y., FANG, X., GAO, Y., ZHU, D., YANG, G., TIAN, J., KANG, X., PIAO, S., OUYANG, H., XIANG, W., LUO, Z., JIANG, H., SONG, X., ZHANG, Y., YU, G., ZHAO, X., GONG, P., YAO, T., & WU, J. (2013): The impacts of climate change and human activities on biogeochemical cycles on the Qinghai-Tibetan Plateau. *Global Change Biology*, 19, 10, 2940–2955.

DORJI, T., MOE, S.R., KLEIN, J.A., & TOTLAND, Ø. (2014): Plant species richness, evenness, and composition along environmental gradients in an alpine meadow grazing ecosystem in Central Tibet, China. *Arctic Antarctic and Alpine Research*, 46, 2, 308–326.

DORJI, T., TOTLAND, Ø., & MOE, S.R. (2013): Are droppings, distance from pastoralist camps, and pika burrows good proxies for local grazing pressure? *Rangeland Ecology and Management*, 66, 1, 26–33.

DU, M., KAWASHIMA, S., YONEMURA, S., ZHANG, X., & CHEN, S. (2004): Mutual influence between human activities and climate change in the Tibetan Plateau during recent years. *Global Planetary Change*, 41, 241–249.

FANG, J., PIAO, S., TANG, Z., PENG, C., & JI, W. (2001): Interannual variability in net primary production and precipitation. *Science*, 293, 5536, 1723–1723.

GAO, J., LI, X.L., CHEUNG, A., & YANG, Y.W. (2013): Degradation of wetlands on the Qinghai-Tibet Plateau: A comparison of the effectiveness of three indicators. *Journal of Mountain Science*, 10, 4, 658–667.

GAO, Q.Z., WAN, Y.F., XU, H.M., LI, Y., JIANGCUN, W.Z., & BORJIGIDAI, A. (2010): Alpine grassland degradation index and its response to recent climate variability in northern Tibet, China. *Quaternary International*, 226, 143–150.

GUERSCHMAN, J.P., HILL, M.J., RENZULLO, L.J., BARRETT, D.J., MARKS, A.S., & BOTHA, E.J. (2009): Estimating fractional cover of photosynthetic vegetation, non-photosynthetic vegetation and bare soil in the Australian tropical savanna region upscaling the EO-1 Hyperion and MODIS sensors. *Remote Sensing of Environment*, 113, 5, 928–945.

GÖTTLICHER, D., OBREGON, A., HOMEIER, J., ROLLENBECK, R., NAUSS, T., & BENDIX, J. (2009): Land-cover classification in the Andes of southern Ecuador using Landsat ETM plus data as a basis for SVAT modelling. *International Journal of Remote Sensing*, 30, 8, 1867–1886.

HAFNER, S., UNTEREGELSBACHER, S., SEEBER, E., LENA, B., XU, X., LI, X., GUGGENBERGER, G., MIEHE, G., & KUZYAKOV, Y. (2012): Effect of grazing on carbon stocks and assimilate partitioning in a Tibetan montane pasture revealed by $^{13}CO_2$ pulse labeling. *Global Change Biology*, 18, 2, 528–538.

HANSEN, M., DEFRIES, R., TOWNSHEND, J., SOHLBERG, R., DIMICELI, C., & CARROLL, M. (2002): Towards an operational MODIS continuous field of percent tree cover algorithm: Examples using AVHRR and MODIS data. *Remote Sensing of Environment*, 83, 1-2, 303–319.

HARDIN, G. (1968): The tragedy of the commons. *Science*, 162, 3859, 1243–1248.

HARRIS, A.T. & ASNER, G.P. (2003): Grazing gradient detection with airborne imaging spectroscopy on a semi-arid rangeland. *Journal of Arid Environments*, 55, 3, 391–404.

HARRIS, R.B. (2010): Rangeland degradation on the Qinghai-Tibetan Plateau: A review of the evidence of its magnitude and causes. *Journal of Arid Environments*, 74, 1, 1–12.

HILKER, T., NATSAGDORJ, E., WARING, R.H., LYAPUSTIN, A., & WANG, Y. (2014): Satellite observed widespread decline in Mongolian grasslands largely due to overgrazing. *Global Change Biology*, 20, 2, 418–428.

HOLZNER, W. & KRIECHBAUM, M. (2001): Pastures in south and central Tibet (China) II: Probable causes of pasture degradation. *Die Bodenkultur*, 52, 1, 37–44.

HOSHINO, A., YOSHIHARA, Y., SASAKI, T., OKAYASU, T., JAMSRAN, U., OKURO, T., & TAKEUCHI, K. (2009): Comparison of vegetation changes along grazing gradients with different numbers of livestock. *Journal of Arid Environments*, 73, 6-7, 687–690.

HOU, X.Y. (1983): Vegetation of China with reference to its geographical distribution. *Annals of the Missouri Botanical Garden*, 70, 3, 509–549.

HOU, X.Y. (Ed.) (2001): Vegetation Atlas of China. Science Press, Beijing.

HUETE, A., LIU, H., BATCHILY, K., & VAN LEEUWEN, W. (1997): A comparison of vegetation indices over a global set of TM images for EOS-MODIS. *Remote Sensing of Environment*, 59, 3, 440 – 451.

IMMERZEEL, W., DROOGERS, P., DE JONG, S., & BIERKENS, M. (2009): Large-scale monitoring of snow cover and runoff simulation in Himalayan river basins using remote sensing. *Remote Sensing of Environment*, 113, 1, 40–49.

IPCC (2014): Climate Change 2014: Impacts, Adaptation, and Vulnerability. Part B: Regional Aspects. Contribution of Working Group II to the Fifth Assessment Report of the Intergovernmental Panel on Climate Change. Cambridge University Press, Cambridge.

JIANG, Y.B., TAO, J., HUANG, Y.Q., ZHU, J.T., TIAN, L., & ZHANG, Y.J. (2015): The spatial pattern of grassland aboveground biomass on Xizang Plateau and its climatic controls. *Journal of Plant Ecology*, 8, 1, 30–40.

KAISER, K., MIEHE, G., BARTHELMES, A., EHRMANN, O., SCHARF, A., SCHULT, M., SCHLUTZ, F., ADAMCZYK, S., & FRENZEL, B. (2008): Turf-bearing topsoils on the central Tibetan Plateau, China: Pedology, botany, geochronology. *Catena*, 73, 3, 300–311.

KLEIN, J.A., HARTE, J., & ZHAO, X.Q. (2007): Experimental warming, not grazing, decreases rangeland quality on the Tibetan Plateau. *Ecological Applications*, 17, 2, 541–557.

LAI, C.H. & SMITH, A.T. (2003): Keystone status of plateau pikas (*Ochotona curzoniae*): Effect of control on biodiversity of native birds. *Biodiversity and Conservation*, 12, 9, 1901–1912.

LEHNERT, L.W., MEYER, H., & BENDIX, J. (2015): hsdar: Manage, Analyse and Simulate Hyperspectral Data. R package version 0.2.1.
URL http://cran.r-project.org/web/packages/hsdar/index.html

LI, X.L., GAO, J., BRIERLEY, G., QIAO, Y.M., ZHANG, J., & YANG, Y.W. (2013): Rangeland degradation on the Qinghai-Tibet Plateau: Implications for rehabilitation. *Land Degradation & Development*, 24, 1, 72–80.

LI, X.Y., MA, Y.J., XU, H.Y., WANG, J.H., & ZHANG, D.S. (2009): Impact of land use and land cover change on environmental degradation in Lake Qinghai watershed, northeast Qinghai-Tibet Plateau. *Land Degradation & Development*, 20, 1, 69–83.

LIU, X.D. & CHEN, B.D. (2000): Climatic warming in the Tibetan Plateau during recent decades. *International Journal of Climatology*, 20, 14, 1729–1742.

LIU, X., ZHU, X., ZHU, W., PAN, Y., ZHANG, C., & ZHANG, D. (2014): Changes in spring phenology in the three-rivers headwater region from 1999 to 2013. *Remote Sensing*, 6, 9, 9130–9144.

LONG, R., DING, L., SHANG, Z., & GUO, X. (2008): The yak grazing system on the Qinghai-Tibetan Plateau and its status. *Rangeland Journal*, 30, 2, 241–246.

LUO, C., XU, G., CHAO, Z., WANG, S., LIN, X., HU, Y., ZHANG, Z., DUAN, J., CHANG, X., SU, A., LI, Y., ZHAO, X., DU, M., TANG, Y., & KIMBALL, B. (2010): Effect of warming and grazing on litter mass loss and temperature sensitivity of litter and dung mass loss on the Tibetan Plateau. *Global Change Biology*, 16, 5, 1606–1617.

MA, J., ZHANG, W., LUO, L., XU, Y., XIE, H., XU, X., LI, Q., ZHENG, J., & SHENG, L. (Eds.) (2013): China Statistical Yearbook. China Statistical Press, Beijing.

MAIN, R., CHO, M.A., MATHIEU, R., O'KENNEDY, M.M., RAMOELO, A., & KOCH, S. (2011): An investigation into robust spectral indices for leaf chlorophyll estimation. *ISPRS Journal of Photogrammetry and Remote Sensing*, 66, 6, 751–761.

MALENOVSKY, Z., HOMOLOVA, L., ZURITA-MILLA, R., LUKES, P., KAPLAN, V., HANUS, J., GASTELLU-ETCHEGORRY, J.P., & SCHAEPMAN, M.E. (2013): Retrieval of spruce leaf chlorophyll content from airborne image data using continuum removal and radiative transfer. *Remote Sensing of Environment*, 131, 85–102.

MIEHE, G., MIEHE, S., BACH, K., NÖLLING, J., HANSPACH, J., REUDENBACH, C., KAISER, K., WESCHE, K., MOSBRUGGER, V., YANG, Y.P., & MA, Y.M. (2011a): Plant communities of central Tibetan pastures in the Alpine Steppe/*Kobresia pygmaea* ecotone. *Journal of Arid Environments*, 75, 8, 711–723.

MIEHE, G., BACH, K., MIEHE, S., KLUGE, J., YONGPING, Y., DUO, L., CO, S., & WESCHE, K. (2011b): Alpine steppe plant communities of the Tibetan highlands. *Applied Vegetation Science*, 14, 4, 547–560.

MIEHE, G., KAISER, K., CO, S., XINQUAN, Z., & JIANQUAN, L. (2008a): Geo-ecological transect studies in northeast Tibet (Qinghai, China) reveal human-made mid-holocene environmental changes in the upper Yellow River catchment changing forest to grassland. *Erdkunde*, 62, 3, 187–199.

MIEHE, G., MIEHE, S., KAISER, K., JIANQUAN, L., & ZHAO, X. (2008b): Status and dynamics of *Kobresia pygmaea* ecosystem on the Tibetan Plateau. *Ambio*, 37, 4, 272–279.

MIEHE, G., MIEHE, S., KAISER, K., REUDENBACH, C., BEHRENDES, L., DUO, L., & SCHLÜTZ, F. (2009): How old is pastoralism in Tibet? An ecological approach to the

making of a Tibetan landscape. *Palaeogeography, Palaeoclimatology, Palaeoecology*, 276, 130–147.

MIEHE, G., MIEHE, S., VOGEL, J., CO, S., & DUO, L. (2007): Highest treeline in the northern hemisphere found in southern Tibet. *Mountain Research and Development*, 27, 2, 169–173.

MYNENI, R. & WILLIAMS, D. (1994): On the relationship between FAPAR and NDVI. *Remote Sensing of Environment*, 49, 3, 200–211.

NIU, K., SCHMID, B., CHOLER, P., & DU, G. (2012): Relationship between reproductive allocation and relative abundance among 32 species of a Tibetan alpine meadow: Effects of fertilization and grazing. *PloS one*, 7, 4, 1–6.

NIU, K., ZHANG, S., ZHAO, B., & DU, G. (2010): Linking grazing response of species abundance to functional traits in the Tibetan alpine meadow. *Plant and Soil*, 330, 1-2, 215–223.

PECH, R.P., JIEBU, ARTHUR, A.D., ZHANG, Y., & LIN, H. (2007): Population dynamics and responses to management of plateau pikas *Ochotona curzoniae*. *Journal of Applied Ecology*, 44, 3, 615–624.

PIAO, S., CIAIS, P., HUANG, Y., SHEN, Z., PENG, S., LI, J., ZHOU, L., LIU, H., MA, Y., DING, Y., FRIEDLINGSTEIN, P., LIU, C., TAN, K., YU, Y., ZHANG, T., & FANG, J. (2010): The impacts of climate change on water resources and agriculture in China. *Nature*, 467, 7311, 43–51.

PIAO, S. & FANG, J. (2002): Terrestrial net primary production and its spatio-temporal patterns in Qinghai-Xizang Plateau, China during 1982-1999. *Journal of Natural Resources*, 17, 3, 373–380.

PIAO, S., FANG, J., & HE, J. (2006): Variations in vegetation net primary production in the Qinghai-Xizang Plateau, China, from 1982 to 1999. *Climatic Change*, 74, 1-3, 253–267.

PICKUP, G. & CHEWINGS, V.H. (1994): A grazing gradient approach to land degradation assessment in arid areas from remotely-sensed data. *International Journal of Remote Sensing*, 15, 3, 597–617.

QIN, J., YANG, K., LIANG, S., & GUO, X. (2009): The altitudinal dependence of recent rapid warming over the Tibetan Plateau. *Climatic Change*, 97, 1-2, 321–327.

SASAKI, T., OKAYASU, T., SHIRATO, Y., UNDARMAA, J., & TAKEUCHI, K. (2007): Quantifying the resilience of plant communities under different grazing intensities in a degraded shrubland: A case study in Mandalgobi, Mongolia. *Grassland Science*, 53, 3, 192–195.

SCHWIEDER, M., LEITÃO, P.J., SUESS, S., SENF, C., & HOSTERT, P. (2014): Estimating fractional shrub cover using simulated EnMAP data: A comparison of three machine learning regressionătechniques. *Remote Sensing*, 6, 4, 3427–3445.

SHEN, M., ZHANG, G., CONG, N., WANG, S., KONG, W., & PIAO, S. (2014a): Increasing altitudinal gradient of spring vegetation phenology during the last decade on the Qinghai-Tibetan Plateau. *Agricultural and Forest Meteorology*, 189-190, 0, 71–80.

SHEN, Z., FU, G., YU, C., SUN, W., & ZHANG, X. (2014b): Relationship between the growing season maximum enhanced vegetation index and climatic factors on the Tibetan Plateau. *Remote Sensing*, 6, 8, 6765–6789.

SHI, Y., WANG, Y., MA, Y., MA, W., LIANG, C., FLYNN, D.F.B., SCHMID, B., FANG, J., & HE, J.S. (2014): Field-based observations of regional-scale, temporal variation in net primary production in Tibetan alpine grasslands. *Biogeosciences*, 11, 7, 2003–2016.

SMITH, A. & FOGGIN, J. (1999): The plateau pika (*Ochotona curziae*) is a keystone species for biodiversity on the Tibetan Plateau. *Animal Conservation*, 2, 235–240.

SMITH, M.O., USTIN, S.L., ADAMS, J.B., & GILLESPIE, A.R. (1990): Vegetation in deserts: I. A regional measure of abundance from multispectral images. *Remote Sensing of Environment*, 31, 1, 1–26.

SOHN, Y.S. & MCCOY, R.M. (1997): Mapping desert shrub rangeland using spectral unmixing and modeling spectral mixtures with TM data. *Photogrammetric Engineering and Remote Sensing*, 63, 6, 707–716.

SUN, J., CHENG, G.W., LI, W.P., SHA, Y.K., & YANG, Y.C. (2013): On the variation of NDVI with the principal climatic elements in the Tibetan Plateau. *Remote Sensing*, 5, 4, 1894–1911.

TIAN, L., ZHANG, Y., & ZHU, J. (2014): Decreased surface albedo driven by denser vegetation on the Tibetan Plateau. *Environmental Research Letters*, 9, 10, 1–11.

TODD, S.W. & HOFFER, R.M. (1998): Responses of spectral indices to variations in vegetation cover and soil background. *Photogrammetric Engineering and Remote Sensing*, 64, 9, 915–921.

TURNER, A.G. & ANNAMALAI, H. (2012): Climate change and the South Asian summer monsoon. *Nature Climate Change*, 2, 8, 587–595.

USTIN, S.L., GITELSON, A., JACQUEMOUD, S., SCHAEPMAN, M., ASNER, G.P., GAMON, J.A., & ZARCO-TEJADA, P. (2009): Retrieval of foliar information about plant pigment systems from high resolution spectroscopy. *Remote Sensing of Environment*, 113, Supplement 1, S67 – S77.

WAN, Y.F., GAO, Q.Z., LI, Y., QIN, X.B., GANJURJAV, ZHANG, W.N., MA, X., & LIU, S. (2014): Change of snow cover and its impact on alpine vegetation in the source regions of large rivers on the Qinghai-Tibetan Plateau, China. *Arctic, Antarctic, and Alpine Research*, 46, 3, 632–644.

WANGDWEI, M., STEELE, B., & HARRIS, R.B. (2013): Demographic responses of plateau pikas to vegetation cover and land use in the Tibet Autonomous Region, China. *Journal of Mammalogy*, 94, 5, 1077–1086.

WU, G.L., LIU, Z.H., ZHANG, L., CHEN, J.M., & HU, T.M. (2010): Long-term fencing improved soil properties and soil organic carbon storage in an alpine swamp meadow of western China. *Plant and Soil*, 332, 1-2, 331–337.

XU, Z.X., GONG, T.L., & LI, J.Y. (2008): Decadal trend of climate in the Tibetan Plateau - regional temperature and precipitation. *Hydrological Processes*, 22, 16, 3056–3065.

XUE, X., GUO, J., HAN, B., SUN, Q., & LIU, L. (2009): The effect of climate warming and permafrost thaw on desertification in the Qinghai-Tibetan Plateau. *Geomorphology*, 108, 3-4, 182–190.

YANG, C. & EVERITT, J. (2012): Using spectral distance, spectral angle and plant abundance derived from hyperspectral imagery to characterize crop yield variation. *Precision Agriculture*, 13, 1, 62–75.

YOU, Q.Y., XUE, X., PENG, F., XU, M.H., DUAN, H.C., & DONG, S.Y. (2014): Comparison of ecosystem characteristics between degraded and intact alpine meadow in the Qinghai-Tibetan Plateau, China. *Ecological Engineering*, 71, 133–143.

YU, F., LI, S., KILPATRICK, W.C., MCGUIRE, P.M., HE, K., & WEI, W. (2012): Biogeographical study of plateau pikas *Ochotona curzoniae* (Lagomorpha, Ochotonidae). *Zoological Science*, 29, 8, 518–526.

ZHOU, H., ZHAO, X., TANG, Y., GU, S., & ZHOU, L. (2005): Alpine grassland degradation and its control in the source region of the Yangtze and Yellow Rivers, China. *Grassland Science*, 51, 3, 191–203.

ZHU, Z.H., WANG, X.A., LI, Y.N., WANG, G., & GUO, H. (2012): Predicting plant traits and functional types response to grazing in an alpine shrub meadow on the Qinghai-Tibet Plateau. *Science China Earth Sciences*, 55, 5, 837–851.

3 A hyperspectral indicator system for rangeland degradation on the Tibetan Plateau

This chapter is published in *Ecological Indicators*, 39, 54 – 64, 2014.
Submitted: 30 May 2013, accepted 2 December 2013

A hyperspectral indicator system for rangeland degradation on the Tibetan Plateau: A case study towards spaceborne monitoring

Lukas W. Lehnert[(1)], Hanna Meyer[(1)], Nele Meyer[(2)], Christoph Reudenbach[(1)], Jörg Bendix[(1)]

[(1)] Department of Geography, Philipps-University of Marburg, Deutschhausstr. 10, 35037 Marburg, Germany

[(2)] Department of Geography, University of Bonn, Meckenheimer Allee 166, 53115 Bonn, Germany

---

Abstract The Tibetan Plateau suffers from progressive degradation caused by over-grazing due to improper livestock management, global climate change and herbivory from small mammals. Therefore, a robust indicator system for rangeland degradation has to be developed and tested. This paper investigates local patterns of degradation at two sites (Lake Namco and Mt. Kailash) in Xizang province (China) that are covered by vegetation types typical of a large portion of the plateau. The suitability of a two-indicator system is analysed using hyperspectral field measurements, and its transferability to spaceborne data is tested. The indicators are (1) land-cover fractions derived from linear spectral unmixing and

(2) chlorophyll content as a proxy for nutrient and water availability calculated using hyperspectral vegetation indices and partial least squares regression. Because cattle remain near settlements overnight in the local semi-nomadic pastoral system, it can be expected that grazing intensity is highest near the settlement and declines with increasing distance. Therefore, we tested the effect of distance on both indicators using a Spearman correlation analysis. The predicted chlorophyll content and land cover fractions of the indicator system were in good agreement with field observations (correlation coefficients between 0.70 and 0.98). High correlations between distance from settlements and land-cover fractions at both study sites demonstrated that the land-cover fraction is a reliable indicator for degradation. A positive correlation between distance from settlements and photosynthetically active vegetation (PV) revealed over-grazing patterns at the first site. Furthermore, the chlorophyll indicator was proven suitable because chlorophyll concentration declined with increasing distance from settlements. This underlines the over-grazing pattern because cattle excrement was the only external source of nutrients in the ecosystem and it was positively correlated with grazing intensity. However, at the second site, we found a significant positive effect of distance on the amount of photosynthetically non-active vegetation; no effect of distance on PV and chlorophyll content was found. Therefore, no evidence of pasture degradation was detected at the second site. Regarding the potential use of satellite data for degradation monitoring, we found that (1) the land-cover indicator derived from multispectral data was more robust than using noise-filtered hyperspectral information and (2) the chlorophyll amount indicator was estimated from simulated EnMAP data with low error rates. Because the proposed two-indicator system can be derived from multi- and hyperspectral satellite data and combines site conditions and local plant cover, it provides a time-saving and robust method to measure pasture degradation across large areas, assuming that respective satellite

data are available.

Keywords Tibetan Plateau, rangeland degradation, remote sensing, field spectroscopy, linear spectral unmixing, partial least squares regression, EnMAP

3.1 Introduction

Degradation is one of the major global threats for ecosystem functioning and services (BALMFORD et al., 2002; CARDINALE et al., 2012). Ecosystem functioning and ecosystem services in the world's largest high-mountain rangeland ecosystem on the Tibetan Plateau play an important role in regional environments and the livelihood of the local and distant population. The plateau and the hydrological regulation function of the (untouched) ecosystem deliver drinking water and hydropower supply to the world's most densely inhabited areas in South and Southeast Asia (BARNETT et al., 2005; PIAO et al., 2010; ZENG et al., 2013). Because the majority of people on the plateau depend directly on livestock grazing, proper rangeland status is of urgent concern for the local economy and political stability. Suspected causes for rangeland degradation on the Tibetan Plateau are overgrazing, improper livestock management, global climate change, herbivory and soil disturbance from small mammals (HARRIS, 2010).

In the semi-nomadic Tibetan grazing system, livestock typically remain in fenced areas near the settlements or campsites overnight. Therefore, herders bring the livestock to the pastures every morning and return to the settlements in the evening. The consequence is that grazing intensity and effects are highest near the settlements and decline with increasing distance away from the settlements (DORJI et al., 2013). Additionally, the high frequency of cattle near the settlements enlarges the effect of trampling on the soil and the vegetation.

To enlarge forage and stock sizes and to improve livestock management, local governments have facilitated the transition from traditional nomadic pastoralism to sedentary land-use forms (MILLER, 2000). This has additionally led to the conversion of marginal croplands and native meadows into pastures (ZHANG et al., 2012), enlarging the area that is potentially subject to pasture degradation.

Rangeland degradation on the Tibetan Plateau is a progressive process (WESCHE & TREIBER, 2012; ZHAOLI et al., 2005; ZHOU et al., 2005). The degree of rangeland degradation on the Tibetan Plateau remains undetermined because degradation estimations from local grassland bureaus are subjective and not comparable; the surveys are undocumented and the criteria are different among the institutions (HARRIS, 2010). Therefore, there are major uncertainties regarding the progress of rangeland degradation on the Tibetan Plateau. A general assumption is that plant cover decreases as degradation increases. This hypothesis is supported by many field studies in the *Kobresia pygmaea* ecosystem (KAISER et al., 2008; MIEHE et al., 2008), which is the dominant zonal vegetation in the eastern part of the Tibetan Plateau. Furthermore, as grazing pressure and the fraction of bare soil increases, wind and water erosion is accelerated. Simultaneously, plant species richness and the plant composition change (HARRIS, 2010; MIEHE et al., 2011).

Unfortunately, a comprehensive attempt to develop a monitoring system for pasture degradation based on the findings of theses valuable field studies is lacking. This is at least partially due to the immense extent of the plateau, which renders operational monitoring by ground observations nearly impossible. Spaceborne remote sensing data may help to overcome this problem, assuming that a reliable indicator system can be developed.

Plant cover was the most frequently applied indicator for rangeland degradation and status during the last few decades if remote sensing data were used (AKIYAMA & KAWAMURA, 2007; GAO et al., 2010; PICKUP et al., 1994). However, the connection between observed plant cover and degradation status may be distorted by local site variables, e.g., nutrient or water availability, because both directly affect plant growth. To address this issue, adequate proxies for nutrient and water availability must be included in degradation estimation analysis, which cannot be appropriately derived from multispectral data used in previous approaches. Chlorophyll content is the most frequently used suitable indicator for the detection of plant stress due to degradation because it is measurable *in situ* and is closely correlated to foliar chemistry parameters, e.g., nitrogen (CLEVERS & KOOISTRA, 2012; OPPELT & MAUSER, 2004; YODER & PETTIGREW-CROSBY, 1995), phosphorus (LOPEZ-CANTARERO et al., 1994) and plant water content (FILELLA & PEÑUELAS, 1994).

As a consequence, the objective of the present study was to estimate pasture degrada-

tion by developing and applying an indicator system at two sites on the Tibetan Plateau covered by widespread vegetation types (*K. pygmaea* meadows and dry alpine steppe vegetation). With respect to the upcoming hyperspectral EnMAP mission (KAUFMANN et al., 2012) and its monitoring capabilities, the goal of this study was also to investigate the hyperspectral data potential for spaceborne degradation monitoring. Therefore, the following three hypotheses were tested:

1. Vegetation cover, the primary investigated indicator for grazing-induced degradation patterns on the Tibetan Plateau, can be physically determined by linear spectral unmixing using hyperspectral data and simulated multispectral data.
2. Chlorophyll content can be estimated with statistical models from hyperspectral and simulated EnMAP data. Because foliar chlorophyll content is a reliable proxy for plant health, the indicator system is able to distinguish between low plant cover caused by local site conditions and grazing-induced degradation.
3. The proposed two-indicator system captures local grazing-induced degradation patterns along gradients of grazing intensity.

The paper is structured as follows: After the descriptions of data and methods (section 3.3), the potential indicators for pasture degradation are justified by comparing *in situ* observations and multi-/hyperspectral satellite information (section 3.4.1 & 3.4.2). Finally, the suitability of the indicators is tested along degradation gradients (section 3.4.3), followed by a discussion of the results.

3.2 Study area

Two sites in the Autonomous Region of Tibet (China), typical for two of the most important grassland types on the Tibetan Plateau, were investigated. The first site was located near the eastern shore of Lake Namco at 4800 m (30°47’ N, 91°8’ E) (Figure 3.1). The second site was situated approximately 50 km west of Mt. Kailash in the western part of the Tibetan Plateau on an ancient flat river terrace at 4300 m (31°9’ N,80°43’ E). Because the forage amount during winter is the most restrictive factor on livestock sizes (LONG et al., 2008), generally, winter pastures are intensively grazed. Thus, we

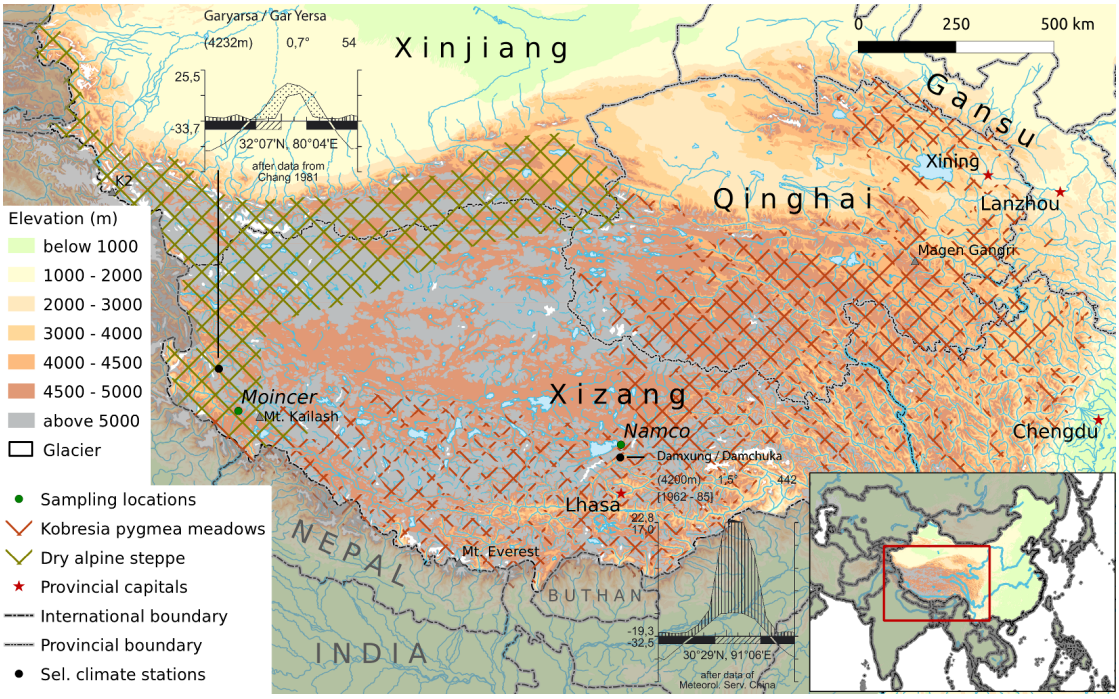

Figure 3.1: Map of sampling locations (green points). Cross-marked parts are areas primarily covered by the vegetation types of both sampling locations. The distribution of vegetation types is from HOU (2001) and MIEHE et al. (2008). Climate diagrams from the closest stations are given for both sampling locations (adapted from MIEHE et al., 2001).

selected sites that were used as winter pastures during recent years. The climate at the Namco site is moderately continental with a mean precipitation of approximately 440 mm and a mean temperature of 1.5 °C. In contrast, the precipitation and mean annual temperature at the Kailash site are considerably lower (approximately 50 mm and 0.7 °C, respectively).

The zonal vegetation type at the Namco site is formed by alpine meadows dominated by *Kobresia pygmaea* (Cyperaceae), a small sedge forming mats similar to golf course lawns. The *K. pygmaea* ecosystem is the most dominant vegetation type on the Tibetan Plateau (MIEHE et al., 2008). Because *K. pygmaea* forms stable turf horizons of multiple decimetre thickness, intact mats are extremely resistant against water and wind erosion (KAISER et al., 2008). Lichens typically cover this turf layer. However, trampling of cattle and ground-dwelling small mammals, e.g., the Plateau Pika (*Ochotona curzoniae*), frequently destroy the turf layer. The vegetation period at Namco ranges from mid-July to mid-September, indicated by dense green grass cover. In late September, frost and

snowfall end the season. Therefore, the aboveground biomass reaches its maximum in late August and early September.

The vegetation at the Kailash site is dominated by two species, the shrub *Caragana versicolor* (Fabaceae) and the tussock-forming grass *Orinus thoroldii* (Poaceae). Livestock typically do not eat *C. versicolor* (CHANDRASEKHAR et al., 2007). Little is known about overgrazing effects on vegetation patterns in the western part of the Tibetan Plateau. In contrast to the thermal limitation of the vegetation period at the Namco site, vegetation at the Kailash site is predominantly limited by aridity. Therefore, the differences in the vegetation during winter and summer are smaller at Kailash than at Namco.

The main nutrient source at both sites is cattle dung because farmers do not use any fertiliser. Therefore, the nutrient amount is correlated with grazing intensities and cattle behaviour. At both sites, cattle are mostly yaks (*Bos grunniens*). It is known from previous studies that yaks mainly ruminate during evening and night (LUMING et al., 2008). This reduces the effect of resting places on nutrient input because cattle remain overnight in small fenced areas near the settlements.

3.3 Materials and methods

This section is divided into a description of field measurements and data analysis. A schematic overview of the methodology, including fieldwork and derivation/testing of indicators for pasture degradation, is presented in Figure 3.2. The development of the first indicator (cover fraction) using linear spectral unmixing is described in section 3.3.2.1; the derivation of the second indicator (chlorophyll content) using hyperspectral indices and PLSR follows in section 3.3.2.2. Finally, the suitability of the indicators is tested in section 3.3.2.3 using Spearman correlation analysis.

3.3.1 Field measurements

We used a transect design to analyse local degradation-related vegetation patterns. Seven transects (three at the Kailash and four at the Namco site) were investigated during the vegetation period in 2012 (August to September). Because both studied sites were grazed during winter, the effects of grazing on vegetation are negligible during the vegetation period, suggesting that vegetation provides a representative status for

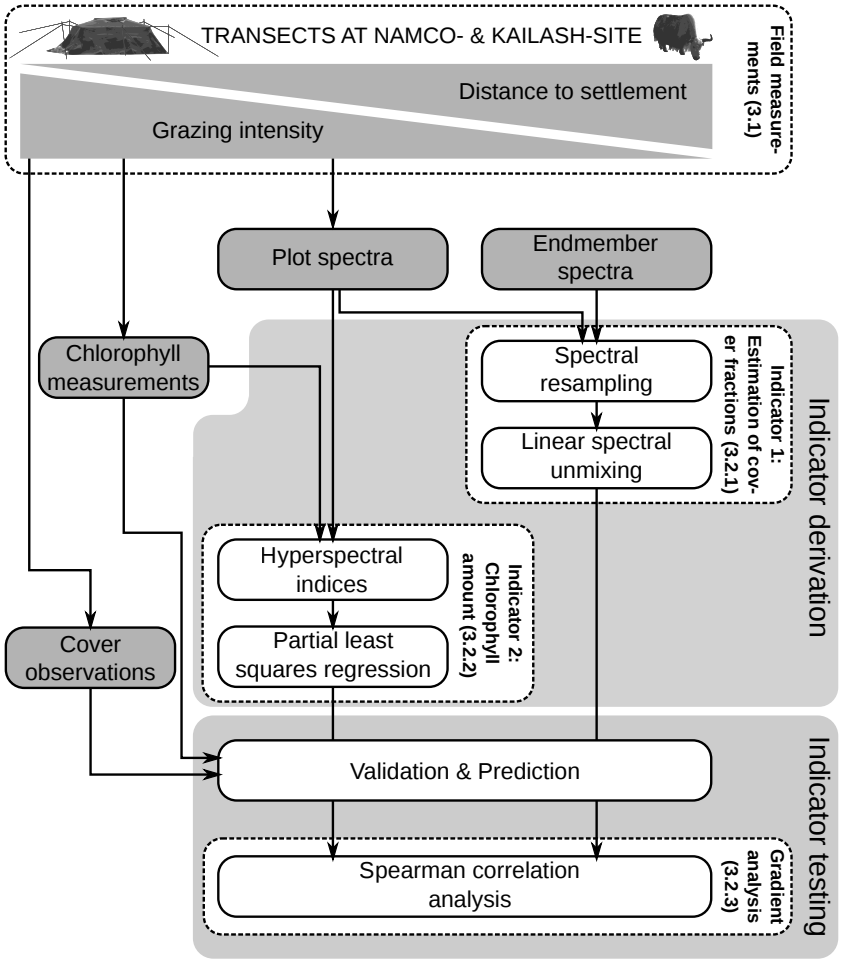

Figure 3.2: Flow chart of the performed data analysis. The division of the methodology into derivation and testing of indicators is symbolised by light grey filled parts. Grey filled boxes symbolise data from field measurements/observations. Numbers in brackets refer to the corresponding section in text.

the vegetation period at field measuring time. Transects started at villages and were drawn with variable lengths depending on the distance to neighbouring settlements and on usage rights of the village under investigation. The direction was chosen such that the aspect and inclination of the slopes remained stable throughout the transects and the dominant vegetation type did not change within the transects. Along each transect, measuring plots were systematically chosen. The distance between measuring plots was 15 m throughout the first third of the transect length near the settlement. Measuring plots within the second and third part of the transects were 30 m and 60 m apart, respectively.

We increased the distance between sampling plots to account for the non-linearity of cattle density with increasing distance from the settlements (STERNBERG, 2012). Hyperspectral measurements were conducted at all plots. On each third plot, the cover fractions were estimated and chlorophyll content was measured.

For *in situ* hyperspectral measurements, a HandySpec® Field spectrometer was used. This device simultaneously measures incoming (downwards) and reflected (upwards) radiation in 1 nm steps from 305 nm to 1705 nm. Reflectance values are automatically derived using a white standard reference spectrum. At each plot, 10 spectra were taken and averaged (plot spectra). To reduce noise in the hyperspectral data, a Savitzky-Golay filter was applied to all spectra after acquisition (filter length = 15). Because a constant device height of 40 cm above ground was chosen for each measurement, the spectrum footprints were circles with a diameter of 40 cm. To avoid errors caused by shadowing of the target, the measuring device was held in the direction of the sun from the user's view. The measuring direction was always directly vertical. All spectra were taken between 10 am and 3 pm local time to reduce the effects of differing sun zenith angles on the reflectance values. SANDMEIER et al. (1998) investigated BRDF effects of grass vegetation and found anisotropic factors of approximately 1 for a similar measurement setup. Because the vegetation height was considerably lower at both field sites than in the study of SANDMEIER et al. (1998), we did not correct spectra for bi-directional effects. Beside measurements at the plots, pure spectra of all land-cover types with high coverage were taken (hereafter called "endmember spectra") with a constant leaf area index of 1 for the vegetation endmembers. A constant leaf area index was chosen to ensure that differences in spectra of different species did not arise from overlapping leaves. This was achieved by measuring arranged leaves cut immediately before measurements. Soil endmember spectra were measured for different soil water contents. Bands between 1350 nm and 1450 nm were removed prior to further analysis because of strong water absorption in this part of the electromagnetic spectrum.

Cover fractions of photosynthetically active vegetation (PV), bare soil, photosynthetically not-active vegetation (NPV), stones, and open turf were independently estimated by four people and subsequently averaged. The geographical location of each plot was recorded using a differential GPS (Topcon HiPer II) in post-processing mode to ensure a high spatial accuracy of the locations.

We measured the chlorophyll content of single species (hereafter called the "target

species") using a Konica Minolta SPAD-502Plus chlorophyll meter. The device returns an index (SPAD-value), which is highly correlated to the foliar chlorophyll content, using the absorption of radiation at 650 nm and 940 nm within leaf samples (COSTE et al., 2010). At each site, we selected one target species for chlorophyll measurements according to the following requirements: (1) leaves had to be large enough to be able to be measured with the device (at least 2 x 3 mm), (2) species had to be present within all degradation stages, (3) species had to be frequent, and (4) must be eaten by the cattle. Because we did not directly compare values of different species, the SPAD-values were not converted to physical units. We selected the pasture species *Carex atrata* (Cyperaceae) at the Namco site and *Orinus thoroldii* (Poaceae) at the Kailash site using these requirements. After performing hyperspectral measurements, 30 independent chlorophyll measurements were conducted and averaged using at least 10 leaves from three individual plants at all plots with at least three plants of the target species within the measurement circle.

3.3.2 Data analysis and indicator development

Data analysis was performed using R (version 2.13.1) with packages "pls" and "hsdar", which was developed to represent the methodology of this article (see the supplementary material for R scripts using hsdar). Our dataset comprised 37 plots for chlorophyll estimation (16 at Namco and 21 at Kailash) and 32 plots for land-cover unmixing at the Namco site and 42 plots at the Kailash site. Hyperspectral measurements were taken at 191 locations at Namco and 111 at Kailash-site. The chlorophyll content was predicted at all plots where the target species was present (103 at Namco and 54 at Kailash).

3.3.2.1 Linear spectral unmixing to develop the land-cover fraction indicator

We performed linear spectral unmixing to derive fractions of land-cover types (endmember) related to degradation. The approach assumes that the spectral signal measured by the sensor is a linear combination of the pure signals of the endmembers and their specific fractions within the pixels (SOHN & MCCOY, 1997). This approach, which originated from the analysis of multispectral satellite data, has been successfully used in hyperspectral data analysis (CHEN & VIERLING, 2006). The variability between 1300 nm and 1800 nm among plant spectra is high because of strong water content-related

absorption within leaves. Because it was expected that the water content significantly differed between plant species and acquisition time, the respective wavelengths may not be represented well by the endmember spectra and were removed for linear spectral unmixing. To test the applicability of the linear spectral unmixing approach on multi-spectral satellite data and to demonstrate its robustness, linear spectral unmixing analysis was performed with hyperspectral data and spectra resampled to EnMAP, Terra MODIS, Landsat-5-TM and WorldView-2 channels. The spectral response function was used to simulate the sensors except EnMAP because the final spectral response function has not yet been determined. Instead, Gaussian fits were used for the spectral resampling to EnMAP channels. EnMAP, Terra MODIS, Landsat-5-TM and WorldView-2 have 242, 17, 4 and 8 bands, respectively, within the spectral range of the spectrometer. To derive cover fractions of degradation-related land-cover types, linear spectral unmixing was applied for all sampling plots using the endmember spectra. The respective predicted fractions were compared to field observations. At the Namco site, the endmembers were bare soil, open turf, stones and PV. At the Kailash site, open turf was replaced by NPV and stones were included in the bare soil class because of the high variability of minerals in stones on the ancient river terrace. At Namco, NPV was completely missing.

3.3.2.2 Partial least squares regression and modelling of chlorophyll indicator

The chlorophyll amount in the vegetation at the plots was estimated using hyperspectral vegetation indices and partial least squares regression. The high potential of hyperspectral indices in the estimation of canopy chemistry has been shown for chlorophyll (LE MAIRE et al., 2008), carotenoid (HERNÁNDEZ-CLEMENTE et al., 2012) and nitrogen content (CLEVERS & KOOISTRA, 2012). Because hyperspectral indices are often highly affected by vegetation cover, plant cover within the footprint of hyperspectral measurements was included in the analysis. Furthermore, we used the target species as additional predictor variables because previous studies outlined the different response of the chlorophyll meter in relation to different plant species (COSTE et al., 2010; UDDLING et al., 2007). The suitability of 82 previously published indices for chlorophyll estimation was separately assessed for both sites using correlation analysis. To test the applicability of our indicator system to be derived from satellite data, the indices were compiled from spectrometer and EnMAP data. A table of the indices is presented in the supplementary material. All

indices with a significant correlation (significance level 0.05) to measured chlorophyll content at both sites were included in the subsequent PLSR analysis. Thus, chlorophyll contents at both sites were predicted using the same set of hyperspectral indices.

The plausibility and robustness of the correlation between hyperspectral indices and chlorophyll content was proven using the canopy reflectance model PROSAIL (JACQUEMOUD et al., 2009) initialised with different chlorophyll values ($C_{a,\,b}$ [μg cm^{-2}]). These values were converted from SPAD-values using the function of COSTE et al. (2010):

$$C_{a,b} = \frac{117.1 \cdot SPAD}{148.84 - SPAD}. \tag{3.1}$$

All other parameters were set to constant values in the centre of the accepted ranges and according to similar previous grassland studies (leaf structure parameter = 1.5, carotenoid content = 8 μg cm^{-2}, brown pigment content = 0, equivalent water thickness = 0.01, dry matter content = 0.009 g cm^{-2}, LAI = 0.7, dry/wet soil factor = 0, and spherical leaf distribution) (DARVISHZADEH et al., 2011, 2008a). The illumination geometry parameters were chosen according to mean field conditions (sun zenith angle = 30.2° and observer zenith angle = 0°).

Partial least squares regression is an approach similar to principle component regression. The predictor and response variable dimensionalities (n x 1 matrix in this study) are reduced to build latent variables. In contrast to principle component regression, the reduction is performed using the information of the response variable(s). For a detailed overview of PLSR, see GELADI & KOWALSKI (1986) and HANSEN & SCHJOERRING (2003). The approach has two advantages compared to normal multivariate regression models. (1) Because the orthogonal components of the predictor variables are used to build latent variables, the predictor variables may be correlated. (2) As a consequence of the dimensionality reduction of the predictor variables, the number of predictors may exceed the number of observations without over-fitting the resulting model. The first point is particularly important in the present analysis because chlorophyll affects various parts of the electromagnetic spectrum, which generally causes a high correlation between different chlorophyll indices: Chlorophyll and other plant pigments absorb radiation from 350 nm to 450 nm and 550 nm to 700 nm. Moreover, it has been shown that chlorophyll content also has an effect on the shape and position of the red edge, although the position of the red-edge may also be affected by other parameters (KIANG et al., 2007).

Using all indices that were significantly correlated to chlorophyll at both sites, the target species and the estimated PV-fraction as predictors, we modelled the chlorophyll content using PLSR. The optimum number of components included in the models was iteratively assessed using calculated root-mean-square errors. The predictive performance of the model was analysed with leave-one-out cross validation.

3.3.2.3 Gradient analysis

To combine both indicators and to test if different stages of local pasture degradation could be identified, we investigated changes in the proposed indicator system with grazing intensity. Therefore, land-cover fractions were derived from all spectra at both sites (111 sites at Kailash and 191 at Namco). Chlorophyll values were estimated for all plots with present target species at both sites using the PLSR-model and the estimated fraction of PV from linear spectral unmixing (54 sites at Kailash and 103 at Namco). The correlation between both indicator systems and distance to closest settlement was investigated with Spearman rank correlation analysis.

3.4 Results

3.4.1 Estimation of the land-cover fraction indicator

The first analysis focuses on the ability to calculate land-cover fractions with hyper- and multispectral remotely sensed data as indicators for rangeland degradation at both field sites. The normalised root-mean-square errors of linear spectral unmixing ranged between 6.95% and 21.79%, depending on the land-cover class and spectral resolution (Table 3.1). Irrespective of the sensor, high error values were observed for bare soil at Namco and PV at Kailash. Stones at Namco and bare soil at Kailash had low error values. In general, the observed error was higher if noise-corrected hyperspectral data were used compared to data resampled to multispectral satellite sensors. The best performing satellite was WorldView 2 at both sites (average Rcv = 0.92). The differences in observed and derived land-cover fraction accuracies within endmember classes were highest for PV at both sites and lowest for open turf and NPV at Namco and Kailash, respectively.

The endmember spectra resampled to WorldView 2 bands and the unmixed end-

Table 3.1: Correlation coefficients and p-values for the hyperspectral indices used as predictors for the chlorophyll content in partial least squares regression. r is the Pearson correlation coefficient of the correlation between the index values and measured chlorophyll values. For definitions and references of the indices, see the table in the supplementary material.

Index	Spectrometer data				EnMAP simulated data			
	Namco		Kailash		Namco		Kailash	
	r	p-value	r	p-value	r	p-value	r	p-value
D1	0.69	0.003	0.65	0.002	0.73	0.001	0.68	< 0.001
D2	-0.62	0.010	-0.62	0.003	-0.72	0.002	-0.64	0.002
Datt1	0.57	0.022	0.72	< 0.001	0.57	0.022	0.72	< 0.001
Datt4	0.90	< 0.001	0.47	0.034	0.90	< 0.001	0.47	0.035
Maccioni	0.67	0.005	0.66	0.002	0.67	0.005	0.66	0.001
MCARI/OSAVI	-0.96	< 0.001	-0.87	< 0.001	-0.96	< 0.001	-0.86	< 0.001
MTCI	0.60	0.014	0.61	0.004	0.60	0.013	0.61	0.004
REP_LE	0.68	0.004	0.59	0.006	0.71	0.002	0.63	0.003
TCARI2/OSAVI2	-0.70	0.003	-0.48	0.033	-0.70	0.003	-0.48	0.033
TCARI/OSAVI	-0.91	< 0.001	-0.87	< 0.001	-0.91	< 0.001	-0.87	< 0.001
TGI	-0.87	< 0.001	-0.54	0.013	-0.87	< 0.001	-0.54	0.013
Vogelmann3					0.53	0.037	0.63	0.003

member fractions are presented in Figure 3.3. Spectrally, all endmembers were clearly distinguishable because curves either intersected or reflectance values in all bands differed substantially (Figure 3.3 top). Plant endmember spectra showed the expected sharp increase at red edge wavelengths for both study sites. The shape of the open turf endmember curve was similar to lichen spectra (KIANG et al., 2007). In general, the reflectance of bare soil was higher at Kailash than at Namco, which is caused by the bedrock and pedogenesis status. The lowest spectral differences were observed between open turf and stones at Namco. Generally, the endmember fractions unmixed from the optical signals (satellite and spectrometer) followed our field observations. The best coincidence was found for the stone fraction at the Namco site and the bare soil fraction at the Kailash site. Overestimations of the linear spectral unmixing routine were observed for the open turf fraction at Namco and the NPV fraction at Kailash. At the Kailash site, our model tended to overestimate high fractions of bare soil; low fractions were underestimated. Unmixed PV fractions at Namco were slightly underestimated; the PV

linear regression line nearly fit the 1:1 line at the Kailash site.

3.4.2 Chlorophyll content indicator estimation

Chlorophyll concentration was considered in our analysis to include an indicator for plant health, which allows us to distinguish between effects of grazing and varying site conditions. At Namco, the mean measured chlorophyll content was higher and the variation was lower than at the Kailash site (52.56% $\pm$ 6.92 at Namco and 50.60% $\pm$ 9.00 at Kailash). The correlations between hyperspectral indices and chlorophyll content for single sites revealed that chlorophyll values derived from spectrometer and EnMAP data had a significant effect on the same 33 vegetation indices for Namco and 13 for Kailash samples (not shown). From these indices, 12 indices derived from simulated EnMAP data were significantly correlated with chlorophyll values at both sites (Table 3.2). If indices were calculated from spectrometer data, the same set, except "Vogelmann3", was significant at both sites. These indices were partly derived from reflectance values, first derivation reflectance values and the red edge position. Reflectance-based indices with close correlations to the chlorophyll content used reflectance values of approximately 680 nm, 710 nm, 750 nm and the range from 780 nm to 850 nm. If derivations were used for indices, the significantly correlated parts of the spectra were in the red-edge part of the electromagnetic spectrum (between 705 nm and 730 nm). The best performing index was MCARI/OSAVI at Namco (r = -0.96) and TCARI/OSAVI at Kailash (r = -0.88).

All significant indices calculated from spectrometer and simulated EnMAP data were linearly dependent on *in situ*-measured chlorophyll values (see Figure 3.4 for selected indices). However, the slopes and intercepts differed between the relationships at both sites for all indices. Although some plots had remarkably high or low values for certain indices, these plots were not removed because the pattern was not consistent throughout all correlations. In general, the index values derived from PROSAIL spectra were similar to the *in situ* measurements. Note that a conversion from SPAD-values to physical units was necessary to simulate spectra in PROSAIL, which may be species dependent. The decrease in MCARI/OSAVI and TCARI/OSAVI values with increasing chlorophyll values was higher for the samples at Namco than at Kailash. In general, spectra at Kailash yielded lower MCARI/OSAVI and TCARI/OSAVI values. The position of the red edge (REP_LE) was at a shorter wavelength at Namco than at Kailash.

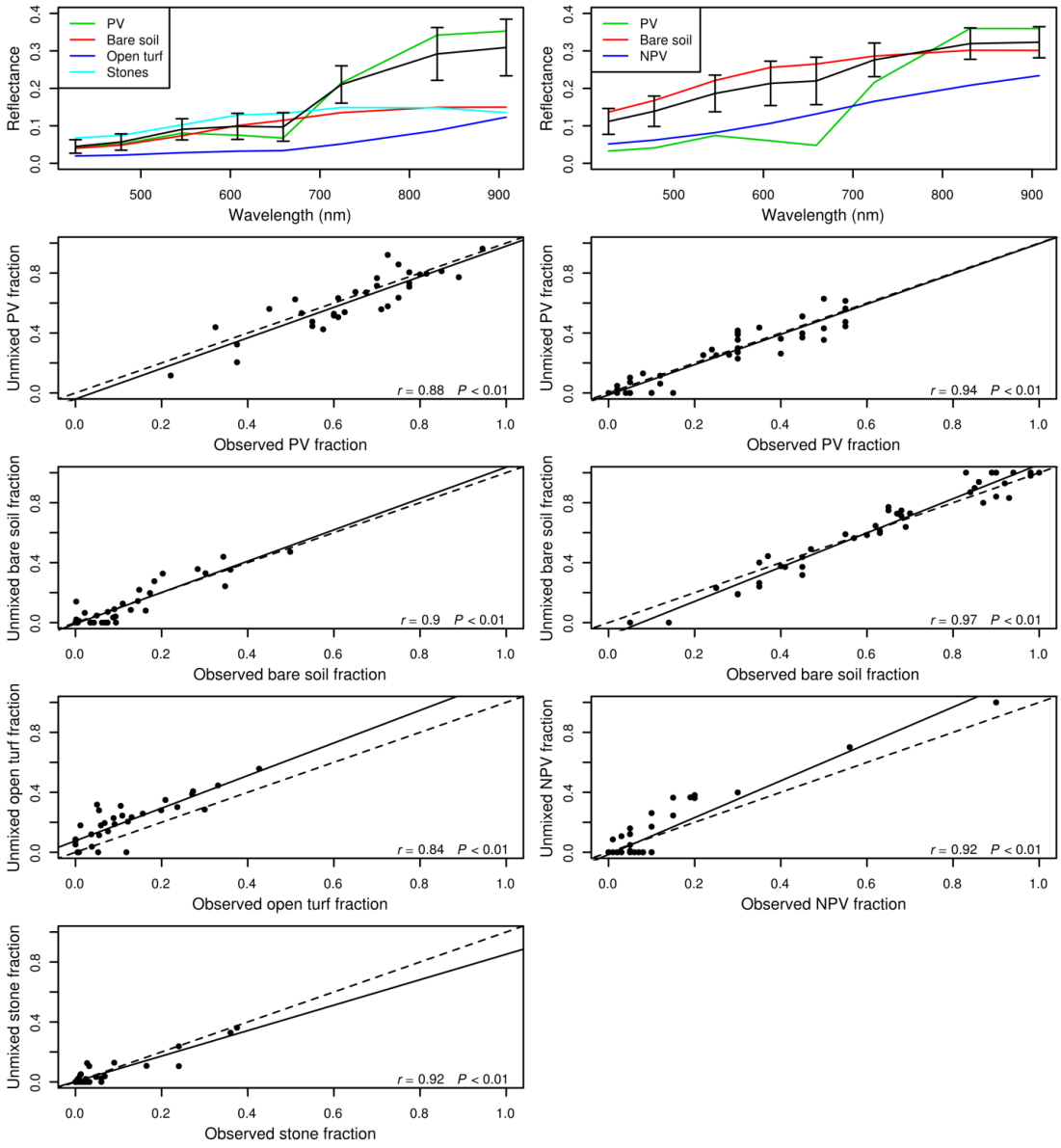

Figure 3.3: Endmember spectra and results of linear spectral unmixing at Namco (left panel) and Kailash (right panel). Plots in the uppermost row show spectra (coloured lines) for all endmembers and the mean (solid black line) and standard deviation (error bars) of the plot spectra. Other plots show derived land-cover fractions compared to observed fractions. Solid lines are regressions and dashed ones are 1:1 lines. r is the Pearson correlation coefficient and P is the p-value of the correlation between unmixed and observed fractions.

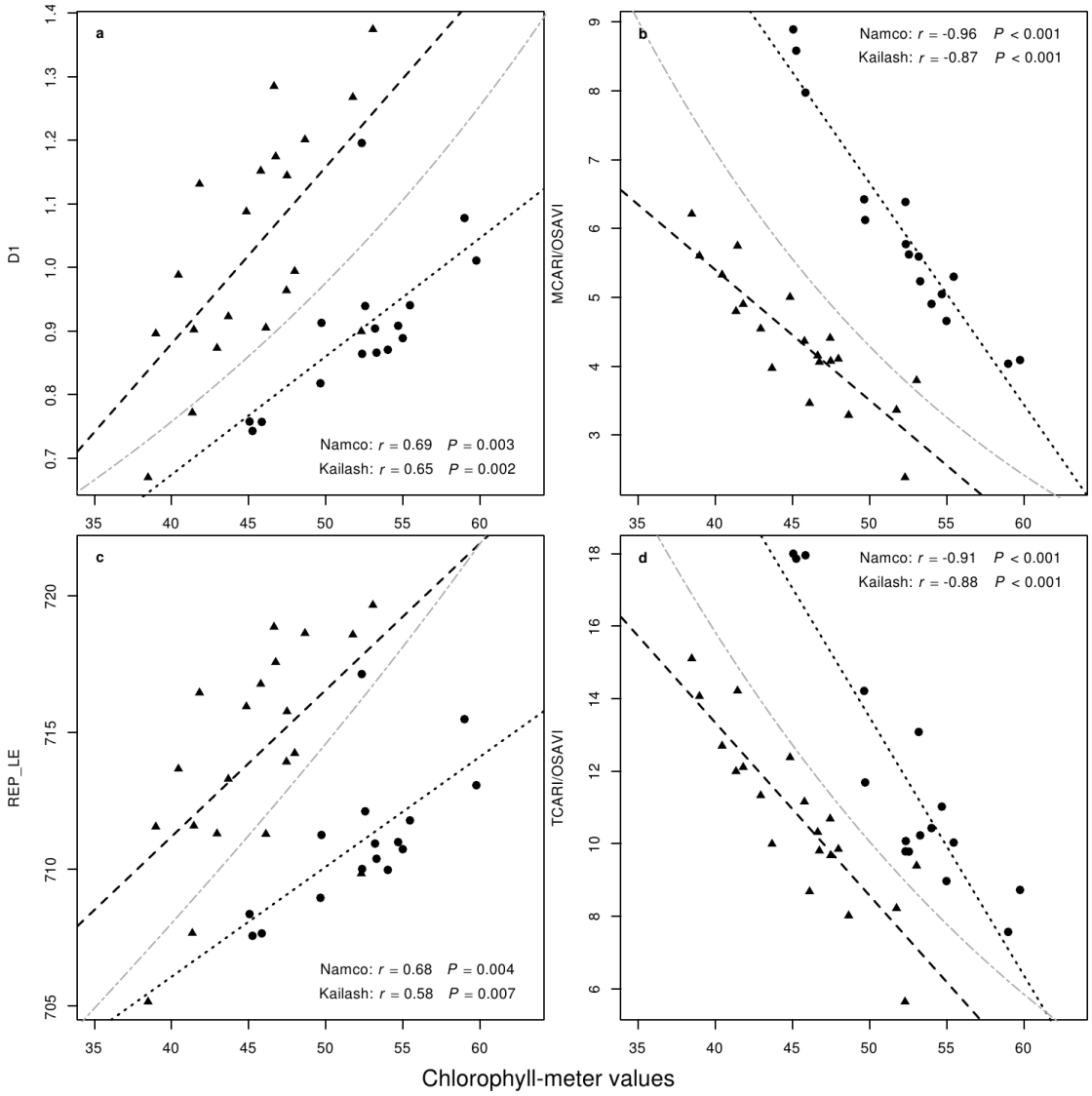

Figure 3.4: Correlations between selected hyperspectral indices (a: D1, b: MCARI/OSAVI, c: REP_LE and d: TCARI/OSAVI) and measured chlorophyll values. For definition and references of the indices, see the table in the supplementary material. Filled circles are Namco and triangles are Kailash samples. Dotted black lines are linear regressions of Namco and dashed lines are for Kailash samples. Grey lines are correlations between PROSAIL-derived indices and chlorophyll concentration. r is the Pearson correlation coefficient and P the p-value of the correlation between index values and measured chlorophyll values. All indices were calculated from spectrometer values.

Table 3.2: Accuracy of land-cover modelling results using linear spectral unmixing. RMSE is the root-mean-square error and nRMSE is the normalised root-mean-square error. Rcv is the coefficient of determination obtained by leave-one-out cross validation.

	Sensor	RMSE	nRMSE	Rcv		Sensor	RMSE	nRMSE	Rcv
Namco					Kailash				
PV	Hyperspectral data	0.180	16.20	0.70	PV	Hyperspectral data	0.104	15.70	0.88
	EnMAP	0.142	15.57	0.76		EnMAP	0.087	13.38	0.90
	MODIS	0.117	13.01	0.82		MODIS	0.079	12.38	0.92
	Landsat5	0.085	10.05	0.91		Landsat5	0.071	11.28	0.94
	WorldView2-8	0.095	11.18	0.88		WorldView2-8	0.071	11.27	0.94
Bare soil	Hyperspectral data	0.074	16.71	0.87	Bare soil	Hyperspectral data	0.080	7.23	0.97
	EnMAP	0.069	14.98	0.91		EnMAP	0.071	6.97	0.98
	MODIS	0.061	12.43	0.93		MODIS	0.073	7.32	0.98
	Landsat5	0.074	15.89	0.87		Landsat5	0.075	7.47	0.97
	WorldView2-8	0.061	12.97	0.90		WorldView2-8	0.074	7.41	0.97
Open turf	Hyperspectral data	0.126	21.79	0.83	NPV	Hyperspectral data	0.091	9.57	0.91
	EnMAP	0.105	18.80	0.87		EnMAP	0.090	9.11	0.92
	MODIS	0.122	20.90	0.85		MODIS	0.092	9.17	0.92
	Landsat5	0.123	21.47	0.84		Landsat5	0.090	9.02	0.91
	WorldView2-8	0.117	20.99	0.84		WorldView2-8	0.090	8.97	0.92
Stones	Hyperspectral data	0.044	9.93	0.92					
	EnMAP	0.054	10.26	0.93					
	MODIS	0.049	10.26	0.91					
	Landsat5	0.049	15.43	0.87					
	WorldView2-8	0.040	11.13	0.92					

RMSE values decreased sharply for an increased number of components in PLSR-models until 8 components if spectrometer data were used (Figure 3.5a). After this RMSE minimum, a further increase in the number of components neither had a positive nor negative effect on the estimation accuracy. If simulated EnMAP data were used to calculate hyperspectral indices, the minimum RMSE was observed using 10 components. The chlorophyll content derived using PLSR was highly correlated with field measurement values (Figure 3.5b) (r = 0.95 for spectrometer data and r = 0.96 for simulated EnMAP data). Irrespective of the use of spectrometer or simulated EnMAP data, low chlorophyll contents mainly belonging to plots at Kailash were slightly overestimated with PLSR. No significant difference in chlorophyll predictive performance of the PLSR model at both sites was observed.

The relationship between measured chlorophyll values and observed fractional plant cover was also assessed to test chlorophyll as a cover-independent indicator. At both

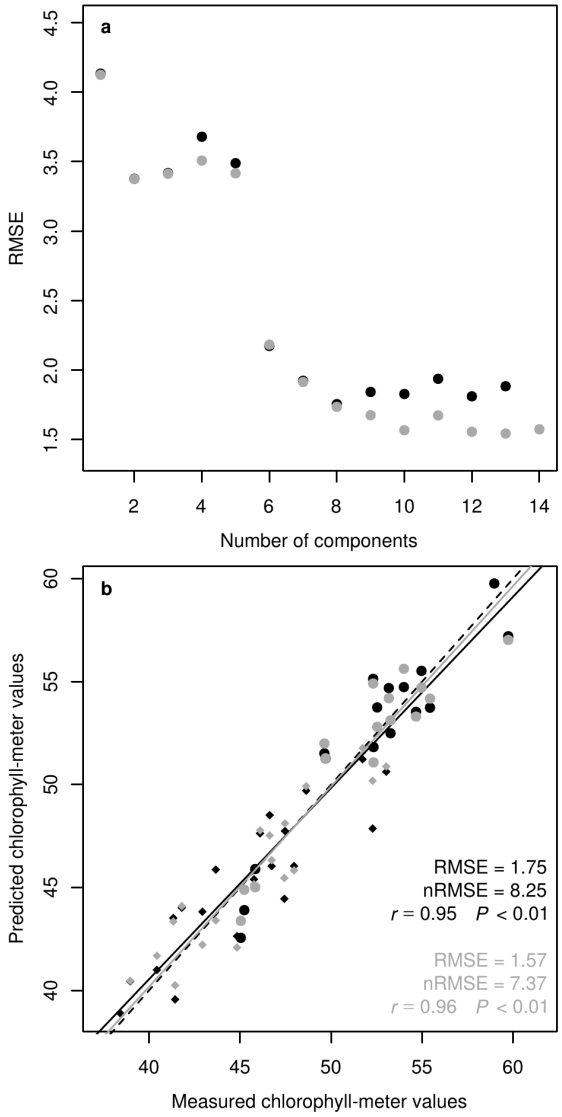

Figure 3.5: The number of components in the PLSR model and resulting RMSE (a). Correlation between predicted and measured chlorophyll values (b). Black points and lines in both plots are results from spectrometer values and grey ones are from EnMAP-simulated spectra. Rectangles in (b) are samples from Kailash and circles are from Namco. The solid line represents the linear regression between predicted and observed chlorophyll values and the dashed line is the 1:1 line. r is the Pearson correlation coefficient and P the p-value of the correlations between predicted and measured chlorophyll values for spectrometer (black font) and EnMAP (grey font) data.

Table 3.3: Summary of Spearman correlation analysis between estimated indicator values and distance to settlements. The number of sites at which the indicators where estimated is represented by n. Bold font indicates significant correlations and italic bold font indicates significant positive correlations.

Site	Indicator	n	ρ	p-value
Namco	PV	***191***	***0.29***	***< 0.001***
	Bare soil	**191**	**-0.17**	**0.017**
	Open turf	191	-0.09	0.197
	Stones	**191**	**-0.26**	**< 0.001**
	Chlorophyll	**103**	**-0.37**	**< 0.001**
Kailash	PV	111	0.16	0.143
	Bare soil	**111**	**-0.27**	**0.013**
	NPV	***111***	***0.24***	***0.029***
	Chlorophyll	54	0.06	0.65

sites, measured chlorophyll values and plant cover were not correlated (Namco: t = -0.10, p = 0.92; Kailash: t = 0.34, p = 0.74).

3.4.3 Indicator testing - Spatial patterns of land-cover fractions and chlorophyll content

While it could be shown that the proposed indicator system comprised of (1) land cover fractions and (2) chlorophyll content could be derived with models based on hyper- and multispectral measurements (spectrometer and satellite), the system must be analysed by means of field surveys if these indicators reflect pasture degradation. This analysis was performed using the spatial gradient approach. At the Namco, highly significant relationships were found between the distance from settlements and PV, stone cover and chlorophyll values (Table 3.3). These correlations were positive for PV and negative for stone cover and chlorophyll values. Bare soil cover was negatively correlated with distance. However, this relationship was only slightly significant. Distances to settlements did not have a significant positive or negative effect on the fraction of open turf.

Slightly significant positive correlations were found between the distance from settlements and NPV fractions at Kailash. In contrast, bare soil cover was negatively correlated

with distance. We did not find any significant effect of the distance on chlorophyll values and PV at Kailash.

3.5 Discussion and Conclusion

Our case study provides the first hyperspectral estimation of degradation-related parameters for two of the most important vegetation types on the Tibetan Plateau. The indicators are related to degradation processes specific for the vegetation at both test sites. Although the results of our two-indicator approach were promising, its assignability to other relevant pasture ecosystems on the Tibetan Plateau must be tested in the future at further sites. The respective ecosystems are particularly summer pastures and wetlands. The small sampling size of the current case study was a direct consequence of the remoteness and difficult access to the region, which underlines the urgent need for a reliable satellite-based monitoring system of pasture degradation on the Tibetan Plateau.

Regarding the first indicator, our unmixing approach to determine vegetation coverage proved to be robust if multispectral data were used instead of hyperspectral data. Thus, widely used satellite sensors were able to characterise land-cover indicators for grassland degradation in our area of investigation. In contrast, using full hyperspectral information (spectrometer and simulated EnMAP data) caused higher error rates in vegetation cover estimates. This finding corroborates the study of Okin et al. (2001), who stated that hyperspectral linear unmixing is not able to estimate plant cover fractions for arid environments with low plant cover. Because the spectral resolution and the spectral configuration of multispectral satellite channels did not largely affect the accuracy of the estimated land-cover factions, plant cover as an indicator for rangeland degradation could be measured with all common satellite systems.

Regarding the second indicator, our statistical approach was able to estimate chlorophyll content with low error rates using spectrometer and simulated hyperspectral EnMAP data and PLSR. Because the hyperspectral index values derived from PROSAIL simulations were similar to the plot-derived values, our method to estimate the chlorophyll content was robust. The final set of estimators comprised indices derived from the green, red and near infrared portions of the spectra, the first derivation, and the shape of the red-edge. We applied four methods to define the wavelength of the red-edge shoulder and tested their effect on chlorophyll values. Only the linear extrapolation method was

significantly correlated to chlorophyll values at both sites. This underlines the high potential of this method for chlorophyll estimation outlined by several previous studies (CHO et al., 2008; CHO & SKIDMORE, 2006; KNOX et al., 2012; MAIN et al., 2011). The high accuracy of the PLSR model in predicting chlorophyll content is in agreement with results of several previous studies comparing different statistical methods for estimating canopy chemistry parameters (DARVISHZADEH et al., 2008b; RAMOELO et al., 2012).

The suitability of the proposed two-indicator monitoring system is underlined by the significant changes among land-cover fractions with increasing distance from settlements at both sites, which may indicate different degradation stages or changes in nutrient availability. At the site in the *Kobresia* ecosystem, the changes were stronger than in the dry alpine steppes. At the first site, a distinct pattern from non-degraded to degraded pasture stages was found. (1) The dense vegetation and turf cover is destroyed which causes higher fractions of bare soil. (2) Once the protective vegetation and turf cover is open, enhanced water and wind erosion leads to an increase in stone cover within non-vegetated parts. It is reported that non-degraded *K. pygmaea* pastures have a total plant cover of > 80% (ZHOU et al., 2005). Applying this threshold for our Namco samplings would indicate that 62% of our plots are degraded to some extent. In the dry alpine steppe, the changes with distance were different. In general, the fraction of NPV increased with increasing distance from settlements. In light of grazing intensities, the reason for this finding may be that livestock rates are low and cattle do not consume all available fodder leading to the observed high proportions of dead leaves partly originating from different vegetation periods. Thus, grazing is not the main driver of vegetation composition at Kailash.

The plant cover changes at the *Kobresia* site may also arise from gradients in nutrient or water availability. In this case, the lower vegetation cover would be caused by reduced productivity and not by high grazing intensities. However, we found a significant negative correlation between chlorophyll content and distance, revealing that chlorophyll is highest at the plots closest to the settlements. In general, chlorophyll content is considered a reliable indicator of nutrient amount and water availability because it is correlated with nitrogen (YODER & PETTIGREW-CROSBY, 1995), phosphorus (KNOX et al., 2012; LOPEZ-CANTARERO et al., 1994) and plant water content (FILELLA & PEÑUELAS, 1994). Thus, we conclude that the changes in land-cover fractions at Namco are correlated to grazing intensities rather than hydrological or pedological factors. At

Kailash, we found evidence of grazing-induced environmental changes. However, these changes were not indicators of over-grazing or degradation.

The proposed two-indicator system provides a reliable method to measure pasture degradation within two of the most widespread vegetation types on the Tibetan Plateau. Because the indicator system can be derived using multi- and hyperspectral satellite data, the approach provides a method to estimate the degradation status across large and remote areas of the Tibetan Plateau if covered by one of the two investigated vegetation types. It is known from previous studies that spectral properties differ substantially among vegetation types on the Tibetan Plateau (SHEN et al., 2008). Thus, the adaption of our indicator system to currently not investigated vegetation types would require additional sampling of reflectance properties and chlorophyll contents. Because the indicator system is sensitive to vegetation cover and varying site conditions, it discriminates grazing-degraded sites from areas where plant growth is negatively affected by site variables, e.g., nutrients or water availability. Therefore, the indicator system provides a solution to the common issue in remote sensing-based degradation studies that an observed low plant cover may be the result of high grazing pressure or the consequence of local site conditions negatively affecting plant growth.

Acknowledgements

We thank Yun Wang from the Senckenberg Museum in Görlitz for the determination of species names and two anonymous reviewers for their constructive comments improving a previous version of the article. The current study was conducted within the framework of the PaDeMoS-Project (“Pasture Degradation Monitoring System”) and was funded by German Federal Ministry of Education and Research (03G0808C).

References

AKIYAMA, T. & KAWAMURA, K. (2007): Grassland degradation in China: Methods of monitoring, management and restoration. *Grassland Science*, 53, 1, 1–17.

BALMFORD, A., BRUNER, A., COOPER, P., COSTANZA, R., FARBER, S., GREEN, R.E., JENKINS, M., JEFFERISS, P., JESSAMY, V., MADDEN, J., MUNRO, K., MY-

ERS, N., NAEEM, S., PAAVOLA, J., RAYMENT, M., ROSENDO, S., ROUGHGARDEN, J., TRUMPER, K., & TURNER, R.K. (2002): Economic reasons for conserving wild nature. *Science*, 297, 5583, 950–953.

BARNETT, T.P., ADAM, J.C., & LETTENMAIER, D.P. (2005): Potential impacts of a warming climate on water availability in snow-dominated regions. *Nature*, 438, 7066, 303–309.

CARDINALE, B.J., DUFFY, J.E., GONZALEZ, A., HOOPER, D.U., PERRINGS, C., VENAIL, P., NARWANI, A., MACE, G.M., TILMAN, D., WARDLE, D.A., KINZIG, A.P., DAILY, G.C., LOREAU, M., GRACE, J.B., LARIGAUDERIE, A., SRIVASTAVA, D.S., & NAEEM, S. (2012): Biodiversity loss and its impact on humanity. *Nature*, 486, 7401, 59–67.

CHANDRASEKHAR, K., RAO, K., MAIKHURI, R., & SAXENA, K. (2007): Ecological implications of traditional livestock husbandry and associated land use practices: A case study from the trans-Himalaya, India. *Journal of Arid Environments*, 69, 2, 299 – 314.

CHEN, X. & VIERLING, L. (2006): Spectral mixture analyses of hyperspectral data acquired using a tethered balloon. *Remote Sensing of Environment*, 103, 3, 338–350.

CHO, M.A., SKIDMORE, A.K., & ATZBERGER, C. (2008): Towards red-edge positions less sensitive to canopy biophysical parameters for leaf chlorophyll estimation using properties optique spectrales des feuilles (PROSPECT) and scattering by arbitrarily inclined leaves (SAILH) simulated data. *International Journal of Remote Sensing*, 29, 8, 2241–2255.

CHO, M.A. & SKIDMORE, A.K. (2006): A new technique for extracting the red edge position from hyperspectral data: The linear extrapolation method. *Remote Sensing of Environment*, 101, 2, 181–193.

CLEVERS, J.G.P.W. & KOOISTRA, L. (2012): Using hyperspectral remote sensing data for retrieving canopy chlorophyll and nitrogen content. *Ieee Journal of Selected Topics In Applied Earth Observations and Remote Sensing*, 5, 2, 574–583.

COSTE, S., BARALOTO, C., LEROY, C., MARCON, E., RENAUD, A., RICHARDSON, A.D., ROGGY, J.C., SCHIMANN, H., UDDLING, J., & HERAULT, B. (2010): Assessing foliar chlorophyll contents with the SPAD-502 chlorophyll meter: A calibration test with thirteen tree species of tropical rainforest in French Guiana. *Annals of Forest Science*, 67, 6, 607.

DARVISHZADEH, R., ATZBERGER, C., SKIDMORE, A., & SCHLERF, M. (2011): Mapping grassland leaf area index with airborne hyperspectral imagery: A comparison study of statistical approaches and inversion of radiative transfer models. *Isprs Journal of Photogrammetry and Remote Sensing*, 66, 6, 894–906.

DARVISHZADEH, R., SKIDMORE, A., SCHLERF, M., & ATZBERGER, C. (2008a): Inversion of a radiative transfer model for estimating vegetation LAI and chlorophyll in a heterogeneous grassland. *Remote Sensing of Environment*, 112, 5, 2592–2604.

DARVISHZADEH, R., SKIDMORE, A., SCHLERF, M., ATZBERGER, C., CORSI, F., & CHO, M. (2008b): LAI and chlorophyll estimation for a heterogeneous grassland using hyperspectral measurements. *Isprs Journal of Photogrammetry and Remote Sensing*, 63, 4, 409–426.

DORJI, T., TOTLAND, Ø., & MOE, S.R. (2013): Are droppings, distance from pastoralist camps, and pika burrows good proxies for local grazing pressure? *Rangeland Ecology and Management*, 66, 1, 26–33.

FILELLA, I. & PEÑUELAS, J. (1994): The red edge position and shape as indicators of plant chlorophyll content, biomass and hydric status. *International Journal of Remote Sensing*, 15, 7, 1459–1470.

GAO, Q.Z., WAN, Y.F., XU, H.M., LI, Y., JIANGCUN, W.Z., & BORJIGIDAI, A. (2010): Alpine grassland degradation index and its response to recent climate variability in northern Tibet, China. *Quaternary International*, 226, 143–150.

GELADI, P. & KOWALSKI, B.R. (1986): Partial least-squares regression: A tutorial. *Analytica Chimica Acta*, 185, 0, 1 – 17.

HANSEN, P. & SCHJOERRING, J. (2003): Reflectance measurement of canopy biomass and nitrogen status in wheat crops using normalized difference vegetation indices and partial least squares regression. *Remote Sensing of Environment*, 86, 4, 542–553.

HARRIS, R.B. (2010): Rangeland degradation on the Qinghai-Tibetan Plateau: A review of the evidence of its magnitude and causes. *Journal of Arid Environments*, 74, 1, 1–12.

HERNÁNDEZ-CLEMENTE, R., NAVARRO-CERRILLO, R.M., & ZARCO-TEJADA, P.J. (2012): Carotenoid content estimation in a heterogeneous conifer forest using narrow-band indices and PROSPECT + DART simulations. *Remote Sensing of Environment*, 127, 0, 298 – 315.

HOU, X.Y. (Ed.) (2001): Vegetation Atlas of China. Science Press, Beijing.

JACQUEMOUD, S.A., VERHOEF, W., BARET, F., BACOUR, C., ZARCO-TEJADA, P.J., ASNER, G.P., FRANCOIS, C., & USTIN, S.L. (2009): PROSPECT + SAIL models: A review of use for vegetation characterization. *Remote Sensing of Environment*, 113, Supplement 1, 0, 56 – 66.

KAISER, K., MIEHE, G., BARTHELMES, A., EHRMANN, O., SCHARF, A., SCHULT, M., SCHLUTZ, F., ADAMCZYK, S., & FRENZEL, B. (2008): Turf-bearing topsoils on the central Tibetan Plateau, China: Pedology, botany, geochronology. *Catena*, 73, 3, 300–311.

KAUFMANN, H., FÖRSTER, S., WULF, H., SEGL, K., GUANTER, L., BOCHOW, M., HEIDEN, U., MÜLLER, A., HELDENS, W., SCHNEIDERHAN, T., LEITÃO, P., VAN DER LINDEN, S., HOSTERT, P., HILL, J., BUDDENBAUM, H., MAUSER, W., HANK, T., KRASEMANN, H., RÖTTGERS, R., OPPELT, N., & HEIM, B. (2012): Science plan of the environmental mapping and analysis program (EnMAP). Technical Report, Deutsches GeoForschungsZentrum GFZ Potsdam.

KIANG, N.Y., SIEFERT, J., GOVINDJEE, & BLANKENSHIP, R.E. (2007): Spectral signatures of photosynthesis. I. Review of earth organisms. *Astrobiology*, 7, 1, 222–251.

KNOX, N.M., SKIDMORE, A.K., PRINS, H.H.T., HEITKONIG, I.M.A., SLOTOW, R., VAN DER WAAL, C., & DE BOER, W.F. (2012): Remote sensing of forage nutrients: Combining ecological and spectral absorption feature data. *ISPRS Journal of Photogrammetry and Remote Sensing*, 72, 27–35.

LE MAIRE, G., FRANŞOIS, C., SOUDANI, K., BERVEILLER, D., PONTAILLER, J.Y., BRÉDA, N., GENET, H., DAVI, H., & DUFRÊNE, E. (2008): Calibration and validation of hyperspectral indices for the estimation of broadleaved forest leaf chlorophyll content, leaf mass per area, leaf area index and leaf canopy biomass. *Remote Sensing of Environment*, 112, 10, 3846–3864.

LONG, R., DING, L., SHANG, Z., & GUO, X. (2008): The yak grazing system on the Qinghai-Tibetan Plateau and its status. *Rangeland Journal*, 30, 2, 241–246.

LOPEZ-CANTARERO, I., LORENTE, F.A., & ROMERO, L. (1994): Are chlorophylls good indicators of nitrogen and phosphorus levels? *Journal of Plant Nutrition*, 17, 6, 979–990.

LUMING, D., RUIJUN, L., ZHANHUAN, S., CHANGTING, W., YUHAI, Y., & SONGHE, X. (2008): Feeding behaviour of yaks on spring, transitional, summer and winter pasture in the alpine region of the Qinghai-Tibetan Plateau. *Applied Animal Behaviour Science*, 111, 3-4, 373 – 390.

MAIN, R., CHO, M.A., MATHIEU, R., O'KENNEDY, M.M., RAMOELO, A., & KOCH, S. (2011): An investigation into robust spectral indices for leaf chlorophyll estimation. *ISPRS Journal of Photogrammetry and Remote Sensing*, 66, 6, 751–761.

MIEHE, G., MIEHE, S., BACH, K., NÖLLING, J., HANSPACH, J., REUDENBACH, C., KAISER, K., WESCHE, K., MOSBRUGGER, V., YANG, Y.P., & MA, Y.M. (2011): Plant communities of central Tibetan pastures in the Alpine Steppe/*Kobresia pygmaea* ecotone. *Journal of Arid Environments*, 75, 8, 711–723.

MIEHE, G., WINIGER, M., BÖHNER, J., & ZHANG, Y. (2001): The climatic diagram map of High Asia. *Erdkunde*, 55, 94–97.

MIEHE, G., MIEHE, S., KAISER, K., JIANQUAN, L., & ZHAO, X. (2008): Status and dynamics of *Kobresia pygmaea* ecosystem on the Tibetan Plateau. *Ambio*, 37, 4, 272–279.

MILLER, D.J. (2000): Tough times for Tibetan nomads in western China: Snowstorms, settling down, fences and the demise of traditional nomadic pastoralism. *Nomadic Peoples*, 4, 1, 83–109.

OKIN, G.S., ROBERTS, D.A., MURRAY, B., & OKIN, W.J. (2001): Practical limits on hyperspectral vegetation discrimination in arid and semiarid environments. *Remote Sensing of Environment*, 77, 2, 212–225.

OPPELT, N. & MAUSER, W. (2004): Hyperspectral monitoring of physiological parameters of wheat during a vegetation period using AVIS data. *International Journal of Remote Sensing*, 25, 1, 145–159.

PIAO, S., CIAIS, P., HUANG, Y., SHEN, Z., PENG, S., LI, J., ZHOU, L., LIU, H., MA, Y., DING, Y., FRIEDLINGSTEIN, P., LIU, C., TAN, K., YU, Y., ZHANG, T., & FANG, J. (2010): The impacts of climate change on water resources and agriculture in China. *Nature*, 467, 7311, 43–51.

PICKUP, G., BASTIN, G.N., & CHEWINGS, V.H. (1994): Remote-sensing-based condition assessment for nonequilibrium rangelands under large-scale commercial grazing. *Ecological Applications*, 4, 3, 497–517.

RAMOELO, A., SKIDMORE, A.K., CHO, M.A., SCHLERF, M., MATHIEU, R., & HEITKONIG, I.M.A. (2012): Regional estimation of savanna grass nitrogen using the red-edge band of the spaceborne rapideye sensor. *International Journal of Applied Earth Observation and Geoinformation*, 19, 151–162.

SANDMEIER, S., MÜLLER, C., HOSGOOD, B., & ANDREOLI, G. (1998): Physical mechanisms in hyperspectral BRDF data of grass and watercress. *Remote Sensing of Environment*, 66, 2, 222–233.

SHEN, M., TANG, Y., KLEIN, J., ZHANG, P., GU, S., SHIMONO, A., & CHEN, J. (2008): Estimation of aboveground biomass using *in situ* hyperspectral measurements

in five major grassland ecosystems on the Tibetan Plateau. *Journal of Plant Ecology*, 1, 4, 247–257.

SOHN, Y.S. & MCCOY, R.M. (1997): Mapping desert shrub rangeland using spectral unmixing and modeling spectral mixtures with TM data. *Photogrammetric Engineering and Remote Sensing*, 63, 6, 707–716.

STERNBERG, T. (2012): Piospheres and pastoralists: Vegetation and degradation in steppe grasslands. *Human Ecology*, 40, 6, 811–820.

UDDLING, J., GELANG-ALFREDSSON, J., PIIKKI, K., & PLEIJEL, H. (2007): Evaluating the relationship between leaf chlorophyll concentration and SPAD-502 chlorophyll meter readings. *Photosynthesis Research*, 91, 37–46.

WESCHE, K. & TREIBER, J. (2012): Abiotic and biotic determinants of steppe productivity and performance - A view from Central Asia. In: J. WERGER & M. VAN STAALDUINEN (Eds.), Eurasian Steppes. Ecological Problems and Livelihoods in a Changing World, Plant and Vegetation. Springer, Dordrecht, pp. 3–43.

YODER, B.J. & PETTIGREW-CROSBY, R.E. (1995): Predicting nitrogen and chlorophyll content and concentrations from reflectance spectra (400-2500 nm) at leaf and canopy scales. *Remote Sensing of Environment*, 53, 3, 199–211.

ZENG, C., ZHANG, F., WANG, Q.J., CHEN, Y.Y., & JOSWIAK, D.R. (2013): Impact of alpine meadow degradation on soil hydraulic properties over the Qinghai-Tibetan Plateau. *Journal of Hydrology*, 478, 148–156.

ZHANG, Z., DUAN, J., WANG, S., LUO, C., CHANG, X., ZHU, X., XU, B., & WANG, W. (2012): Effects of land use and management on ecosystem respiration in alpine meadow on the Tibetan Plateau. *Soil and Tillage Research*, 124, 161–169.

ZHAOLI, Y., NING, W., DORJI, Y., & JIA, R. (2005): A review of rangeland privatisation and its implications in the Tibetan Plateau, China. *Nomadic Peoples*, 9, 1-2, 31–51.

ZHOU, H., ZHAO, X., TANG, Y., GU, S., & ZHOU, L. (2005): Alpine grassland degradation and its control in the source region of the Yangtze and Yellow Rivers, China. *Grassland Science*, 51, 3, 191–203.

4 Retrieval of grassland plant coverage on the Tibetan Plateau based on a multi-scale, multi-sensor and multi-method approach

This chapter is accepted for publication in *Remote Sensing of Environment*.
Submitted: 11 July 2014, accepted: 18 April 2015

Retrieval of grassland plant coverage on the Tibetan Plateau based on a multi-scale, multi-sensor and multi-method approach

Lukas W. Lehnert[(1)], Hanna Meyer[(1)], Yun Wang[(2)], Georg Miehe[(1)], Boris Thies[(1)], Christoph Reudenbach[(1)], Jörg Bendix[(1)]

[(1)] Department of Geography, Philipps-University of Marburg, Deutschhausstr. 10, 35037 Marburg, Germany

[(2)] Senckenberg Museum of Natural History, Am Museum 1, 02826 Görlitz, Germany

---

Abstract Plant coverage is a basic indicator of the biomass production in ecosystems. On the Tibetan Plateau, the biomass of grasslands provides major ecosystem services with regard to the predominant transhumance economy. The pastures, however, are threatened by progressive degradation, resulting in a substantial reduction in plant coverage with currently unknown consequences for the hydrological/climate regulation function of the plateau and the major river systems of SE Asia that depend on it and provide water for the adjacent lowlands. Thus, monitoring of changes in plant coverage is of utmost importance, but no reliable tools have been available to date to monitor the changes on the entire plateau. Due to the wide extent and remoteness of the Tibetan Plateau, remote sensing is the only tool that can recurrently provide area-wide data for monitoring purposes. In this study, we develop and

present a grassland-cover product based on multi-sensor satellite data that is applicable for monitoring at three spatial resolutions (WorldView type at 2-5 m, Landsat type at 30 m, MODIS at 500 m), where the data of the latter resolution cover the entire plateau. Four different retrieval techniques to derive plant coverage from satellite data in boreal summer (JJA) were tested. The underlying statistical models are derived with the help of field observations of the cover at 640 plots and 14 locations, considering the main grassland vegetation types of the Tibetan Plateau. To provide a product for the entire Tibetan Plateau, plant coverage estimates derived by means of the higher-resolution data were upscaled to MODIS composites acquired between 2011 and 2013. An accuracy assessment of the retrieval methods revealed best results for the retrieval using support vector machine regressions (RMSE: 9.97%, 7.13% and 5.51% from the WorldView to the MODIS scale). The retrieved values coincide well with published coverage data on the different grassland vegetation types.

Keywords Tibetan Plateau, plant coverage, degradation monitoring, MODIS, SVM regression, partial least squares regression, linear spectral unmixing, spectral angle mapper, vegetation indices

4.1 Introduction

Plant coverage is a key proxy used to estimate and monitor important ecosystem parameters and functions by remote sensing, particularly for such expanses as the grasslands on the Tibetan Plateau. Important cover-related parameters and functions are primary production (PP; SEAQUIST et al., 2003), evapotranspiration (ET; MU et al., 2007) and leaf area index (LAI; SOUDANI et al., 2006), where PP is commonly used as a proxy of CO_2 fluxes (WYLIE et al., 2003) and ET is used to investigate interactions among vegetation, hydrology and climate (MURRAY et al., 2013). In addition, plant coverage and its changes over time have been directly used as an indicator for grassland degradation in

several studies (e.g., GAO et al., 2010). The Tibetan Plateau hosts the world's largest high-mountain grassland ecosystem, and it significantly influences the hydrology of East and South-East Asia (PIAO et al., 2010). The plateau, with its extended pastures, serves as a globally important "water tower", providing water for nearly 40% of the world's population (BARNETT et al., 2005; XU et al., 2008), and it plays an important role in monsoon generation (DING & CHAN, 2005; MÖLG et al., 2014). Despite their great importance, the pastures of the plateau are threatened by environmental change. To date, there is strong evidence that degradation of the grassland due to climate change and over-grazing may alter the phenology of the vegetation, thus adversely affecting ecosystem stability on the plateau (HARRIS, 2010; ZHANG et al., 2013). Consequently, monitoring the state changes of the Tibetan grasslands under conditions of global environmental change is of utmost importance.

Information about plant coverage of the grasslands on the Tibetan Plateau is important for various stakeholders. On the local scale (covered by WorldView-type satellite data), a plant coverage monitoring product would improve the early detection of over-grazing and would allow adjustment of the carrying capacities of the spacious rangeland ecosystems (CAO et al., 2013). On the regional scale (covered by Landsat-type satellite data), knowledge of changes in plant coverage is essential for county administrators who assign rangeland to the farmers (BANKS et al., 2003). On the plateau scale (MODIS data), detailed knowledge on pasture degradation is particularly interesting for scientists, e.g., to simulate the effect of land-use changes on hydrological and atmospheric processes (CUI & GRAF, 2009).

Because of the enormous spatial extent and remoteness of the Tibetan pastures, it is obvious that remote sensing is the only tool for assessing and monitoring the plateau's plant coverage. To be suitable for the different stakeholders mentioned above, a remotely sensed plant coverage product for the grasslands of the Tibetan Plateau must have a spatial resolution fine enough to cover local terrain effects and to differentiate the pastures belonging to a village. To warrant its suitability for monitoring purposes, the temporal resolution must be high enough to allow comparisons between seasons and to investigate differences among years. Thus, satellite systems offering continuous and consistent data over a long time are a precondition for an operational monitoring product.

Previous attempts at plant coverage monitoring on the Tibetan grasslands using remote sensing have mainly been based on the analysis of normalized difference vegetation

index (NDVI) data, either by inspecting NDVI time-series (ZHANG et al., 2013) or conducting change-detection analysis (GAO et al., 2010). However, the link between plant coverage and NDVI is sometimes ambiguous because the index is highly sensitive to the soil background signal, particularly in arid (and/or degraded) environments with low vegetation cover (HUETE et al., 1997). Thus, to make the plant coverage product suitable for estimation and monitoring purposes regarding, e.g., the provisioning of ecosystem services by pastures, the satellite reflectance values must be transformed into plant coverage. This transformation can be achieved using field-derived transfer functions, which have been established for single sites (e.g., LIU et al., 2014) but not for the entire plateau. Other possibilities to derive plant coverage from remotely sensed images are the application of linear spectral unmixing (LSU, GÖTTLICHER et al., 2009) and spectral angle mapper (SAM; YANG & EVERITT, 2012) techniques. One simple and fast method to translate reflectance values or SAM distances into plant coverage values is linear-regression analysis. This method has been applied in a variety of studies (MEYER et al., 2013; PSOMAS et al., 2011; ZHA et al., 2003). More advanced multivariate methods used to retrieve plant coverage from satellite data encompass partial least squares regressions (PLSR) and machine-learning algorithms such as support vector machines (SVM), which have been evaluated as a valuable tool to cope with non-linear relations and highly correlated predictor variables. Thus, SVM might be advantageous in studies of complex interacting systems. For instance, SCHWIEDER et al. (2014) recently highlighted the high potential of SVM for the determination of fractions of land cover types in satellite images.

However, none of the previous studies have answered the question of which method is most suitable for deriving plant coverage, particularly on the Tibetan Plateau. Consequently, reliable and area-wide information on plant coverage and its changes over time is lacking to date. Therefore, the paper has two objectives:

- Objective one is to compare different methods to derive the summer plant coverage of the grasslands on the Tibetan Plateau. In this context, plant coverage information is derived along a cascade of satellite data with three spatial resolutions. This allows for a direct link between locally observed plant coverage and satellite-derived values. The methods to be compared are (i) LSU, (ii) SAM in combination with linear regression, (iii) PLSR and (iv) SVM regression based on the same

feature space comprised by vegetation indices (VI) and normalized difference indices (NDI).

- Objective two is to apply the method with the highest accuracy to generate a summer (JJA) plant coverage dataset for the grasslands of the Tibetan Plateau for the years with field data at hand (2011 – 2013), based on Moderate Resolution Imaging Spectroradiometer (MODIS) imagery.

First, a short overview of the considered grassland vegetation types on the Tibetan Plateau is given. Then, the upscaling methodology to compare the different estimation methods to derive plant coverage on three spatial scales is described. In the third part, we present and discuss the results, including the finally generated grassland cover data set.

4.2 Grasslands on the Tibetan Plateau

Plant coverage on the Tibetan Plateau is calculated for the most widespread and grazed grassland vegetation types. For further processing, grassland areas were pre-assigned to the five major grassland vegetation types on the Tibetan Plateau as proposed by HOU (2001): (1) *Kobresia pygmaea* pastures, (2) *K. humilis* pastures, (3) swamps and salt marshes, (4) montane and (5) alpine steppes. The distribution of the grassland vegetation types under investigation is shown in Figure 4.1.

Kobresia humilis pastures (Figure 4.2a) are widespread in the north-eastern Tibetan Plateau between 3300 and 3600 m, and they grow under 400-600 mm of mainly summer precipitation. The plant cover normally exceeds 80%, and a typical *Kobresia* pasture is composed of 30 to 40 species. In less-grazed areas, grasses up to 40 cm of height overgrow the widespread Cyperaceae, which reach 10 to 20 cm in height. If pastures are intensively grazed, grazing weeds (*Stellera chamaejasme*, *Ligularia tangutica*, *Iris* spp., *Cryptothladia kokonorica*), which are generally taller than the Cyperaceae, may cover up to 30% of the area. Since the mid-Holocene optimum (8,000 BP), these grasslands have replaced forests of *Picea crassifolia* and *Juniperus przewalskii* due to human impact (MIEHE et al., 2014).

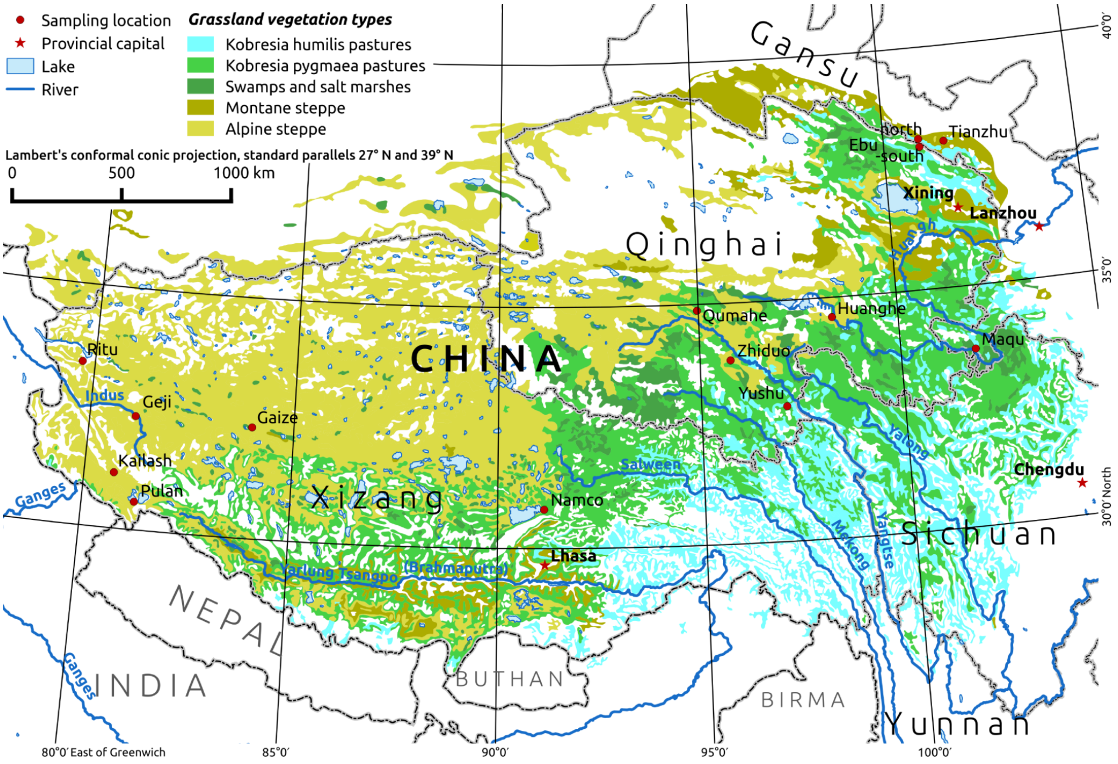

Figure 4.1: Distribution of grassland vegetation types. The extent of *Kobresia pygmaea* pastures is taken from MIEHE et al. (2008b), with other vegetation types taken from HOU (2001). Sampling locations are shown as red points.

Montane steppe is also a secondary grassland vegetation type. It occurs in areas with lower rainfall and terrain altitude. Tussocks of *Stipa splendens* and the poisonous bunch grass *Achnatherum inebrians* grow up to 80 cm tall in a grazing lawn of 2-5 cm consisting of matted *Sibbaldianthe adpressa*, *Potentilla bifurca*, *Heteropappus* spp, and annual *Artemisia* spp. The total cover of the steppe, with its approximately 20 species, ranges between 30 and 60%. The number and cover of matted and rosette grazing weeds is highest in comparison to the other grassland vegetation types considered in this study.

Kobresia pygmaea pastures cover the humid south-eastern quarter of the Tibetan Plateau (450,000 km^2; Figure 4.2b). The altitudinal range of this alpine plant community is globally unique, forming the world's highest alpine vegetation (up to 5960 m) on sunny slopes. In the core area, the tiny sedge *Kobresia pygmaea* (2-4 cm in height, Figure 4.2c) forms a nearly monotypic pasture on a felty turf with up to 98% cover, dominating the plant composition by 90% abundance. The closed grasslands are generally species-poor

(average 10 species). In areas of *Kobresia pygmaea* pastures with higher disturbance and in the ecotone towards the Alpine steppe (Figure 4.2d), the mosaics of *Kobresia pygmaea* turfs are surrounded by a vegetation on open sands and gravels composed of rosette plants and alpine cushions (average 24 species).

Alpine steppes are Central Asian short-grass steppes in the arid northwest of the Tibetan Plateau associated with alpine cushions plants. This grassland vegetation type covers an area of approx. 800,000 km^2. The less diverse *Carex moorcroftii* desert steppe normally consists of 2-8 species. Cushion plants dominate at 50-100 mm of summer precipitation at elevations between 4500 and 5400 m in the remote north of the Tibetan Plateau (Figure 4.2e). The moister eastern region with 100-400 mm of rainfall is characterized by a mean cover of 35% and an average of 25 species. *Carex montis everestii* is common in the south, while *Stipa purpurea* is found throughout the area. The majority of the species are resistant against grazing.

The swamps of the Tibetan Plateau are largely dominated by felty hummocks of *Kobresia schoenoides*, a plant forming tussocks up to 30 cm high (Figure 4.2f). They cover approximately 80,000 km^2 on the Tibetan Plateau. Intact swamps not containing too much salt in the water have a closed vegetation cover.

4.3 Data and Methods

In this paper, plant coverage is derived along a cross-scale set of satellite data with three spatial resolutions (scales) using RGB and hyperspectral field surveys as references. At each scale, four methods (SAM, LSU, PLSR, and SVM) were applied to retrieve plant coverage from the satellite data. First, we briefly outline the field-sampling methods. The second and main part of this section describes the upscaling methodology, the four methods used to derive plant coverage at each scale and the error propagation and validation approaches.

4.3.1 Field methods and data

Field data were taken during the growing seasons in 2011, 2012 and 2013. Overall, the field studies of grassland vegetation at 14 locations covered all major grassland vegetation types of the Tibetan Plateau (Figure 4.1).At all sampling locations, plant coverage was

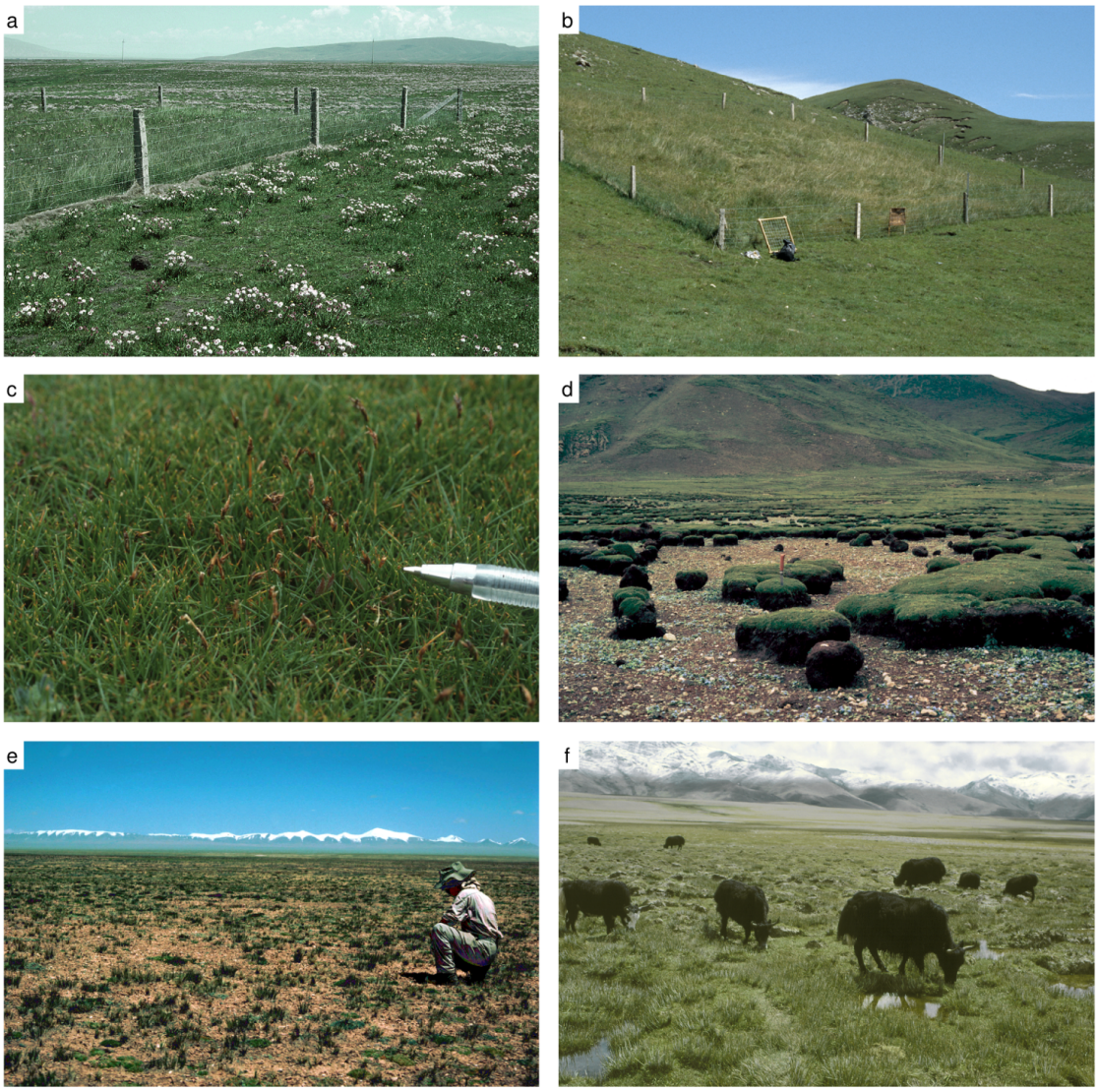

Figure 4.2: Photographs of the investigated grassland vegetation types on the Tibetan Plateau. *Kobresia humilis* pastures are widespread in the montane belt of the north-eastern highlands. Selective free-range, which is the traditional livestock management practice, results in high abundances of grazing weeds such as *Stellera* (white flowers) (**a**). *K. pygmaea* (**b**-**d**) pastures cover a huge altitudinal range between the montane belt, probably replacing former forest (**b**), and build firm felty grazing lawns in the alpine belt (**c**). The disintegration process of those felty root mats (**d**) is poorly understood but is widespread in the ecotone between both major ecosystems. The alpine steppe (**e**) is a Central Asian short grass steppe with cushion plants, which is widely grazing resilient. *Kobresia schoenoides* swamps (**f**) are the most important grazing reserves and are under great grazing pressure. The steppes' vulnerability is the bottleneck of the pastoral system of the entire plateau.

recorded by analyzing digital photographs and visual estimations. Previous field studies on the Tibetan Plateau have demonstrated a positive correlation between plant coverage and distance to settlements (DORJI et al., 2013; LEHNERT et al., 2013, 2014; MEYER et al., 2013). Consequently, we applied a unified transect design for the field surveys to cover the entire range of vegetation-degradation stages at each location. Transects started at villages or camp sites. Transect length was kept variable depending on the distance to neighboring settlements and the land-use rights of the village under investigation. Digital photos/visual plant coverage estimates were taken/conducted along transects with a constant distance. The geographic locations of the sampling sites were recorded by using a GPS-device. The digital photos with a vertical field of view were taken with a common digital camera. The height and the focal length of the camera were always kept constant. To calculate the ground size of each photo, a measuring tape was arranged at the edge of the photos. Additionally, plant coverage estimates were visually conducted by an experienced observer on 10x10-m plots at the starting and ending points of each transect.

The definitions of pure reference spectra (spectral endmember) of the surface types of interest (e.g., pasture species, soil) are generally required to apply LSU and SAM. These reference spectra can be either extracted directly from satellite images or measured *in situ* with a spectrometer or a hyperspectral camera. A common problem when reference spectra are extracted from satellite images is the mixed pixel effect, with increasing pixel resolution preventing the capture of pure spectral endmember information. This is especially problematic in arid areas, where vegetation is usually characterized by very small-scale patches in subpixel resolution. To avoid this problem, we used endmember spectra measured *in situ* at each sampling location using a HandySpec field spectrometer. This instrument provides reflectance values between 305 and 1705 nm with a spectral resolution of 1 nm. Soil spectra were measured with different soil water contents (soil endmember spectra). Vegetation spectra were taken from single plants (species endmember spectra). To this end, leaves were cut and arranged to achieve a leaf area index of one. For noise reduction in the captured data, all spectra were filtered with a Savitzky-Golay filter (filter length = 15 nm). To generate endmember spectra for the grassland vegetation types, all species endmember spectra from each grassland vegetation type were averaged (vegetation endmember).

4.3.2 Calculation of plant coverage from digital images

Using the digital photographs taken from each measuring plot, we derived the plant coverage within the footprint of the digital photo. We calculated an image (e) from the RGB values in which green vegetation was enhanced using the following formula (WOEBBECKE et al., 1995):

$$e = 2g - r - b, \tag{4.1}$$

where g, r, and b are the digital values in the green, red, and blue channels. By applying a manual threshold, we selected green vegetation pixels and calculated the plant coverage of the green vegetation in the images.

4.3.3 Satellite and auxiliary data

We used satellite data with three spatial resolution levels: (i) WorldView-2 (2 m nominal spatial resolution), Quickbird (2 m) and RapidEye (5 m) at the local scale; (ii) Landsat 7 (30 m) and Landsat 8 data (30 m) at the regional scale; and (iii) MODIS BRDF-corrected composites (MCD43A4; SCHAAF et al., 2002; 500 m) at the plateau scale.

Data at the WorldView scale were ordered prior to field surveys to minimize the time lag between field and satellite observations. For the regional-scale analysis, Landsat scenes were downloaded from United States Geological Survey (USGS) website (http://earthexplorer.usgs.gov). All Landsat data used are taken at a time-span of one month around the acquisition time of the corresponding WorldView-scale imagery. For a summary of satellite data used at the WorldView and Landsat scales, see Table 4.2 in the supplementary material. MODIS 16-day composites were downloaded from the Atmosphere Archive and Distribution System (LAADS) FTP server for summer months between 2011 and 2013.

The Aster digital elevation model data (GDEM, TACHIKAWA et al., 2011) were used to generate altitude data for the topographic correction of satellite data. On the MODIS scale, the MODIS MCD43A2 quality product data was used to exclude pixels for further processing contaminated by snow. An important step is the pre-selection of MODIS pixels on the plateau that are covered by grassland vegetation for which MODIS data was principally masked. This step was performed with the help of the digital and co-located map presented in Figure 4.1 (HOU, 2001). Because of the pre-assignment of the pixels

based on only one GIS map, land-use changes potentially appearing over the time span of the MODIS time series might blur the pre-assignment. Thus, MODIS pixels affected by land-cover changes (mostly to croplands and urban/built-up areas) were eliminated from later plant coverage retrieval based on land use information in the annually available MODIS land-cover product (MCD12Q1, FRIEDL et al., 2010), which is used to mask each MODIS composite of the same year. For the calculation of the final plant coverage map, only pixels were included that were classified as grasslands in all years. However, it should be stressed that pixels affected by changes from grassland to the classes "barren or sparsely vegetated" were not removed from further processing because the change may contain important information regarding the usage of the product for pasture degradation monitoring.

4.3.4 Preprocessing of satellite data of the WorldView and Landsat scales

Preprocessing of satellite data of the WorldView and Landsat scales encompassed three steps: (i) geometric, (ii) atmospheric and (iii) topographic correction.

Geometric correction was performed to ensure that spatially corresponding pixels from the two scales overlapped. The WorldView scale was used as the reference where Landsat scale data was co-registered to the WorldView-scale by selecting corresponding ground control points (GCPs) in both images. For each image pair, at least six GCPs were identified. A first-order polynomial was used for transformation.

Atmospheric correction was conducted to ensure the spectral comparability of reflectance values in different satellite scenes of the same sensor. To match satellite-retrieved reflectances, a proper atmospheric correction is required, particularly for the SAM and LSU methods, which rely on reference spectra measured on the ground. To cope with the huge volume of image data in atmospheric correction, a modified and fully automatic version of the 6S radiative transfer code extended for spatial raster applications was developed and applied (for the 6S code, refer to VERMOTE et al., 1997; for the modifications, see CURATOLA FERNÁNDEZ et al., 2015). The atmosphere at the time of image acquisition was approximated by using the pressure, temperature and humidity profiles from NCEP reanalysis data (KALNAY et al., 1996). Ozone and aerosol contents were taken from Aura OMI data DOBBER et al. (2006); LEVELT et al. (2006).

To properly process the state-of-the-art sensor data, WorldView-2, RapidEye, Quickbird, and Landsat-8 sensors with their respective spectral response functions and acquisition geometries were included in the 6S code.

To remove the effects of topography and illumination on reflectance values of the satellite data, the statistical-correction method of TEILLET et al. (1982) was applied to the data at the Landsat scale. Therefore, the digital elevation data model was bilinearly resampled to the resolution of the satellite data.

At the Landsat scale, cloud-free image composites covering the respective field transects were compiled. In the first step, clouds and cloud shadows were classified manually. Then, if only Landsat 7 data were available, the pixels affected by scanner errors were excluded and added to the cloud masks. For further processing, only pixels without errors and clouds were selected. If two or more scenes could provide the same pixel for the composite, the pixels with the greatest proximity of acquisition time between the Landsat and WorldView-scale imagery were used. A statistical radiometric normalization was applied to inter-calibrate the different scenes in each composite (ELVIDGE et al., 1995). For this purpose, the Landsat scale image in closest temporal proximity to the spatially corresponding WorldView scale image was selected as a reference. Pairwise linear regression models were fitted between the reflectance values of the Landsat scale reference image and each other Landsat scale image by only considering pixels not affected by clouds or scanner errors in both images. The derived regression model was afterward applied to all other reflectance values of the images to be normalized.

4.3.5 Upscaling of plant coverage from ground transects to MODIS scale

4.3.5.1 Concept and overview

The general processing scheme for upscaling grassland plant coverage is depicted in Figure 4.3 and encompasses the following steps:

- At the WorldView scale, the plant coverage values were only estimated for pixels that are covered by field observations and the surroundings of those pixels inside the spatially collocated Landsat pixel. To transform pixel reflectance values into plant coverage, several methods (SAM, LSU, PLSR, and SVM) were applied as

described in the following sections in more detail. The plant coverage values derived from the in depth analysis of digital photographs taken during field work at the locations of Worldview scale pixels were used to derive statistical regression models between satellite and *in-situ* values. An exception is the LSU method, where the endmember fractions of vegetation were directly used as plant coverage values. Afterward, the plant coverage values determined at the WorldView scale were spatially aggregated to the Landsat scale (30-m nominal pixel resolution) by averaging all pixel values from the WorldView scale spatially belonging to each respective and co-located Landsat pixel.

- At the Landsat scale, all Landsat pixels were selected that covered at least one sampling site and the surroundings of those pixels inside the spatially collocated MODIS pixel. Their spectral information was then used to train new regression models. As reference data to train the linear (SAM), PLSR and SVM regression models, the co-located and spatially aggregated values previously calculated from the WorldView scale were used. The resulting models were then applied to the entire Landsat dataset to estimate plant coverage values for all Landsat pixels. Afterward, the plant coverage values were spatially aggregated to the MODIS scale by spatially averaging all Landsat-derived plant coverage values belonging to each respective and co-located MODIS pixel.

- At the MODIS scale, the same model training and validation approach described for the Landsat scale was used to estimate plant coverage values for all relevant MODIS pixels. Thus, the spatially aggregated plant coverage estimates from the Landsat scale were used accordingly.

After validation of the entire model cascade (see 3.5.3), the approach with the highest accuracy was selected. Its associated regression model was then applied to all MODIS scenes (see http://pademos.org for data access). Finally, the mean plant coverage of grasslands on the Tibetan Plateau was calculated from the estimation maps using the MODIS land-cover products and the grassland vegetation types from HOU (2001) for the selection of grassland pixels.

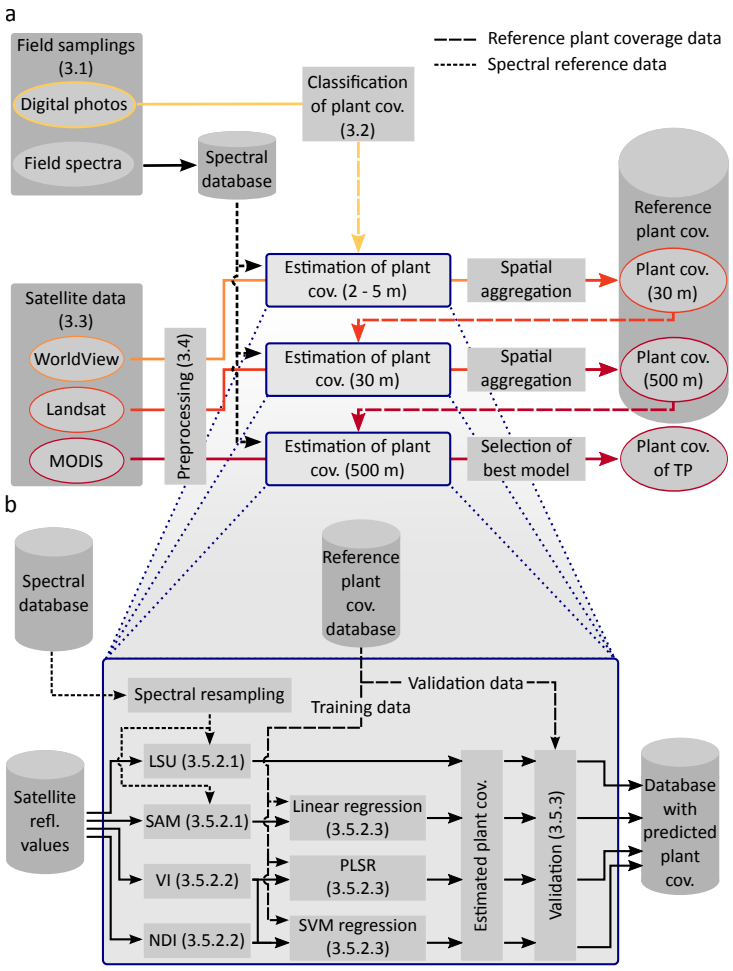

Figure 4.3: Flow chart of the methodology: overall upscaling approach (**a**) and plant coverage estimation performed at each scale (**b**). The blue boxes in (**a**) correspond to the blue box in (**b**). Scales of satellite and *in situ* data are indicated by colors of lines and ellipses in (**a**). Numbers in brackets indicate the relevant section in the text.

4.3.5.2 Methods to derive plant coverage

Because the first aim of the article is to compare different methods to derive plant coverage on the Tibetan Plateau (Figure 4.3), these methods will be outlined below in more detail.

4.3.5.2.1 Linear spectral unmixing and spectral angle mapper. — LSU was applied to directly calculate the percentage of each of land-cover type (endmember) in mixed pixels (LEHNERT et al., 2014; SOHN & MCCOY, 1997). Because we aim to

estimate plant coverage across large scales, it must be noted that our knowledge of the spectral properties of the vegetation and soil over the grasslands of the entire plateau is certainly limited to our transect areas. Thus, we presume that the mean of all dry-soil spectra acquired in the field can be taken as a first guess for a representative average soil endmember for the whole plateau. Regarding vegetation analysis with LSU, we used different green vegetation spectra for each vegetation type (vegetation endmember). All endmember spectra taken in the field were spectrally resampled to the spectral bands of the respective sensor using the band-specific spectral response functions.

SAM is a frequently used measurement of distance between a known reference spectrum, e.g., ground measurement, and the reflectance values taken from satellite images (KRUSE et al., 1993). We used the green vegetation endmember spectra as calculated for LSU as reference data.

4.3.5.2.2 Calculation of vegetation indices and normalized band indices. — To derive plant coverage values from the satellite data without using spectral reference data taken at the ground, we extracted a feature space from the reflectance values encompassing a set of previously defined vegetation indices (enhanced vegetation index, EVI, HUETE et al., 1997; soil-adjusted vegetation index, SAVI, QI et al., 1994; modified SAVI, MSAVI, HUETE, 1988) (Table 4.3 in the supplementary material) and all NDVI-like normalized difference indices for each satellite sensor (NDI; THENKABAIL et al., 2000) as predictors used for PLSR and SVM based plant coverage estimates (next section). The vegetation indices selected were required to be derivable from all sensors in our study.

4.3.5.2.3 Prediction of plant coverage using linear regression, partial least squares regression and support vector machines. — Regression techniques are required to convert the SAM distances and the feature space into plant coverage values. Here, we applied three different approaches: (i) linear regression, (ii) partial least squares regression and (iii) support vector machine regression.

1. In the linear-regression model, the SAM distances were fitted against the reference plant coverage values. We did not take non-linear relationships into account because the initial tests did not indicate any non-linearity between SAM distances and plant coverage.

2. PLSR was applied to estimate plant coverage values using the feature space comprised by the vegetation indices and the NDI values as predictors. To build PLSR models, one free parameter, the number of components used for the regression model, has to be defined. Therefore, the entire range of possible values (from 1 to the number of predictor variables) was tested and the optimum number of components was selected comparing the R^2 values from the cross validation.

3. SVM regression was the second approach to estimate plant coverage values using the same feature space as for PLSR as predictors. One of the important benefits of SVM regression models is the very good balance between estimation accuracy and overfitting (MOUNTRAKIS et al., 2011). We selected SVM regression for two additional reasons: (1) the indices must not be linearly dependent on plant coverage values, and (2) correlated predictors do not have an effect on the performance of the resulting SVM model. In general, there are three parameters that must be well defined to fit SVM models with high predictive performance: the cost value (C), the threshold for residuals that do not contribute to the regression fit (ε) and the Parzen window width (γ) for the radial basis function used as kernel. To define γ, C and ε, we tested exponential ranges of parameter values in a grid search as proposed by SCHWIEDER et al. (2014). SVM regression models to estimate plant coverage were fitted for all possible combinations of the three parameters. The cross-validation of the derived models is described in the following section. The model resulting in the highest R^2 from cross-validation was chosen for further analyses.

4.3.5.3 Error propagation and validation of plant coverage predictions

Each approach in the model cascade at each scale was validated with a test dataset that was not used for model training at the same scale. If the dataset comprised more than 40 samples/pixels, one-third of the samples were used as test data to validate the predictive performance of the resulting model. If the number of samples was below 40, a leave-one-out cross-validation was performed. As error measurement, the root mean-square error, the cross-validation correlation coefficient (r_{cv}) and the R^2-value of the linear relationship between predicted and observed plant coverage values were calculated.

The 30-m-resolution training samples used to fit the regression models at the MODIS scale encompass estimation errors at the Landsat scale model output. To quantify this error, we used Monte-Carlo simulations as proposed by, e.g., GESSNER et al. (2013).

- The pixel estimates of plant coverage from the WorldView scale model were spatially aggregated to the MODIS scale resolution and assigned to the geographically corresponding MODIS pixels. Note that this aggregation was only possible if the MODIS pixel was completely covered by the respective satellite dataset at the WorldView scale.
- Then, the estimates of plant coverage derived from the Landsat scale model were spatially aggregated to MODIS pixels and then subtracted from the estimates of the WorldView scale data spatially aggregated to the MODIS pixels.
- Several distribution density functions (exponential, gamma, log normal, normal, Weibull) were fitted to the frequency distribution of the pixel differences, and the best-fitting ones regarding the PLSR and SVM regressions were selected. The success of the fitting was assessed by Kolmogorov-Smirnov tests and visual interpretation, respectively. In both cases, the normal distribution was selected as the best-fitting distribution density function.
- In Monte-Carlo simulations, the training samples at the MODIS scale were manipulated using random values from the respective error distribution functions. Afterward, the PLSR and SVM regression models were fitted with the manipulated training data and validated against the original data as described above. This step was performed 10,000 times.

4.4 Results

4.4.1 Accuracy of models to estimate plant coverage

Regarding the performances of the four different methods (LSU, SAM, PLSR, and SVM) used to estimate plant coverage on the Tibetan Plateau on three different scales, we found large differences in their estimation accuracies (Table 4.1). Regardless of the scale of the satellite data used for estimation, the highest error rates were observed in plant coverage

Table 4.1: Accuracy of plant coverage estimations for sensors and methods applied in the approach. Underlined values are the method with the highest accuracy comparing RMSE values. Italic font symbolizes the method with the lowest accuracy.

Method	WorldView-scale				Landsat-scale				MODIS-scale			
	Sensor	RMSE	r_{cv}	R^2	Sensor	RMSE	r_{cv}	R^2	Sensor	RMSE	r_{cv}	R^2
SAM	Quickbird	15.88	0.70	0.49	Landsat7	10.26	0.75	0.56	MODIS	8.00	0.77	0.59
	RapidEye	8.15	0.83	0.70	Landsat8	14.80	0.75	0.56				
	WorldView2-8	11.00	0.82	0.67								
LSU	Quickbird	*17.16*	*0.63*	*0.40*	Landsat7	*15.87*	*0.67*	*0.45*	MODIS	*12.65*	*0.94*	*0.88*
	RapidEye	*24.59*	*0.72*	*0.51*	Landsat8	*56.95*	*0.65*	*0.43*				
	WorldView2-8	*29.97*	*0.49*	*0.24*								
PLSR	Quickbird	13.28	0.78	0.60	Landsat7	8.05	0.92	0.84	MODIS	8.20	0.93	0.86
	RapidEye	13.28	0.78	0.60	Landsat8	5.38	0.98	0.95				
	WorldView2-8	6.45	0.90	0.81								
SVM	Quickbird	12.28	0.81	0.66	Landsat7	7.01	0.94	0.88	MODIS	5.59	0.95	0.91
	RapidEye	6.17	0.91	0.83	Landsat8	3.95	0.99	0.98				
	WorldView2-8	7.01	0.93	0.87								

values estimated by LSU, followed by those estimated by SAM. Higher accuracies were observed using NDI and vegetation indices in combination with PLSR. The best results were obtained for SVM regression.

In the approach for plant coverage estimation, six different sensors with three classes of spatial resolutions were used. At the WorldView scale, we found low accuracies in estimations based on Quickbird imagery. If RapidEye or WorldView-2 imageries were available, the error rates were much lower. This ranking was inverted for LSU, where the lowest errors were observed if the Quickbird data were unmixed. By comparing the two Landsat sensors, Landsat 7 revealed higher error rates than Landsat 8, except for LSU and SAM.

Regarding the estimation accuracies at the three scales of the cascade, we found the highest error rates at the local scale. Intermediate accuracies were observed at the Landsat scale, while the best results (RMSE below 6%) were yielded with MODIS at the plateau scale. Figure 4.4 shows the predictions of the validation data at each scale using the SVM regression models. In general, no bias, and thus, no evidence for systematic under- or overestimation, was observed. However, scatter (and thus RMSE) is obviously decreasing toward lower-resolution imagery. Here, it must be stressed that the number of samples is declining with decreasing pixel resolution because several plots of the

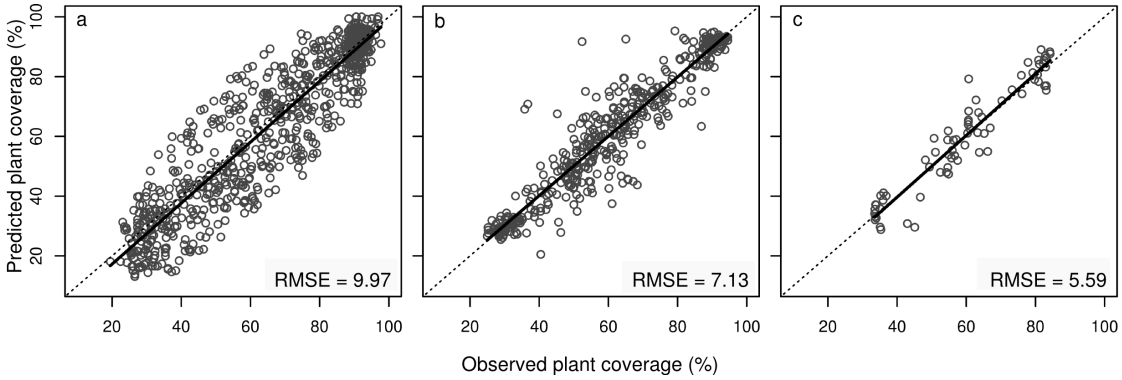

Figure 4.4: Predicted vs. observed plant coverage for all sensors at the WorldView (**a**), Landsat (**b**) and MODIS scales (**c**) using SVM regression. The dotted lines are the 1:1 lines, and solid lines are linear regressions between observed and predicted plant coverage values.

WorldView and Landsat scales are covered by only one co-located pixel in the Landsat- and MODIS-scale imagery, respectively. For PLSR, the pattern was similar to the results obtained from SVM regression (Figure 4.8 in the supplementary material). However, the variation around the 1:1 line was far higher, especially at the WorldView scale. The largest variation was found for LSU estimates at all three scales. For LSU, a considerable overestimation of low plant coverage values was observed at the WorldView and Landsat scales.

4.4.2 Cross-scale error propagation

Although the accuracies regarding each single estimation model were promising, the cross-scale error had to be assessed, which was performed using Monte-Carlo simulations. Figure 4.5 shows the results of the error propagation analysis for PLSR and SVM regression from the Landsat to the MODIS scale. The errors at the MODIS scale are partly the result of errors already introduced in the Landsat training samples used for training of PLSR and SVM regression models to derive plant coverage at the MODIS scale. The sensitivity to the error committed at the Landsat scale was much higher in PLSR than SVM. In the PLSR regression, RMSE values up to 13% were observed, whereas the maximum RMSE values of the SVM regressions were still below the RMSE value of the PLSR model trained on the original data (dashed line in Figure 4.5a).

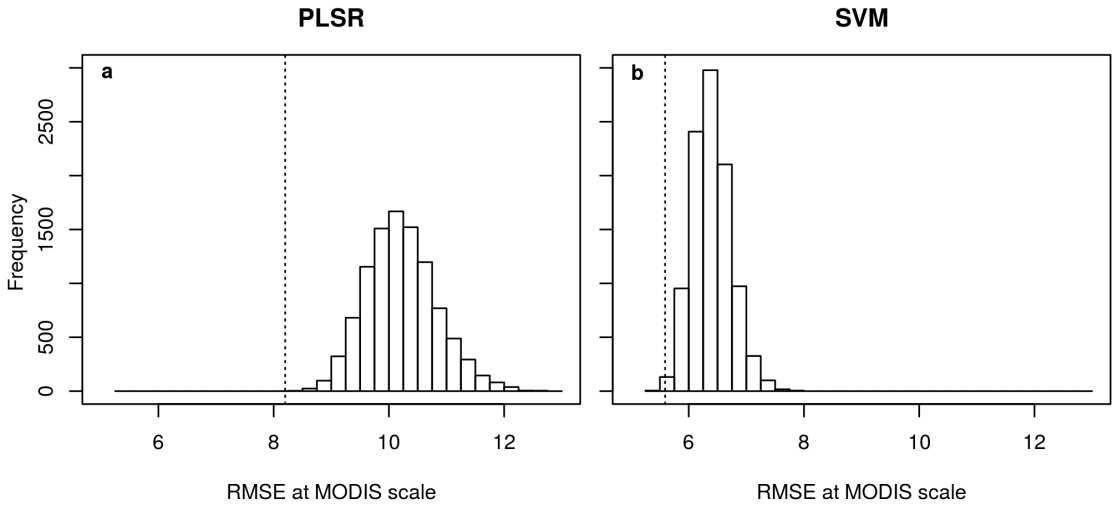

Figure 4.5: Histograms of RMSE values from 10,000 Monte-Carlo simulations of plant coverage estimates at the MODIS scale with training samples randomly manipulated by the error distribution. The dashed vertical line is the RMSE obtained without manipulation.

4.4.3 Spatial configuration of estimation errors

The spatial distribution of the estimation errors is shown in Figure 4.6 for the SVM regression models. The highest errors at the local scale were observed in the central and northeastern region of the plateau, whereas error rates at sampling locations in the western and eastern region of the plateau were lower. At the Landsat scale, no clear geographical pattern of accuracies was observed. At the MODIS scale, a remarkably high error was found at Ebu North.

4.4.4 Application of the best performing model to estimate plant coverage of Tibetan grasslands

Figure 4.7a shows the mean summer plant coverage of the grasslands on the Tibetan Plateau between 2011 and 2013 as calculated by the best-performing method (SVM regression) on the plateau scale based on MODIS data. In the western and north-western regions of the map, the mean plant coverage during the summer months was approximately 30%. In the eastern and south-eastern regions, values up to 95% were observed. The transition zone between both areas was approximately along the headwater

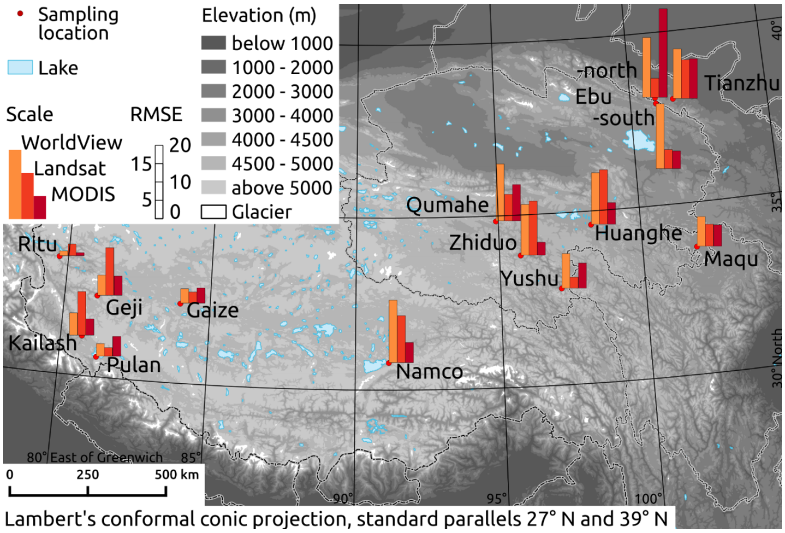

Figure 4.6: Prediction errors of SVM regression at all sampling locations. The bar colors indicate the scale of plant coverage prediction. The bar heights correspond to the RMSE at the sampling location.

regions of the large East Asian rivers. The histograms and boxplots in Figure 4.7b depict the distribution of plant coverage estimates for all important grassland vegetation types. They show that the part covered by *Kobresia pygmaea* pastures had the largest numerical range of plant coverage values (9% and 84%), with higher values in the south-eastern region. Approximately 40% plant coverage was observed in the transition zone between *K. pygmaea* pastures and Alpine steppe vegetation. The highest mean plant coverage was observed in areas covered by *K. humilis* pastures (63%). The alpine-steppe vegetation is characterized by a low spatial variability and a small range of plant coverage values (30 – 44%).

4.5 Discussion

In this study, plant coverage was estimated along a cross-scale model cascade based on satellite data with decreasing spatial resolution. Although the accuracy of the estimations differed among the four methods applied, the quality of the estimations of the vegetation indices and normalized difference indices in combination with PLSR and SVM regressions was promising. The predictions using SVM regression were in particularly good agreement with the reference data of plant coverage.

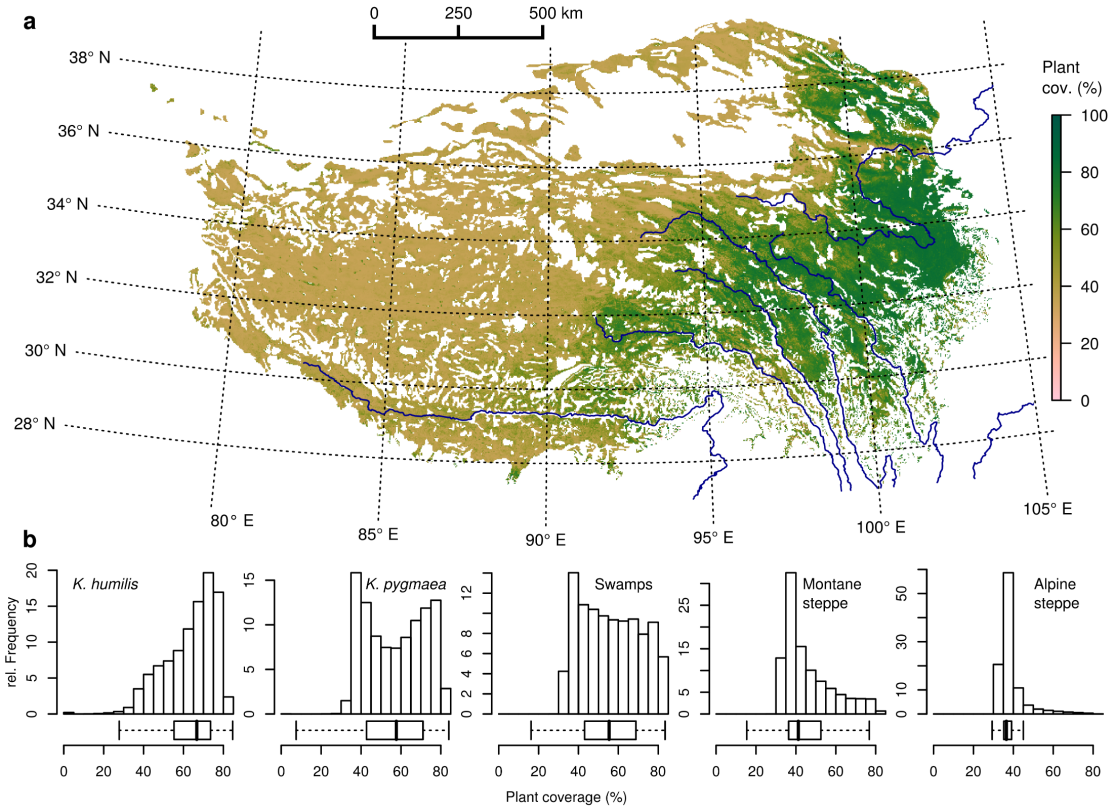

Figure 4.7: Plant coverage (%) of the grasslands on the Tibetan Plateau. Colors indicate the mean values of all MODIS scenes acquired between 2011 and 2013 in June, July and August (summer period; **a**). White areas are not covered by grasslands of any of the investigated types. Histograms (rel. frequencies) and boxplots in (**b**) show the distribution of plant-cover values within grassland vegetation types (outliers are omitted in the boxplots; lines and boxes correspond to extreme values, the first quartile, third quartile, and the median).

According to a comparison of the estimation accuracies of the different approaches, the methods based on *in situ* spectral data (SAM, LSU) provided by a spectrometer at ground generally produced higher error rates than the methods using only the feature space derived from the reflectance values of the satellite imagery as predictors for plant coverage (PLSR, SVM). Comparing the two methods requiring spectral ground information, we found that LSU was unable to predict plant coverage on larger scales for the whole Tibetan Plateau. This finding shows that the great potential of LSU to estimate plant coverage for small areas on the Tibetan Plateau (LEHNERT et al., 2014; SOMERS et al., 2011) might not extend to the plateau scale. The reason might be that LSU requires spectral knowledge (endmembers) of all major land-cover types and their variations over

space and time. These requirements were difficult to meet for two reasons: (i) First, the area of our analysis encompasses all grazed grasslands on the Tibetan Plateau, so there are substantial knowledge gaps regarding the spectral properties of soils and non-organic components in areas not covered by field measurements. This inherent uncertainty led us to include only soil and vegetation as endmembers in the LSU analysis. A better result might be achievable if more endmembers, such as stones, would be included in LSU as shown in a previous study (LEHNERT et al., 2014). However, the spectral properties of the stones depend on various factors, such as mineral composition, that greatly vary across the plateau and whose variation is largely unknown. (ii) Second, the spectral properties of soil within the spectral range of our sensors depend largely on the soil moisture content (NAGLER et al., 2000). Therefore, the soils are spectrally highly variable in space and time, even between the time of our measurements and the acquisition of the satellite images. In general, it might be possible that the high LSU error also arises from an improper spectral description of the vegetation endmembers. For instance, the change in chlorophyll content at the end of the vegetation period may cause that *in situ* measured vegetation endmembers do not represent the vegetation in the satellite data. If so, the finding that the error rates of SAM were far lower than those of LSU would not be explainable. Therefore, we conclude that the vegetation endmember is not the primary source of error in our LSU analysis.

The accuracies of the PLSR and SVM regressions were higher than those for LSU and SAM. Because neither method depended on the *in situ* measured spectral data, this finding implies that our results were in better agreement with reference data when we relied only on the feature space calculated from reflectance values than when spectral properties of plants measured *in situ* were incorporated into the analysis. This may be explained by the time lag between the sampling of the vegetation spectra and the acquisition of the satellite data. Alternatively, the atmosphere may cause the satellite surface-reflectance values to differ from those measured *in situ*, or the choice of reference spectra in the SAM analysis may not reflect the spatial variability of the spectral properties of vegetation. The best method to derive plant coverage of pastures on the Tibetan Plateau was the combination of NDI values and vegetation indices in SVM regression. This finding underlines the great potential of SVM regression to analyze satellite imagery, as previously documented in several studies (CAMPS-VALLS et al., 2006; SCHWIEDER et al., 2014; SUN et al., 2009).

Irrespective of the method applied, the error rates decreased at lower spatial resolutions of the satellite data, a pattern that has already been addressed by previous studies deriving vegetation cover along satellite data of multiple scales (GESSNER et al., 2013; HANSEN et al., 2002). At the WorldView scale, where the highest error was observed, the most likely reason is that *in situ* observations were compared to satellite data only at this scale. The comparison of *in situ* observations with satellite data may cause higher error rates because of the unavoidable time lags between the acquisition of the reference and the high-resolution satellite data. At the Landsat and the MODIS scales, the differences in accuracies were lower than those between the WorldView and the Landsat scales. Although the overall lowest error rate was observed for Landsat 8, the total error of Landsat 7 and 8 was higher than at the MODIS scale. This occurred because the number of samples in Landsat 8 was considerably lower than that in Landsat 7. The reason is that the data from Landsat 8 were only available for the year 2013.

The spatial analysis of the accuracy of plant coverage estimates showed that SVM regression produced higher error rates in the central part of the Tibetan Plateau, where plant coverage is intermediate, than in areas with low or high plant coverage. The reason for this pattern was that the range of observed plant coverage values was highest at locations in the *Kobresia pygmaea* ecosystem in central Tibet. Here, cover values below 10% were observed in extremely degraded areas, while the cover values reached 90% at non-degraded plots. Because the landscape is extremely patchy, often with less than 10 m distance between degraded and non-degraded plots, a spatial uncertainty of a few meters may cause high error rates at the WorldView scale. Subsequently, even if our field measurements indicated heavy degradation, the signal at the satellite sensor may be a mixture of degraded and less degraded vegetation because the spatial extent (1 m) of heavily degraded areas is frequently below the spatial resolution of the satellite data available at the WorldView scale. This may also explain why the error rates decreased at the Landsat and MODIS scales for locations in the *Kobresia pygmaea* ecosystem.

The geographical pattern in the configuration of error rates may also explain the large differences among sensors at the WorldView scale. Here, we found remarkably lower accuracies using Quickbird than RapidEye or WorldView-2 data. We had only three Quickbird images (Kailash, Namco and Qmarrhexiang) at our disposal. Thus, two of three scenes were located in the *Kobresia pygmaea* ecosystem. We compared the results of the plant coverage estimates using Quickbird and WorldView-2 imagery at the Kailash

location and found nearly equal error rates. Thus, the accuracies of the estimations based on the Quickbird imagery were lower than for the RapidEye or WorldView-2 data because of the location of the Quickbird scenes in the transition zone between *K. pygmaea* and Alpine Steppe rather than the spectral resolution or spectral configuration of the Quickbird sensor.

The results of the plant coverage estimations at MODIS scale are affected by the estimation errors committed at the Landsat scale. In particular, we found a low sensitivity at MODIS scale on this estimation error if plant coverage was estimated with SVM regression. If PLSR was used, the error at the Landsat scale had a far greater effect on the accuracy of the estimations at the MODIS scale. Thus, we conclude that the error committed at the Landsat scale only slightly influences the total accuracy of the product.

The second objective of the article was to create the first plant coverage product for the grasslands of the Tibetan Plateau. Here, the mean plant coverage of the Tibetan grasslands ranges from 30% in the western and north-western regions to 95% in the eastern and south-eastern regions. Care must be taken in comparing the values to other ground data derived at other scales published in the literature. The values predicted from our model are generalized due to the coarse spatial resolution of our product, and most of the available sources from on-site observations report sums of species cover rather than plant coverage. Compared to field samples of previous studies in the area, the model tends to overestimate plant coverage in the western region by approx. 10% (MIEHE et al., 2011b). This overestimation results from the low number of ground samplings in the far western region, which is the most remote area and the most difficult to access. The central region, including the transition between *Kobresia* pastures and Alpine steppe, has a plant coverage of 40% to 60%, which is very close to published data based on field samplings in the area (BABEL et al., 2014; MIEHE et al., 2011a, 2008a). A cover of approximately 85% is reported for non-degraded grasslands in the hydrologically important headwaters of the Yangtze and Huang Rivers (ZHOU et al., 2005), which is slightly above the mean plant coverage predicted by our model.

4.6 Conclusions

In this study, we presented the first plant coverage product for the grasslands of the Tibetan Plateau to be fully validated against ground data sampled in the field. We

tested four different methods (SAM, LSU, PLSR and SVM regression) in a cross-scale cascade of satellite data (WorldView-2, Landsat, MODIS) with decreasing pixel resolution and found that the methods using only satellite reflectance values (PLSR, SVM regression) yielded better results than those based on spectral endmembers (SAM, LSU). Because the error rates of the SVM regression models were low, the final product may help stakeholders at local and regional scales to define livestock storage capacities or redistribute pastures to villages and families. Furthermore, the plant coverage data may serve as data sources for future estimations of LAI, biomass and primary production. Such datasets are urgently required to improve the simulation of vegetation dynamics and vegetation-climate interactions on the Tibetan Plateau.

Acknowledgments

This study was conducted within the framework of the PaDeMoS-Project ("Pasture Degradation Monitoring System") and was funded by the German Federal Ministry of Education and Research (03G0808C). We are grateful that the MODIS and Landsat data could be obtained free of charge from the United States Geological Survey (USGS) ftp server (ftp://e4ftl01.cr.usgs.gov/) and website (http://earthexplorer.usgs.gov). We thank Yuanliang Jin, Michael Göbel, Alexander Groos, Nele Meyer, Stefan Pinkert, Sebastian Semella, Junnan Wang, and Eva-Vanessa Wilzek for their help in the field and processing the large datasets. We highly appreciate the valuable comments of Mark Friedl and anonymous reviewers on a previous version of this manuscript.

References

BABEL, W., BIERMANN, T., CONERS, H., FALGE, E., SEEBER, E., INGRISCH, J., SCHLEUSS, P.M., GERKEN, T., LEONBACHER, J., LEIPOLD, T., WILLINGHÖFER, S., SCHÜTZENMEISTER, K., SHIBISTOVA, O., BECKER, L., HAFNER, S., SPIELVOGEL, S., LI, X., XU, X., SUN, Y., ZHANG, L., YANG, Y., MA, Y., WESCHE, K., GRAF, H.F., LEUSCHNER, C., GUGGENBERGER, G., KUZYAKOV, Y., MIEHE, G., & FOKEN, T. (2014): Pasture degradation modifies the water and carbon cycles of the Tibetan highlands. *Biogeosciences*, 11, 8861–8923.

BANKS, T., RICHARD, C., LI, P., & YAN, Z.L. (2003): Community-based grassland management in western China - Rationale, pilot project experience, and policy implications. *Mountain Research and Development*, 23, 2, 132–140.

BARNETT, T.P., ADAM, J.C., & LETTENMAIER, D.P. (2005): Potential impacts of a warming climate on water availability in snow-dominated regions. *Nature*, 438, 7066, 303–309.

CAMPS-VALLS, G., GÓMEZ-CHOVA, L., MUÑOZ-MARÍ, J., VILA-FRANCÉS, J., AMORÓS-LÓPEZ, J., & CALPE-MARAVILLA, J. (2006): Retrieval of oceanic chlorophyll concentration with relevance vector machines. *Remote Sensing of Environment*, 105, 1, 23–33.

CAO, J.J., YEH, E.T., HOLDEN, N.M., YANG, Y.Y., & DU, G.Z. (2013): The effects of enclosures and land-use contracts on rangeland degradation on the Qinghai-Tibetan Plateau. *Journal of Arid Environments*, 97, 3–8.

CHEN, W., SAKAI, T., MORIYA, K., KOYAMA, L., & CAO, C. (2013): Estimation of vegetation coverage in semi-arid sandy land based on multivariate statistical modeling using remote sensing data. *Environmental Modeling & Assessment*, 18, 5, 547–558.

CUI, X. & GRAF, H.F. (2009): Recent land cover changes on the Tibetan Plateau: A review. *Climatic Change*, 94, 1-2, 47–61.

CURATOLA FERNÁNDEZ, G.F., OBERMEIER, W.A., GERIQUE, A., SANDOVAL, M.F.L., LEHNERT, L.W., THIES, B., & BENDIX, J. (2015): Land cover change in the Andes of southern Ecuador - Patterns and drivers. *Remote Sensing*, 7, 3, 2509–2542.

DING, Y.H. & CHAN, J.C.L. (2005): The East Asian summer monsoon: An overview. *Meteorology and Atmospheric Physics*, 89, 1-4, 117–142.

DOBBER, M., DIRKSEN, R., LEVELT, P., VAN DEN OORD, G.H.J., VOORS, R., KLEIPOOL, Q., JAROSS, G., KOWALEWSKI, M., HILSENRATH, E., LEPPELMEIER, G., DE VRIES, J., DIERSSEN, W., & ROZEMEIJER, N. (2006): Ozone monitoring instrument calibration. *IEEE Transactions on Geoscience and Remote Sensing*, 44, 5, 1209–1238.

DORJI, T., TOTLAND, Ø., & MOE, S.R. (2013): Are droppings, distance from pastoralist camps, and pika burrows good proxies for local grazing pressure? *Rangeland Ecology and Management*, 66, 1, 26–33.

ELVIDGE, C. D AND, Y.D., WEERACKOON, R.D., & LUNETTA, R.S. (1995): Relative radiometric normalization of Landsat Multispectral Scanner (MSS) data using an automatic scattergram-controlled regression. *Photogrammetric Engineering and Remote Sensing*, 61, 1255–1260.

FRIEDL, M.A., SULLA-MENASHE, D., TAN, B., SCHNEIDER, A., RAMANKUTTY, N., SIBLEY, A., & HUANG, X. (2010): MODIS collection 5 global land cover: Algorithm refinements and characterization of new datasets. *Remote Sensing of Environment*, 114, 168–182.

GAO, Q.Z., WAN, Y.F., XU, H.M., LI, Y., JIANGCUN, W.Z., & BORJIGIDAI, A. (2010): Alpine grassland degradation index and its response to recent climate variability in northern Tibet, China. *Quaternary International*, 226, 143–150.

GESSNER, U., MACHWITZ, M., CONRAD, C., & DECH, S. (2013): Estimating the fractional cover of growth forms and bare surface in savannas. A multi-resolution approach based on regression tree ensembles. *Remote Sensing of Environment*, 129, 90–102.

GÖTTLICHER, D., OBREGON, A., HOMEIER, J., ROLLENBECK, R., NAUSS, T., & BENDIX, J. (2009): Land-cover classification in the Andes of southern Ecuador using Landsat ETM plus data as a basis for SVAT modelling. *International Journal of Remote Sensing*, 30, 8, 1867–1886.

HANSEN, M., DEFRIES, R., TOWNSHEND, J., MARUFU, L., & SOHLBERG, R. (2002): Development of a MODIS tree cover validation data set for Western Province, Zambia. *Remote Sensing of Environment*, 83, 1/2, 320–335.

HARRIS, R.B. (2010): Rangeland degradation on the Qinghai-Tibetan Plateau: A review of the evidence of its magnitude and causes. *Journal of Arid Environments*, 74, 1, 1–12.

HOU, X.Y. (Ed.) (2001): Vegetation Atlas of China. Science Press, Beijing.

HUETE, A. (1988): A soil-adjusted vegetation index (SAVI). *Remote Sensing of Environment*, 25, 295–309.

HUETE, A., LIU, H., BATCHILY, K., & VAN LEEUWEN, W. (1997): A comparison of vegetation indices over a global set of TM images for EOS-MODIS. *Remote Sensing of Environment*, 59, 3, 440 – 451.

KALNAY, E., KANAMITSU, M., KISTLER, R., COLLINS, W., DEAVEN, D., GANDIN, L., IREDELL, M., SAHA, S., WHITE, G., WOOLLEN, J., ZHU, Y., LEETMAA, A., REYNOLDS, R., CHELLIAH, M., EBISUZAKI, W., HIGGINS, W., JANOWIAK, J., MO, K.C., ROPELEWSKI, C., WANG, J., JENNE, R., & JOSEPH, D. (1996): The NCEP/NCAR 40-Year Reanalysis Project. *Bulletin of the American Meteorological Society*, 77, 3, 437–471.

KRUSE, F.A., LEFKOFF, A.B., BOARDMAN, J.W., HEIDEBRECHT, K.B., SHAPIRO, A.T., BARLOON, P.J., & GOETZ, A.F.H. (1993): The spectral image processing system (SIPS) - interactive visualization and analysis of imaging spectrometer data. *Remote Sensing of Environment*, 44, 2-3, 145–163.

LEHNERT, L.W., MEYER, H., MEYER, N., REUDENBACH, C., & BENDIX, J. (2013): Assessing pasture quality and degradation status using hyperspectral imaging: A case study from western Tibet. In: Proceedings of the SPIE, volume 8887. Dresden, pp. 88 870I–88 870I–13.

LEHNERT, L.W., MEYER, H., MEYER, N., REUDENBACH, C., & BENDIX, J. (2014): A hyperspectral indicator system for rangeland degradation on the Tibetan Plateau: A case study towards spaceborne monitoring. *Ecological Indicators*, 39, 54 – 64.

LEVELT, P.F., VAN DEN OORD, G.H.J., DOBBER, M.R., MALKKI, A., VISSER, H., DE VRIES, J., STAMMES, P., LUNDELL, J.O.V., & SAARI, H. (2006): The ozone monitoring instrument. *IEEE Transactions on Geoscience and Remote Sensing*, 44, 5, 1093–1101.

LIU, B., SHEN, W.S., LIN, N.F., LI, R., & YUE, Y.M. (2014): Deriving vegetation fraction information for the alpine grassland on the Tibetan Plateau using *in situ* spectral data. *Journal of Applied Remote Sensing*, 8, 083 630.

MEYER, H., LEHNERT, L.W., WANG, Y., REUDENBACH, C., & BENDIX, J. (2013): Measuring pasture degradation on the Qinghai-Tibet Plateau using hyperspectral dissimilarities and indices. In: Proceedings of the SPIE, volume 8893. Dresden, pp. 88 931F–88 931F–13.

MIEHE, G., MIEHE, S., BACH, K., NÖLLING, J., HANSPACH, J., REUDENBACH, C., KAISER, K., WESCHE, K., MOSBRUGGER, V., YANG, Y.P., & MA, Y.M. (2011a): Plant communities of central Tibetan pastures in the Alpine Steppe/*Kobresia pygmaea* ecotone. *Journal of Arid Environments*, 75, 8, 711–723.

MIEHE, G., BACH, K., MIEHE, S., KLUGE, J., YONGPING, Y., DUO, L., CO, S., & WESCHE, K. (2011b): Alpine steppe plant communities of the Tibetan highlands. *Applied Vegetation Science*, 14, 4, 547–560.

MIEHE, G., KAISER, K., CO, S., XINQUAN, Z., & JIANQUAN, L. (2008a): Geo-ecological transect studies in northeast Tibet (Qinghai, China) reveal human-made mid-holocene environmental changes in the upper Yellow River catchment changing forest to grassland. *Erdkunde*, 62, 3, 187–199.

MIEHE, G., MIEHE, S., BÖHNER, J., KAISER, K., HENSEN, I., MADSEN, D., LIU, J.Q., & OPGENOORTH, L. (2014): How old is the human footprint in the world's largest alpine ecosystem? A review of multiproxy records from the Tibetan Plateau from the ecologists' viewpoint. *Quaternary Science Reviews*, 86, 190–209.

MIEHE, G., MIEHE, S., KAISER, K., JIANQUAN, L., & ZHAO, X. (2008b): Status and dynamics of *Kobresia pygmaea* ecosystem on the Tibetan Plateau. *Ambio*, 37, 4, 272–279.

MÖLG, T., MAUSSION, F., & SCHERER, D. (2014): Mid-latitude westerlies as a driver of glacier variability in monsoonal High Asia. *Nature Climate Change*, 4, 1, 68–73.

MOUNTRAKIS, G., IM, J., & OGOLE, C. (2011): Support vector machines in remote sensing: A review. *ISPRS Journal of Photogrammetry and Remote Sensing*, 66, 3, 247 – 259.

MU, Q., HEINSCH, F.A., ZHAO, M., & RUNNING, S.W. (2007): Development of a global evapotranspiration algorithm based on MODIS and global meteorology data. *Remote Sensing of Environment*, 111, 4, 519–536.

MURRAY, S., WATSON, I., & PRENTICE, I. (2013): The use of dynamic global vegetation models for simulating hydrology and the potential integration of satellite observations. *Progress in Physical Geography*, 37, 1, 63–97.

NAGLER, P., DAUGHTRY, C., & GOWARD, S. (2000): Plant litter and soil reflectance. *Remote Sensing of Environment*, 71, 2, 207 – 215.

PIAO, S., CIAIS, P., HUANG, Y., SHEN, Z., PENG, S., LI, J., ZHOU, L., LIU, H., MA, Y., DING, Y., FRIEDLINGSTEIN, P., LIU, C., TAN, K., YU, Y., ZHANG, T., & FANG, J. (2010): The impacts of climate change on water resources and agriculture in China. *Nature*, 467, 7311, 43–51.

PSOMAS, A., KNEUBUEHLER, M., HUBER, S., ITTEN, K., & ZIMMERMANN, N.E. (2011): Hyperspectral remote sensing for estimating aboveground biomass and for exploring species richness patterns of grassland habitats. *International Journal of Remote Sensing*, 32, 24, 9007–9031.

QI, J., CHEHBOUNI, A., HUETE, A., KERR, Y., & SOROOSHIAN, S. (1994): A modified soil adjusted vegetation index. *Remote Sensing of Environment*, 48, 2, 119–126.

SCHAAF, C.B., GAO, F., STRAHLER, A.H., LUCHT, W., LI, X.W., TSANG, T., STRUGNELL, N.C., ZHANG, X.Y., JIN, Y.F., MULLER, J.P., LEWIS, P., BARNSLEY, M., HOBSON, P., DISNEY, M., ROBERTS, G., DUNDERDALE, M., DOLL, C., D'ENTREMONT, R.P., HU, B.X., LIANG, S.L., PRIVETTE, J.L., & ROY, D. (2002): First operational BRDF, albedo nadir reflectance products from MODIS. *Remote Sensing of Environment*, 83, 1-2, PII S0034–4257(02)00 091–3.

SCHWIEDER, M., LEITÃO, P.J., SUESS, S., SENF, C., & HOSTERT, P. (2014): Estimating fractional shrub cover using simulated EnMAP data: A comparison of three machine learning regressionătechniques. *Remote Sensing*, 6, 4, 3427–3445.

SEAQUIST, J., OLSSON, L., & ARDÖ, J. (2003): A remote sensing-based primary production model for grassland biomes. *Ecological Modelling*, 169, 1, 131 – 155.

SOHN, Y.S. & MCCOY, R.M. (1997): Mapping desert shrub rangeland using spectral unmixing and modeling spectral mixtures with TM data. *Photogrammetric Engineering and Remote Sensing*, 63, 6, 707–716.

SOMERS, B., ASNER, G.P., TITS, L., & COPPIN, P. (2011): Endmember variability in spectral mixture analysis: A review. *Remote Sensing of Environment*, 115, 7, 1603–1616.

SOUDANI, K., FRANCOIS, C., LE MAIRE, G., LE DANTEC, V., & DUFRENE, E. (2006): Comparative analysis of IKONOS, SPOT, and ETM+ data for leaf area index estimation in temperate coniferous and deciduous forest stands. *Remote Sensing of Environment*, 102, 1-2, 161–175.

SUN, D., LI, Y., & WANG, Q. (2009): A unified model for remotely estimating chlorophyll a in Lake Taihu, China, based on SVM and *in situ* hyperspectral data. *IEEE Transactions on Geoscience and Remote Sensing*, 47, 8, 2957–2965.

TACHIKAWA, T., HATO, M., KAKU, M., & IWASAKI, A. (2011): Characteristics of ASTER GDEM version 2. In: Geoscience and Remote Sensing Symposium (IGARSS), IEEE International. pp. 3657–3660.

TEILLET, P.M., GUINDON, B., & GOODEONUGH, D.G. (1982): On the slope-aspect correction of multispectral scanner data. *Canadian Journal of Remote Sensing*, 8, 84–106.

THENKABAIL, P.S., SMITH, R.B., & PAUW, E.D. (2000): Hyperspectral vegetation indices and their relationships with agricultural crop characteristics. *Remote Sensing of Environment*, 71, 2, 158 – 182.

VERMOTE, E.F., TANRE, D., DEUZE, J.L., HERMAN, M., & MORCETTE, J.J. (1997): Second simulation of the satellite signal in the solar spectrum, 6S: An overview. *IEEE Transactions on Geoscience and Remote Sensing*, 35, 3, 675–686.

WOEBBECKE, D.M., MEYER, G.E., VONBARGEN, K., & MORTENSEN, D.A. (1995): Color indexes for weed identification under various soil, residue, and lighting conditions. *Transactions of the ASAE*, 38, 1, 259–269. A021979057.

WYLIE, B.K., JOHNSON, D.A., LACA, E., SALIENDRA, N.Z., GILMANOV, T.G., REED, B.C., TIESZEN, L.L., & WORSTELL, B.B. (2003): Calibration of remotely sensed, coarse resolution NDVI to CO_2 fluxes in a sagebrush-steppe ecosystem. *Remote Sensing of Environment*, 85, 2, 243–255.

XU, X., LU, C., SHI, X., & GAO, S. (2008): World water tower: An atmospheric perspective. *Geophysical Research Letters*, 35, 20.

YANG, C. & EVERITT, J. (2012): Using spectral distance, spectral angle and plant abundance derived from hyperspectral imagery to characterize crop yield variation. *Precision Agriculture*, 13, 1, 62–75.

ZHA, Y., GAO, J., NI, S.X., LIU, Y.S., JIANG, J.J., & WEI, Y.C. (2003): A spectral reflectance-based approach to quantification of grassland cover from Landsat TM imagery. *Remote Sensing of Environment*, 87, 2-3, 371–375.

ZHANG, G.L., ZHANG, Y.J., DONG, J.W., & XIAO, X.M. (2013): Green-up dates in the Tibetan Plateau have continuously advanced from 1982 to 2011. *Proceedings of the National Academy of Sciences*, 110, 11, 4309–4314.

ZHOU, H., ZHAO, X., TANG, Y., GU, S., & ZHOU, L. (2005): Alpine grassland degradation and its control in the source region of the Yangtze and Yellow Rivers, China. *Grassland Science*, 51, 3, 191–203.

Supplementary material

Supplementary Table 4.2: Summary of fieldwork and satellite data at the WorldView and Landsat scale.

Location	Fieldwork				WorldView scale		Landsat scale		
			Number of						
	Begin	End	trans-ects	plots	Sensor	Acquisition date	No	Sensor	Acquisition date
Ebu North	2013-06-16	2013-06-17	1	2	RapidEye	2013-07-15	1	Landsat 8	2013-06-28
							2	Landsat 8	2013-07-05
							3	Landsat 8	2013-07-21
Ebu South	2013-06-18	2013-06-19	1	3	RapidEye	2013-07-15	1	Landsat 8	2013-06-28
							2	Landsat 8	2013-07-05
							3	Landsat 8	2013-07-21
Gaize	2013-07-10	2013-07-11	1	2	RapidEye	2013-10-06	4	Landsat 8	2013-10-24
Geji	2013-07-12	2013-07-13	1	2	RapidEye	2013-10-06	5	Landsat 8	2013-10-06
Huanghe	2011-08-27	2011-08-30	3	14	RapidEye	2011-08-28	6	Landsat 7	2011-06-29
							6	Landsat 7	2011-07-15
							7	Landsat 7	2011-07-31
							8	Landsat 7	2011-08-16
							10	Landsat 7	2011-09-17
Kailash	2012-09-01	2012-09-09	3	9	Quickbird	2012-07-23	11	Landsat 7	2012-07-07
							12	Landsat 7	2012-07-23
					WorldView-2	2012-07-23	11	Landsat 7	2012-07-07
							12	Landsat 7	2012-07-23
Maqu	2011-08-12	2011-08-15	3	18	RapidEye	2011-08-26	13	Landsat 7	2011-08-11
							14	Landsat 7	2011-10-14
	2012-07-08	2012-07-13	5	126	WorldView-2	2012-09-02	15	Landsat 7	2012-09-05
							16	Landsat 7	2012-09-14
							17	Landsat 7	2012-09-30
							18	Landsat 7	2012-10-16
Namco	2012-08-19	2012-08-26	4	129	Quickbird	2012-09-12	19	Landsat 7	2012-08-14
							20	Landsat 7	2012-08-30
							21	Landsat 7	2012-09-15
							22	Landsat 7	2012-10-01
Pulan	2013-07-17	2013-07-18	1	2	RapidEye	2013-07-28	23	Landsat 8	2013-08-03
Qumahe	2012-07-30	2012-08-04	9	265	Quickbird	2012-09-05	24	Landsat 7	2012-09-17
							25	Landsat 7	2012-10-19
Ritu	2013-07-15	2013-07-16	1	2	RapidEye	2013-09-20	26	Landsat 8	2013-09-18
Tianzhu	2011-08-03	2011-08-04	1	13	WorldView-2	2011-09-12	27	Landsat 7	2011-09-10
							28	Landsat 7	2011-09-26
Yushu	2013-06-06	2013-06-12	1	3	RapidEye	2013-08-04	29	Landsat 8	2013-08-13
Zhiduo	2011-09-05	2011-09-08	2	11	WorldView-2	2011-08-07	30	Landsat 7	2011-08-07
							31	Landsat 7	2011-08-30
							32	Landsat 7	2011-09-15
	2012-08-10	2012-08-11	2	41	WorldView-2	2012-08-13	33	Landsat 7	2012-08-16
							34	Landsat 7	2012-09-01
							24	Landsat 7	2012-09-17

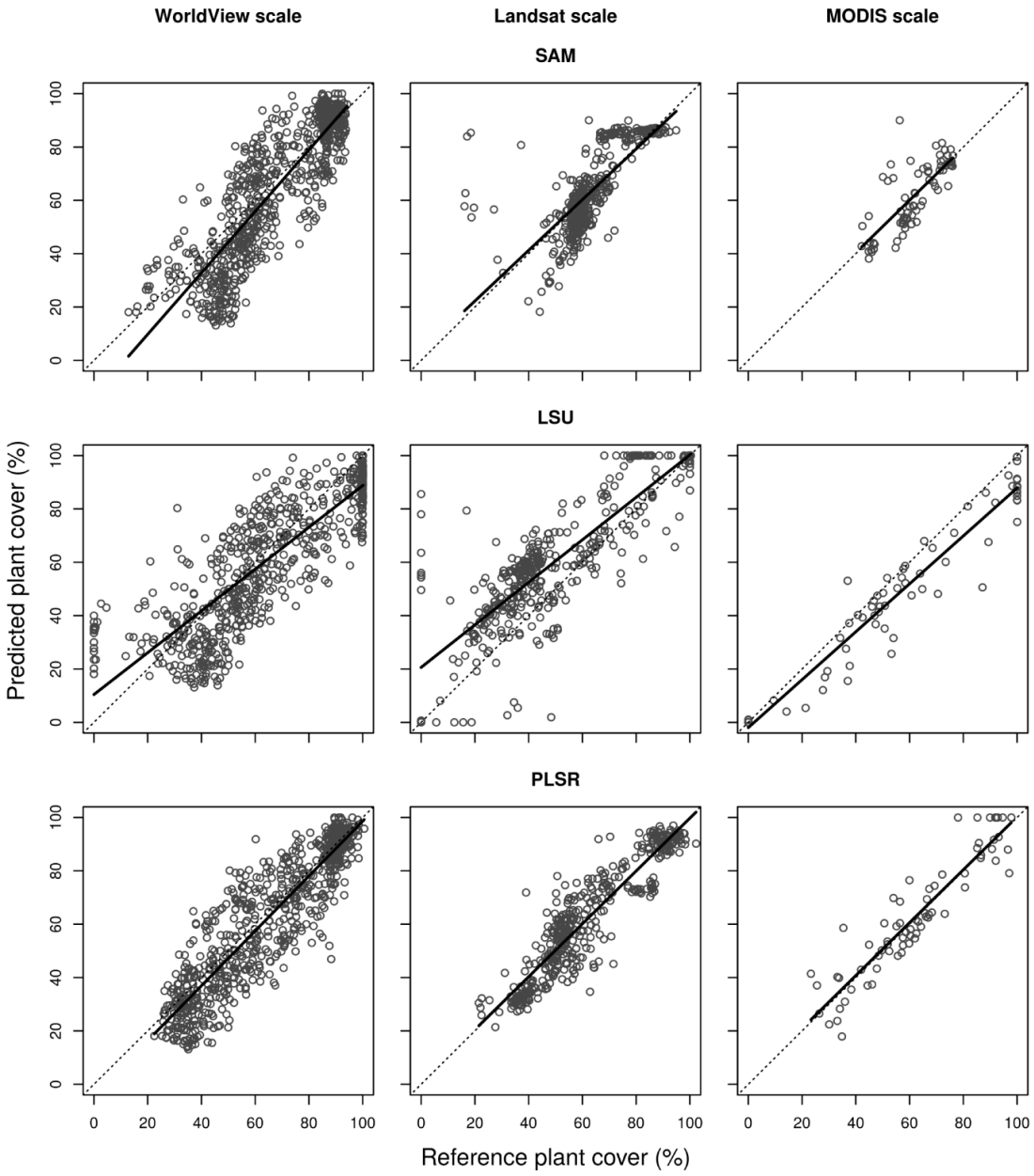

Supplementary Figure 4.8: Predicted vs. observed plant coverage for all sensors at the WorldView (left panel), Landsat (central panel) and MODIS scales (right panel) using SAM (upper panel), LSU (central panel) and PLSR (lower panel). The dotted lines are the 1:1 lines, and solid lines are linear regressions between observed and predicted plant-cover values.

Supplementary Table 4.3: Vegetation indices used in this study. Note that the NDVI is already included in the NDI-indices.

Index	Definition	Source
EVI	$2.5\frac{R_{800} - R_{670}}{R_{800} - 6 \cdot R_{670} - 7.5 \cdot R_{475} + 1}$	HUETE et al. (1997)
MSAVI	$0.5\left(2 \cdot R_{800} + 1 - \left(\left(2 \cdot R_{800} + 1\right)^2 - 8\left(R_{800} - R_{670}\right)\right)^{0.5}\right)$	QI et al. (1994)
SAVI[1]	$(1 + L)\,\frac{R_{800} - R_{670}}{R_{800} + R_{670} + L}$	HUETE (1988)

[1] L was set to an intermediate and constant value of 0.5 (CHEN et al., 2013).

5 Climate variability rather than overstocking causes degradation of Tibetan pastures

This chapter is under review at *Global Change Biology*.
Submitted: 16 April 2015

Climate variability rather than overstocking causes recent degradation of Tibetan pastures

Lukas W. Lehnert[(1)], Karsten Wesche[(2, 3)], Katja Trachte[(1)], Christoph Reudenbach[(1)], Jörg Bendix[(1)]

[(1)] Department of Geography, Philipps-University of Marburg, Deutschhausstr. 10, 35037 Marburg, Germany

[(2)] Senckenberg Museum of Natural History, Am Museum 1, 02826 Görlitz, Germany

[(3)] German Centre for Integrative Biodiversity Research (iDiv) Halle-Jena-Leipzig, Deutscher Platz 5e, 04103 Leipzig, Germany

---

Abstract The Tibetan Plateau (TP) is a globally important "water tower" that provides water for nearly 40% of the world's population. In addition to melting glaciers, pasture degradation and the associated loss of water regulation and supply functions have been discussed as key threats to the TP. To determine the interactions among vegetation dynamics, climate change and human impacts on the TP, we analyzed trends in a new high-resolution dataset of grassland cover. The results revealed that the vegetation cover has increased since 2000 in the northeastern part of the TP due to increases in precipitation. In contrast, the vegetation cover has declined in the central and western parts of the TP due to increases in temperature and the number of livestock; the latter is a result of land use change. As demonstrated by simulation studies on the TP,

the large-scale reduction in vegetation cover results in an increase in the sensible heat fluxes and a decrease in the average precipitation. In addition, higher-intensity convective rainfall will increase. Furthermore, the water retention capacity of the soils is decreasing, which will lead to discharge extremes in the headwater regions of Bramaputra and Salween.

Keywords Tibetan Plateau, Grassland degradation, Climate vegetation interactions, Global change, Time series analysis, Land use change

5.1 Introduction

Degradation of grasslands is a global threat for human welfare (BALMFORD et al., 2002). Estimates of grassland degradation in China vary, and as much as 90% of the grasslands is considered to be degraded (LIU & DIAMOND, 2005). Depending on the assessment methods that are used, the changes have been found to be the result of either climate change or human-induced overgrazing (CUI & GRAF, 2009); however, conclusive evidence for both effects is lacking (HARRIS, 2010). Within China, the TP forms the world's largest high mountain grassland ecosystem and is a globally important "water tower" that provides water for nearly 40% of the world's population living in East China, India and Southeast Asia (XU et al., 2008). This water supply function of the TP is threatened by melting glaciers (MÖLG et al., 2014; YAO et al., 2012) and local land use change (LIU & DIAMOND, 2005). Climatic controls are pronounced in the high and often dry region, where the ecosystems are generally vulnerable to climate change (PIAO et al., 2011). It was recently shown that vegetation changes alter the sensible heat fluxes and causes feedbacks to the atmosphere, which demonstrates the interaction between land cover change and climate change on the TP (CUI et al., 2006). Because the TP has been grazed since at least the mid-Holocene climatic optimum (8800 BP), the vegetation is generally well-adapted to grazing (MIEHE et al., 2009). However, land use on the TP is now undergoing significant changes because of the sedentarization of the Tibetan nomads, which has had large effects on livestock stocking numbers and pasture use

rights. This causes that pasture degradation and the associated loss of water regulation and supply functions have been discussed as key threats to the TP (CUI & GRAF, 2009; HU et al., 2008; LIU & DIAMOND, 2005) threatening the areas along the middle and lower reaches of the rivers (ZHANG et al., 2011). Thus, accurate high-resolution data are needed to detect potentially divergent trends in different regions of the TP.

The most significant effect of pasture degradation is a reduction in the net biomass production followed by a reduction in plant cover, which have been demonstrated by grazing enclosure experiments on the TP (HAFNER et al., 2012; WU et al., 2009) and confirmed using remote sensing (LEHNERT et al., 2014). In the grazing enclosure experiments, a relatively short response time of the ecosystem to grazing was found (< 10 years) (HAFNER et al., 2012; MIEHE et al., 2009). The large spatial extent of the TP makes field investigations and the monitoring of plant cover as an indicator for changes in climate and livestock numbers (e.g., sheep, goats, and yaks; hereafter LN) extremely expensive. Thus, remote sensing approaches provide the only opportunity to investigate recent and widespread changes in plant cover.

Feedback mechanisms of vegetation change on climate change have been simulated with general circulation models (GCMs). However, these GCM-based studies have only led to very general statements because the data on the spatiotemporal change of vegetation that were used as boundary conditions for the GCM simulations were extremely generalized (CUI et al., 2006). Here, we use a recently generated MODIS-based high-resolution and wide area dataset of vegetation cover (LEHNERT et al., 2015) to overcome these spatial deficits and to delineate regions of change since 2000. By comparing the trends in air temperature, precipitation and LN, we identify the drivers of vegetation change. This approach allows us to provide area-wide and region-specific evidence of the interactions and feedbacks between vegetation, land use and climate change on the TP.

5.2 Materials and methods

5.2.1 Vegetation cover

A time series (from 2000 to 2013) of a novel vegetation cover product for grasslands on the TP was used to investigate the recent changes in vegetation dynamics (LEHNERT

et al., 2015). The data are derived from MODIS BRDF composites (MCD43A4) with a spatial resolution of 500 m and a temporal resolution of 16 days. The vegetation cover values are calculated from a cascade of satellite data of increasing spatial resolutions using support vector machine (SVM) regression models, which are trained and validated against plant cover surveys from more than 600 field plots that span the entire TP.

It was recently reported that the Terra MODIS sensor is suffering from degradation (WANG et al., 2012). This implies that the reflectance values that are used for plant cover calculations are progressively decreasing. WANG et al. (2012) provided degradation factors over time for each Terra MODIS band. To test the maximum effect of sensor degradation on plant cover values, we used the maximum sensor degradation factors for each band and manipulated the reflectance values prior to their transfer into plant cover values in the vegetation cover product. Afterwards, the differences in plant cover values were compared as calculated with and without manipulation of the reflectance values. Here, we found extremely small and thus negligible effects (root mean square error of below 0.8% plant cover).

5.2.2 Precipitation and temperature data

Daily rainfall data that were provided by the Tropical Rainfall Measuring Mission (TRMM, 3B42) were used for the precipitation analysis (HUFFMAN et al., 2007). The dataset was validated against field measurements and was successfully tested for its suitability to provide reliable estimates of rainfall variability on the TP (MAUSSION et al., 2014). The TRMM data have a spatial resolution of 0.25° x 0.25°, which was resampled to 20 km using the nearest neighbor approach. Resampling has been performed to use one single projection facilitating the comparison of the different datasets. The new spatial resolution was chosen to be close to the original one so that rescaling was kept to a minimum.

The 2-m air temperature values were derived from ERA-Interim reanalysis data (DEE et al., 2011). This dataset has a spatial resolution of 0.75° x 0.75°, which was resampled to 60 km. The quality of the ERA-Interim air temperature values in the TP has been demonstrated by the very high correlations to data from meteorological stations (GAO et al., 2014; WANG & ZENG, 2012).

5.2.3 Livestock numbers

LN for the provinces Qinghai and TAR were taken from the official statistical surveys published in China Statistical Yearbooks (MA et al., 2000-2013). Data for prefectures of the TAR were provided by the PEOPLES'S REPUBLIC OF CHINA (2000-2013). Absolute numbers of different animals were converted to sheep equivalents according to FAO (2005).

5.2.4 Time series analysis

The plant cover values were averaged over June, July and August (the growing season) because this period is characterized by vegetation activity across the entire TP (YU et al., 2010). Vegetation activity during the growing season is not necessarily influenced by only summer precipitation and temperatures. The winter precipitation may also be important for the greening-up of the C3 plant-dominated grasslands in the spring and thus may contribute substantially to plant growth in the early summer. Therefore, the inter-annual relationship between the grassland vegetation cover and climate factors was assessed for each pixel and climate dataset by a linear multi-temporal correlation analysis. Temporal lags from 0 to 6 months were tested at 1 month intervals. For each pixel, the climate data were aggregated for the lag period that corresponded to the time period that revealed the best correlation.

In each dataset, temporal trends across the entire time span of 14 years were calculated. For the vegetation cover, the values averaged over the summer period were used. For both climate datasets and each pixel, the average temperature values and precipitation sums of the time period were used which revealed the closest correlation to plant cover values. Anomalies ($\hat{x}$) were calculated for each dataset and pixel using the following formula:

$$\hat{x}_{i,j} = \frac{x_{i,j} - \overline{x}_{i,j}}{\sigma_{i,j}}, \tag{5.1}$$

where $x_{i,j}$ denotes the values of the time series (plant cover, precipitation or temperature) between 2000 and 2013 of the pixel in column i and row j in the respective dataset. $x_{i,j}$ and $\sigma_{i,j}$ are corresponding mean and standard deviation values.

Trends within the anomalies were calculated separately for each pixel and dataset. Because most of the data were not normally distributed, the trends in the anomalies of the

plant cover data and climate variables were calculated by the Mann-Kendall correlation techniques. We did not directly compare the time series of the different datasets in a multivariate analysis because of the coarser spatial resolution of the precipitation and temperature datasets compared to plant cover values.

5.3 Results

5.3.1 Inter-annual relationships between climate variables and plant coverage

Vegetation cover mostly responds to precipitation and temperature within very short periods on the TP (Fig. 5.1a, b). Only in the arid western and central part of the TAR, the response time was higher (up to 6 month). Here, winter precipitation considerably influenced vegetation growth in summer. We analyzed the differences between the absolute values of the maximum and minimum correlation coefficients which is a measurement of the magnitude of the inter-annual dependence of vegetation growth on temperature and precipitation values within a specific season. These differences followed the pattern in the lag periods (Fig. 5.1c, d). This corresponds to the magnitude of the inter-annual variability in precipitation and temperature which is generally lower in the arid western part but also reflects the influence of the summer monsoon in the southern and south-western part of the TAR. In areas with a distinct annual cycle in climate elements, these differences were higher than in areas with low inter-annual variability. In general, the correlation coefficients between climate variables and plant coverage were high (Fig. 5.1e, f). For precipitation values up to 0.99 were observed while figures for temperature were slightly lower (up to 0.97). In most parts of the area, the correlation coefficient of the relationship between precipitation and plant coverage were slightly higher than those between temperature and plant coverage.

5.3.2 Changes in livestock numbers on the Tibetan Plateau

The major part of the TP belongs administratively to two different provinces, Qinghai in the north-eastern part and the Tibetan Autonomous Region (TAR) covering the southern and western part (see Fig. 5.6 for a location map). Since regional politics and social

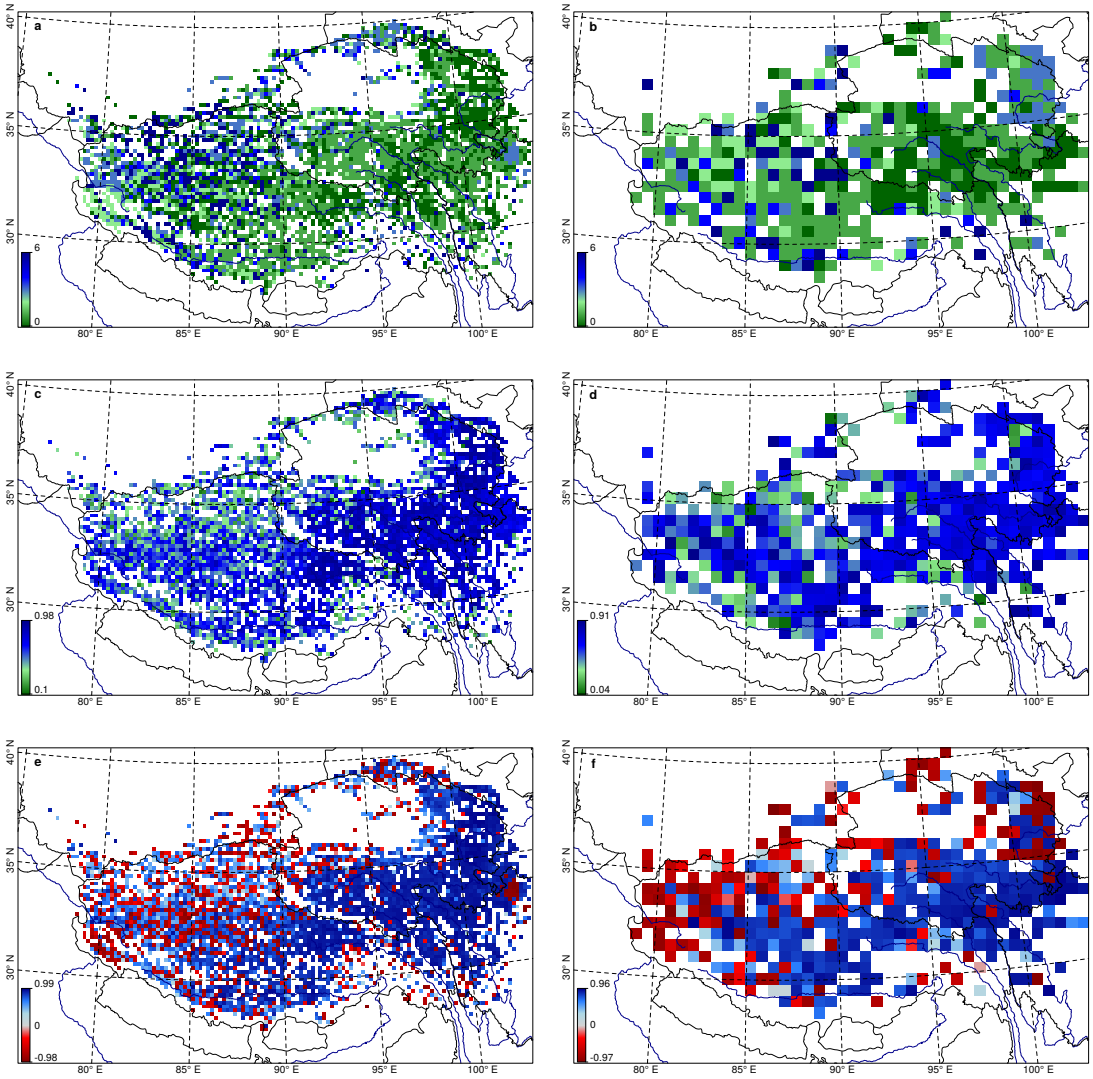

Figure 5.1: Maps depicting relationships between plant cover and precipitation (left panel) and plant cover and air temperature (right panel) as revealed by the linear multi-temporal correlation analysis. (a & b) Time lags in months resulting in the maximum correlation coefficient; (c & d) absolute difference between maximum and minimum correlation coefficient observed for all tested time lags; (e & f) maximum correlation coefficient.

structures are considerably different, it is worthwhile to separately analyze LN in both provinces to find out if they evolved differently during the last decades. LN increased dramatically between 2000 and 2006 in the TAR (Fig. 5.2). In contrast, LN decreased considerably during the 1990s and have remained almost constant since 2000 in adjacent

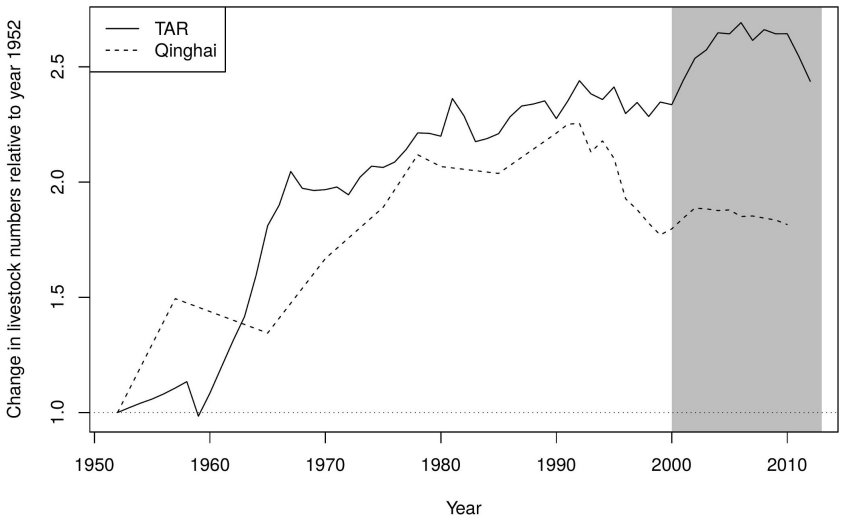

Figure 5.2: Changes in LN in TAR and Qinghai in sheep equivalents (relative to year 1952). Grey marked area is the investigated time period when satellite data and thus, the area-wide plant cover product were available. For location purposes refer to Fig. 5.6.

Qinghai Province. In the TAR, LN increased at the beginning of the new millennium in all prefectures except Shannan (Fig. 5.6). LN decreased slightly in the second half of the time series in most of the prefectures.

5.3.3 Changes in precipitation, temperature and vegetation cover between 2000 and 2013

The vegetation cover increased significantly between 2000 and 2013 along a large belt that encompasses southern Qinghai, the headwater region of the Yangtze and the eastern part of Qinghai (Fig. 5.3a). The largest increase was observed south of Lake Koko Nor. In contrast, the vegetation cover in the western and southern parts of the TAR has decreased, with the strongest negative trends being observed in the upper reaches of the Indus River. The southeastern part of the TP does not show clear trends. A remarkable significantly negative trend was observed in the Altun Shan in the north-western part of Qinghai. The comparison of the spatially accumulated vegetation cover trends between the main provinces of Qinghai and the TAR underline these substantially different patterns with positive trends for Qinghai and negative trends for the TAR (Fig. 5.3b).

Precipitation has increased significantly in southern Qinghai and along a small north-

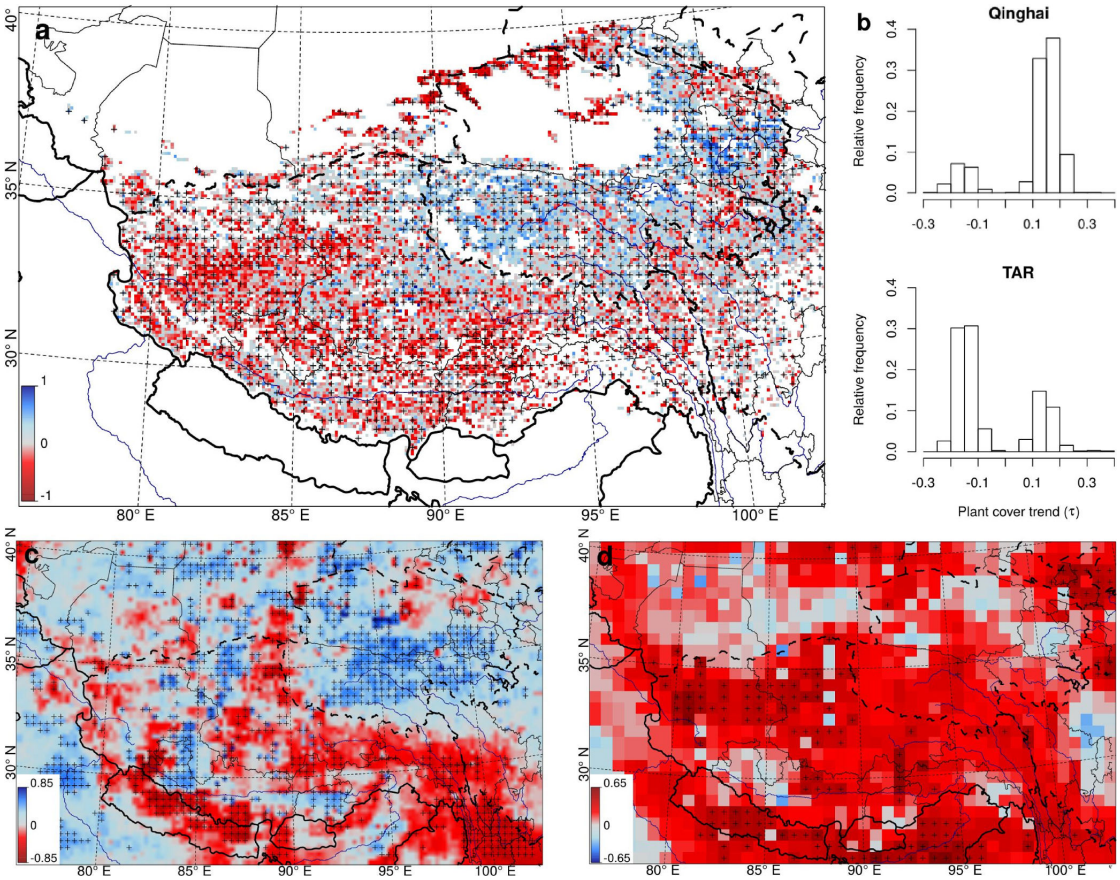

Figure 5.3: Trends in vegetation cover and climate variables between 2000 and 2013. (a) shows plant cover trends during the growing season. Histograms in (b) reveal the relative frequencies of significant plant cover trends in Qinghai and TAR (significance level 0.05). Note that the distributions are bimodal because only significant changes are considered. The bottom maps depict trends in precipitation sums (c) and in the mean 2 m air temperature (d). Colors indicate the τ-values of Mann-Kendall correlations. (+) labeling marks areas where correlations are significant at the 0.05 confidence level. Note for interpretation that all correlations were calculated from anomalies of the variables.

south trending band at 85° E (Fig. 5.3c). Significant negative trends were observed in the upper reaches of the Mekong and Salween rivers in northern Yunnan. To date, these negative anomalies have been attributed to the weakening of the East Asian monsoon (Fu, 2003). Precipitation also decreased significantly in the Himalayas and the southern TAR between 2000 and 2013 which was also attributed to a negative monsoon development (Yao et al., 2012).

Long term temperature trends on the central Tibetan Plateau were generally positive

Table 5.1: Pearson correlation statistics of the temporal trend analysis of temperature values (1980 - 2014). Data was taken from ERA-interim data and averaged for the area where thawing permafrost soils are considered as cause of increasing coverage (33°N - 36°N, 86.25°E - 90.75°E). All variables were tested on normality.

Variable	Season	t	df	p value	r
Temperature	Year	3.33	34	< 0.01	0.50
	Winter	0.63	34	0.532	0.11
	Spring	2.20	34	0.035	0.35
	Summer	4.17	34	< 0.01	0.58
	Fall	1.82	34	0.078	0.30
No. of month with t > 0°C		3.22	34	< 0.01	0.48

during the last three decades (Fig. 5.4). However, significant positive trends were observed mainly in summer, whereas temperature values in winter did not significantly change (Tab. 5.1). From a spatial perspective, temperatures increased across nearly the entire TP between 2000 and 2013 (Fig. 5.3d). However, significant positive trends were only observed in the western part of the TAR, to the south of the Himalayas and north of Qilian Shan. No significant negative temperature trends were found.

Fig. 5.5 presents a comparison between the trends in the climate variables and plant cover. Positive trends in all three variables were observed in southern Qinghai and the northern part of the TAR (Fig. 5.5a). Simultaneous occurrences of negative precipitation and plant cover trends were found in the far western part of the TAR and in some areas in the central TAR (Fig. 5.5b). Positive plant cover trends corresponded to negative precipitation trends at the northern border between Qinghai and the TAR (Fig. 5.5c) while the co-occurrence of the opposite trends was observed in the western part of the TAR and in the Qilian Shan (Fig. 5.5d).

5.4 Discussion

The results show unexpected and pronounced differences in the temporal trends of vegetation cover on the TP that are accompanied by differing trends of the potential atmospheric forcings. The trends differ between the provinces of Qinghai and the TAR, which may either be influenced by land use policy or reflect changes in individual climate

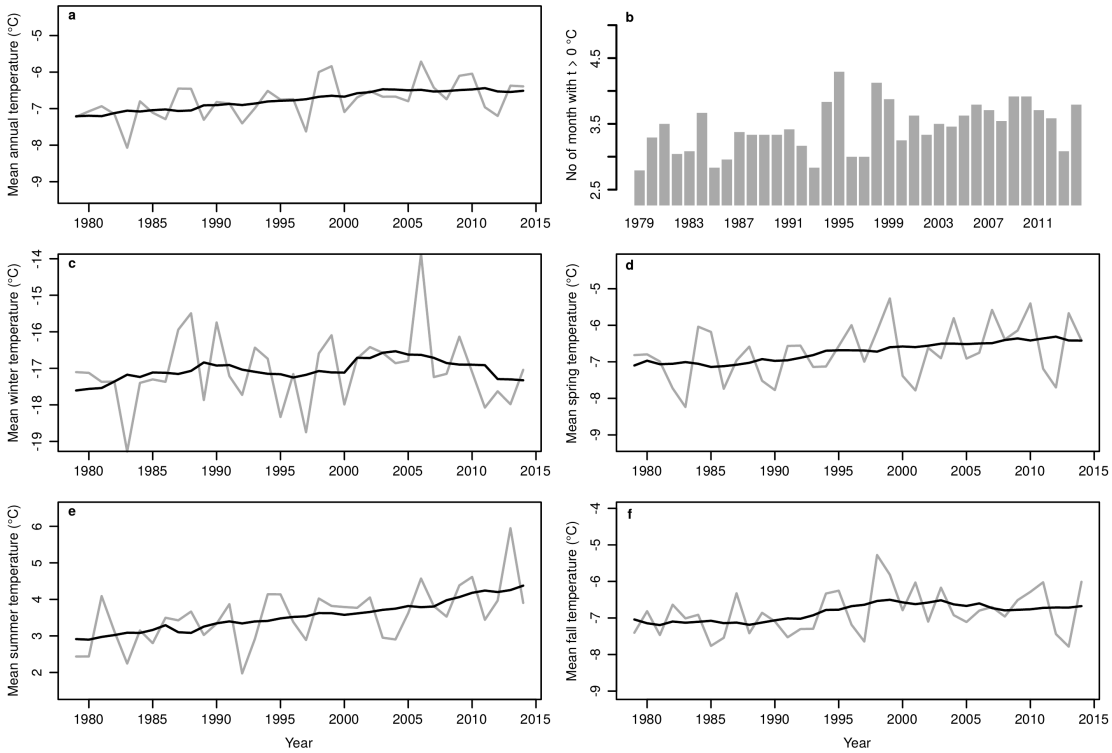

Figure 5.4: Mean air temperature between 1980 and 2014 extracted from ERA-interim data for the area where thawing permafrost soils are considered as cause of increasing coverage. (a) Mean annual temperature. (b) Number of months per year, where mean temperatures were above 0°C. (c-f) Mean temperature in winter (December to February), spring (March to May), summer (June to August), and fall (September to November). The gray lines are the mean values and the black ones the moving averages across 5 years. Spatial extent of the extracted data: 33°N - 36°N, 86.25°E - 90.75°E.

elements. Both explanations are theoretically plausible. On the one hand, LN and thus potential overgrazing are strongly influenced by regional land use policies, which differ in the two provinces in that the sedentarization programs began earlier in Qinghai. During these sedentarization programs, the land use system and the storage numbers changed dramatically leading to severe degradation at least in some areas (HARRIS, 2010; MIEHE et al., 2011). On the other hand, the border between the provinces parallels the Tangula mountain ridge, which may also function as a climatic divide between the southern and northern TP.

Changes in vegetation cover can be caused by changes in climate, such as precipitation, temperature, or a combination of both depending on which is the main local limiting

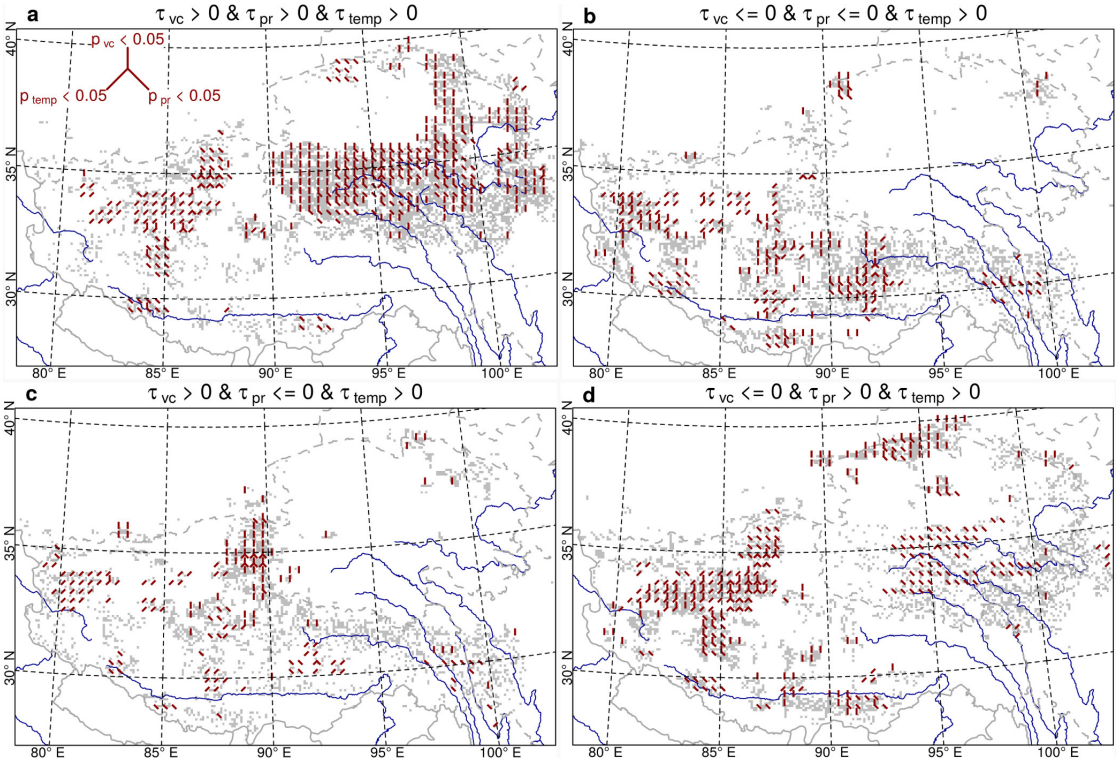

Figure 5.5: Interactions between vegetation cover and climate variables. (a) Positive trends in vegetation cover, precipitation and temperature. (b) Positive trends in temperature but negative trends in vegetation cover and precipitation. (c) Positive trends in vegetation cover and temperature but negative trends in precipitation. (d) Positive trends in precipitation and temperature but negative trends in vegetation cover. Red section lining marks areas where correlations are significant at 0.05 level (see inset in a for an explanation of section lining).

factor for vegetation growth. Precipitation and vegetation cover are positively correlated on a global scale (FANG et al., 2001), which has also been confirmed along transects in Inner Mongolia (BAI et al., 2004, 2007) and across the TP (SHI et al., 2014). Thus, the significant increase of vegetation cover between 2000 and 2013 in southern and eastern Qinghai can be explained by the positive trend in precipitation in these regions (Fig. 5.5a). There are only a few areas of the TAR in which precipitation changes can be the reason for the vegetation trends. Negative precipitation trends correspond to declining vegetation cover in the valleys of Salween and Mekong in eastern Tibet, central Tibet around Lhasa and in the area north of the border with Nepal (Fig. 5.5b). The progressive melting of permafrost soils due to local warming could result in the indirect increase in the plant available water (DAVIDSON & JANSSENS, 2006). This

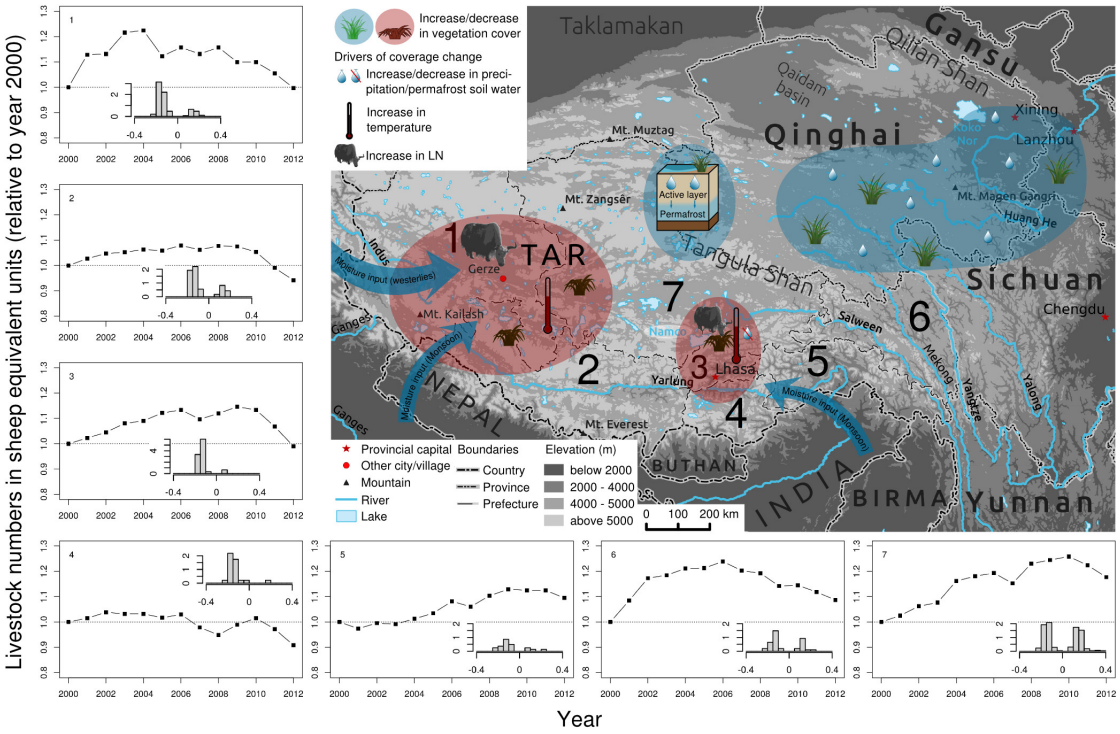

Figure 5.6: General synopsis of the drivers for significant vegetation cover changes by area, encompassing livestock numbers between 2000 and 2012 in prefectures of the TAR. In the map the resulting conceptual model of land-use (anthropogenic degradation) and climatic impacts on vegetation cover, including all locations mentioned in the text, is shown (for further discussions see text). Blue colors mark areas with dominant positive cover changes while red symbolizes negative trends. Blue arrows show the main atmospheric moisture transport paths towards the TP, driven by the monsoon system and the extratropical westerlies. Histograms show relative distributions (in percentages) of significant plant cover trends by prefecture area. Considered prefectures are: Ngari (1), Shigatze (2), Lhasa (3), Shannan (4), Nyingtri (5), Qamdo (6), and Nagqu (7).

effect might counter-balance the negative precipitation trends and has been demonstrated in the region at the southwestern border between Qinghai and the TAR (Fig. 5.5c), where the permafrost soils began melting after 2000 (Li et al., 2014). This is confirmed by the significant increase in air temperature in the respective region (Fig. 5.4a, c-f), especially in the summer (Tab. 5.1), and the increase in the number of months with a mean air temperature above 0°C (Fig. 5.4b).

Significant positive temperature trends have only been observed in the central and northwestern TAR, where the vegetation cover is generally declining (Fig. 5.5b, d). Because

former permafrost soils have already melted in these arid regions and only discontinuous permafrost islands remained (CHENG et al., 2012), it is unlikely that thawing permafrost soils provided additional water for the vegetation. In this case, the available water did not change, but the increasing air temperature accelerated evapotranspiration, which caused water stress on the vegetation and led to the observed decrease in vegetation cover. This mechanism has been confirmed with field experiments in central Tibet (YOU et al., 2014).

The reduction of plant cover in the Altun Shan cannot be explained by changes in temperature, precipitation or melting permafrost. However, the region is exposed to severe dust storms in spring originating from the Taklamakan or the Qaidam basin which cover the grass-dominated vegetation with sand and delays the greening-up. Although the frequency of dust storms is decreasing (FAN et al., 2014), the intensity increased since 1999 (TAN et al., 2014), which most likely contributes to the observed negative vegetation cover trends.

The main impacts of climate and human activities on the vegetation cover trends are summarized in Fig. 5.6. The changes in land use, which are indicated by the increasing stocking numbers, contribute to the predominantly negative trends in the vegetation cover of the TAR. Except for Shannan, all of the prefectures in the TAR experienced increasing LN since 2000. In the western (Ngari prefecture) and eastern (Qamdo prefecture) parts of the TAR, the negative trends in the vegetation cover are the result of the increasing LN as well as the less suitable environment for plant growth. In other areas of the TAR, such as the northern central region (Nagqu prefecture), the effects of the increasing LN are apparently mitigated by improving climatic conditions, which were getting more suitable for plant growth.

A reduction of plant cover in the TAR is alarming because it leads to higher erosion, lower water retention capacity of the soils, and thus to an acceleration of extreme runoff (ZHANG et al., 2011). These direct negative impacts may be further exacerbated because the reduction of vegetation cover significantly feeds back to atmospheric processes (CUI et al., 2006; PIAO et al., 2010; ZHAI et al., 2005) by means of a reduction of transpiration and thus latent heat fluxes. This causes an increase in the sensible heat fluxes, which may accelerate convective precipitation processes according to the catalysis hypothesis if moist air masses are advected at higher atmospheric levels; this can occur even if local water recycling is reduced by a loss of vegetation cover, such as due to overstocking.

Evidence for this mechanism is provided by the finding that the dominant fractions of atmospheric moisture transport towards the TP occur in the western and southwestern parts of the plateau (CURIO et al., 2014; FU et al., 2006), where negative vegetation cover and positive precipitation trends were observed (Fig. 5.5c). This interrelationship led to an increase in higher intensity convective rainfall, while the average precipitation decreased and led to changes in the spatiotemporal patterns of precipitation. Thus, the water cycle of the TP has been altered, which may impact the monsoonal system and contribute to a higher frequency of extreme precipitation events in southern China (DUAN et al., 2012).

In summary, our study documented clear changes in the grassland vegetation on the TP. While increasing precipitation counterbalances the degradation of grassland in large parts of Qinghai, the increase in LN in the TAR, the rising temperatures and the slight decrease in precipitation have resulted in an alarming reduction of grassland plant cover in the western and central parts of the TP. This, in turn, has affected the regional climate and thus the headwater regions of the large river systems of southeast Asia and India. However, LN are not the only cause for the decrease in vegetation cover. If adverse plant cover developments are not adequately monitored in the future, sustainable countermeasures cannot be taken. Further degradation would have negative effects on the stability of the ecosystem of the Tibetan pastures, which could have impacts on the political stability of the TP region and human prosperity in the densely populated areas of south and southeast Asia that strongly depend on the proper water regulation of the TP.

References

BAI, Y., HAN, X., WU, J., CHEN, Z., & LI, L. (2004): Ecosystem stability and compensatory effects in the Inner Mongolia grassland. *Nature*, 431, 7005, 181–184.

BAI, Y., WU, J., PAN, Q., HUANG, J., WANG, Q., LI, F., BUYANTUYEV, A., & HAN, X. (2007): Positive linear relationship between productivity and diversity: Evidence from the Eurasian Steppe. *Journal of Applied Ecology*, 44, 5, 1023–1034.

BALMFORD, A., BRUNER, A., COOPER, P., COSTANZA, R., FARBER, S., GREEN, R.E., JENKINS, M., JEFFERISS, P., JESSAMY, V., MADDEN, J., MUNRO, K., MY-

ERS, N., NAEEM, S., PAAVOLA, J., RAYMENT, M., ROSENDO, S., ROUGHGARDEN, J., TRUMPER, K., & TURNER, R.K. (2002): Economic reasons for conserving wild nature. *Science*, 297, 5583, 950–953.

CHENG, W., ZHAO, S., ZHOU, C., & CHEN, X. (2012): Simulation of the decadal permafrost distribution on the Qinghai-Tibet Plateau (China) over the past 50 years. *Permafrost and Periglacial Processes*, 23, 4, 292–300.

CUI, X. & GRAF, H.F. (2009): Recent land cover changes on the Tibetan Plateau: A review. *Climatic Change*, 94, 1-2, 47–61.

CUI, X., GRAF, H.F., LANGMANN, B., CHEN, W., & HUANG, R. (2006): Climate impacts of anthropogenic land use changes on the Tibetan Plateau. *Global and Planetary Change*, 54, 1-2, 33 – 56.

CURIO, J., MAUSSION, F., & SCHERER, D. (2014): A twelve-year high-resolution climatology of atmospheric water transport on the Tibetan Plateau. *Earth System Dynamics Discussions*, 5, 2, 1159–1196.

DAVIDSON, E.A. & JANSSENS, I.A. (2006): Temperature sensitivity of soil carbon decomposition and feedbacks to climate change. *Nature*, 440, 7081, 165–173.

DEE, D.P., UPPALA, S.M., SIMMONS, A.J., BERRISFORD, P., POLI, P., KOBAYASHI, S., ANDRAE, U., BALMASEDA, M.A., BALSAMO, G., BAUER, P., BECHTOLD, P., BELJAARS, A.C.M., VAN DE BERG, L., BIDLOT, J., BORMANN, N., DELSOL, C., DRAGANI, R., FUENTES, M., GEER, A.J., HAIMBERGER, L., HEALY, S.B., HERSBACH, H., HOLM, E.V., ISAKSEN, L., KALLBERG, P., KOEHLER, M., MATRICARDI, M., MCNALLY, A.P., MONGE-SANZ, B.M., MORCRETTE, J..J., PARK, B..K., PEUBEY, C., DE ROSNAY, P., TAVOLATO, C., THEPAUT, J..N., & VITART, F. (2011): The ERA-Interim reanalysis: Configuration and performance of the data assimilation system. *Quarterly Journal of the Royal Meteorological Society*, 137, 656, 553–597.

DUAN, A., WANG, M., LEI, Y., & CUI, Y. (2012): Trends in summer rainfall over China associated with the Tibetan Plateau sensible heat source during 1980-2008. *Journal of Climate*, 26, 1, 261–275.

FAN, B., GUO, L., LI, N., CHEN, J., LIN, H., ZHANG, X., SHEN, M., RAO, Y., WANG, C., & MA, L. (2014): Earlier vegetation green-up has reduced spring dust storms. *Scientific Reports*, 4, 1–6.

FANG, J., PIAO, S., TANG, Z., PENG, C., & JI, W. (2001): Interannual variability in net primary production and precipitation. *Science*, 293, 5536, 1723–1723.

FAO (2005): Livestock sector brief, China. Food and Agriculture Organization of the United Nations - Livestock Information, Sector Analysis and Policy Branch (AGAL), Rome.

FU, C. (2003): Potential impacts of human-induced land cover change on East Asia monsoon. *Global Planetary Change*, 37, 219–229.

FU, R., HU, Y., WRIGHT, J.S., JIANG, J.H., DICKINSON, R.E., CHEN, M., FILIPIAK, M., READ, W.G., WATERS, J.W., & WU, D.L. (2006): Short circuit of water vapor and polluted air to the global stratosphere by convective transport over the Tibetan Plateau. *Proceedings of the National Academy of Sciences*, 103, 15, 5664–5669.

GAO, L., HAO, L., & CHEN, X.W. (2014): Evaluation of ERA-interim monthly temperature data over the Tibetan Plateau. *Journal of Mountain Science*, 11, 5, 1154–1168.

HAFNER, S., UNTEREGELSBACHER, S., SEEBER, E., LENA, B., XU, X., LI, X., GUGGENBERGER, G., MIEHE, G., & KUZYAKOV, Y. (2012): Effect of grazing on carbon stocks and assimilate partitioning in a Tibetan montane pasture revealed by $^{13}CO_2$ pulse labeling. *Global Change Biology*, 18, 2, 528–538.

HARRIS, R.B. (2010): Rangeland degradation on the Qinghai-Tibetan Plateau: A review of the evidence of its magnitude and causes. *Journal of Arid Environments*, 74, 1, 1–12.

HU, Z., YU, G., FU, Y., SUN, X., LI, Y., SHI, P., WANGW, Y., & ZHENG, Z. (2008): Effects of vegetation control on ecosystem water use efficiency within and among four grassland ecosystems in China. *Global Change Biology*, 14, 7, 1609–1619.

HUFFMAN, G.J., BOLVIN, D.T., NELKIN, E.J., WOLFF, D.B., ADLER, R.F., GU, G., HONG, Y., BOWMAN, K.P., & STOCKER, E.F. (2007): The TRMM multisatellite

precipitation analysis (TMPA): Quasi-global, multiyear, combined-sensor precipitation estimates at fine scales. *Journal of Hydrometeorology*, 8, 1, 38–55.

LEHNERT, L.W., MEYER, H., MEYER, N., REUDENBACH, C., & BENDIX, J. (2014): A hyperspectral indicator system for rangeland degradation on the Tibetan Plateau: A case study towards spaceborne monitoring. *Ecological Indicators*, 39, 54 – 64.

LEHNERT, L.W., MEYER, H., WANG, Y., MIEHE, G., THIES, B., REUDENBACH, C., & BENDIX, J. (2015): Retrieval of grassland plant coverage on the Tibetan Plateau based on a multi-scale, multi-sensor and multi-method approach. *Remote Sensing of Environment*, 164, 197–207.

LI, Y.K., LIAO, J.J., GUO, H.D., LIU, Z.W., & SHEN, G.Z. (2014): Patterns and potential drivers of dramatic changes in Tibetan lakes, 1972-2010. *Plos One*, 9, 11, e111 890.

LIU, J. & DIAMOND, J. (2005): China's environment in a globalizing world. *Nature*, 435, 7046, 1179–1186.

MA, J., ZHANG, W., LUO, L., XU, Y., XIE, H., XU, X., LI, Q., ZHENG, J., & SHENG, L. (Eds.) (2000-2013): China Statistical Yearbook. China Statistical Press, Beijing.

MAUSSION, F., SCHERER, D., MÖLG, T., COLLIER, E., CURIO, J., & FINKELNBURG, R. (2014): Precipitation seasonality and variability over the Tibetan Plateau as resolved by the high asia reanalysis. *Journal of Climate*, 27, 5, 1910–1927.

MIEHE, G., MIEHE, S., BACH, K., NÖLLING, J., HANSPACH, J., REUDENBACH, C., KAISER, K., WESCHE, K., MOSBRUGGER, V., YANG, Y.P., & MA, Y.M. (2011): Plant communities of central Tibetan pastures in the Alpine Steppe/*Kobresia pygmaea* ecotone. *Journal of Arid Environments*, 75, 8, 711–723.

MIEHE, G., MIEHE, S., KAISER, K., REUDENBACH, C., BEHRENDES, L., DUO, L., & SCHLÜTZ, F. (2009): How old is pastoralism in Tibet? An ecological approach to the making of a Tibetan landscape. *Palaeogeography, Palaeoclimatology, Palaeoecology*, 276, 130–147.

MÖLG, T., MAUSSION, F., & SCHERER, D. (2014): Mid-latitude westerlies as a driver of glacier variability in monsoonal High Asia. *Nature Climate Change*, 4, 1, 68–73.

PEOPLES'S REPUBLIC OF CHINA (2000-2013): Tibet Statistical Yearbook. Tibet Statistics Bureau, China Statistical Press, Beijing.

PIAO, S., CIAIS, P., HUANG, Y., SHEN, Z., PENG, S., LI, J., ZHOU, L., LIU, H., MA, Y., DING, Y., FRIEDLINGSTEIN, P., LIU, C., TAN, K., YU, Y., ZHANG, T., & FANG, J. (2010): The impacts of climate change on water resources and agriculture in China. *Nature*, 467, 7311, 43–51.

PIAO, S., WANG, X., CIAIS, P., ZHU, B., WANG, T., & LIU, J. (2011): Changes in satellite-derived vegetation growth trend in temperate and boreal Eurasia from 1982 to 2006. *Global Change Biology*, 17, 10, 3228–3239.

SHI, Y., WANG, Y., MA, Y., MA, W., LIANG, C., FLYNN, D.F.B., SCHMID, B., FANG, J., & HE, J.S. (2014): Field-based observations of regional-scale, temporal variation in net primary production in Tibetan alpine grasslands. *Biogeosciences*, 11, 7, 2003–2016.

TAN, M., LI, X., & XIN, L. (2014): Intensity of dust storms in China from 1980 to 2007: A new definition. *Atmospheric Environment*, 85, 0, 215–222.

WANG, A.H. & ZENG, X.B. (2012): Evaluation of multireanalysis products with *in situ* observations over the Tibetan Plateau. *Journal of Geophysical Research – Atmospheres*, 117, D05 102.

WANG, D., MORTON, D., MASEK, J., WU, A., NAGOL, J., XIONG, X., LEVY, R., VERMOTE, E., & WOLFE, R. (2012): Impact of sensor degradation on the MODIS NDVI time series. *Remote Sensing of Environment*, 119, 55–61.

WU, G.L., DU, G.Z., LIU, Z.H., & THIRGOOD, S. (2009): Effect of fencing and grazing on a *Kobresia*-dominated meadow in the Qinghai-Tibetan Plateau. *Plant and Soil*, 319, 1-2, 115–126.

XU, X., LU, C., SHI, X., & GAO, S. (2008): World water tower: An atmospheric perspective. *Geophysical Research Letters*, 35, 20.

YAO, T., THOMPSON, L., YANG, W., YU, W., GAO, Y., GUO, X., YANG, X., DUAN, K., ZHAO, H., XU, B., PU, J., LU, A., XIANG, Y., KATTEL, D.B., & JOSWIAK, D.

(2012): Different glacier status with atmospheric circulations in Tibetan Plateau and surroundings. *Nature Climate Change*, 2, 9, 663–667.

YOU, Q.Y., XUE, X., PENG, F., XU, M.H., DUAN, H.C., & DONG, S.Y. (2014): Comparison of ecosystem characteristics between degraded and intact alpine meadow in the Qinghai-Tibetan Plateau, China. *Ecological Engineering*, 71, 133–143.

YU, H., LUEDELING, E., & XU, J. (2010): Winter and spring warming result in delayed spring phenology on the Tibetan Plateau. *Proceedings of the National Academy of Sciences*, 107, 51, 22 151–22 156.

ZHAI, P., ZHANG, X., WAN, H., & PAN, X. (2005): Trends in total precipitation and frequency of daily precipitation extremes over China. *Journal of Climate*, 18, 7, 1096–1108.

ZHANG, W., AN, S., XU, Z., CUI, J., & XU, Q. (2011): The impact of vegetation and soil on runoff regulation in headwater streams on the east Qinghai-Tibet Plateau, China. *Catena*, 87, 2, 182–189.

6 Conclusions and Outlook

The aims of the present study were to detect recent changes in the degradation status of the pastures on the Tibetan Plateau and to identify their drivers. To achieve this, the prerequisite was the development of a satellite-based pasture degradation monitoring system which is relying on a suitable set of indicators and which incorporate ground truth data to assess the amount of uncertainty in the product.

The selection of the indicators was the subject of the first working package (**WP 1**) in which the following two hypotheses have been tested:

H 1 The degradation of the pastures on the Tibetan Plateau is accompanied by a reduction in plant coverage, which can be derived on the local scale from multi- and hyperspectral datasets.

H 2 The combination of plant coverage and chlorophyll content provides a useful indicator system to distinguish between effects of grazing pressure and effects of other environmental factors on the local scale.

Regarding **H 1**, it was shown in a case study at two sites on the Tibetan Plateau that plant coverage can be delineated with high accuracies on the local scale from hyper- and multispectral data using linear spectral unmixing. With this technique, it was furthermore possible to estimate fractions of other land-cover types, such as bare soil, stones, dead organic material, and open *Kobresia pygmaea* turf. Spatial patterns within the land-cover fractions of open turf and dead organic material estimations underlined the degradation pattern revealed by the plant coverage estimations and additionally allowed a better insight into the processes leading to degradation. Regarding the second indicator for pasture degradation, it was demonstrated that the estimation of the chlorophyll content of grasses is possible by combining hyperspectral vegetation indices and partial least squares regression. The delineation of land-cover fractions and chlorophyll contents was successfully performed at over 300 plots at the two sites. With respect to **H 2**, the

combination of both indicators was proven to be a suitable set of indicators for pasture degradation in the Alpine Steppe and *K. pygmaea* pastures. Particularly, the new indicator system allowed to distinguish between low plant coverage values caused by degradation and low plant coverage values caused by local site effects such as water and nutrient availability. The proposed new indicator system can be easily transferred to other sites on the Tibetan Plateau if hyperspectral and reference data are available. In this context, the latter has to measured *in situ*. In contrast, the upcoming EnMAP mission (KAUFMANN et al., 2012) will provide area-wide and remotely acquired hyperspectral data sets. In the present thesis, simulated hyperspectral EnMAP data sets were proven to be suitable for the derivation of the indicator system. Thus, area-wide estimations of the degradation status at local scales can be provided by the new indicator system in future.

Plant coverage was proven to be a suitable indicator for pasture degradation on the Tibetan Plateau. Consequently, a satellite-based plant coverage product was developed in **WP 2** by deriving plant coverage from different satellite data. In this scope, the following hypothesis has been tested:

H 3 Plant coverage of the Tibetan Plateau can be derived along a cascade of multispectral satellite data with increasing spatial resolution from the local to the plateau scale.

The predictive performance of four different methods was assessed for the estimation of plant coverage from satellite data with high (2 - 5 m, WorldView, Quickbird, RapidEye), medium (30 m, Landsat) and low (500 m, MODIS) spatial resolution. The methods were spectral angle mapper, linear spectral unmixing, partial least squares, and support vector machine (SVM) regression. The latter two methods were based on a feature space comprised by several vegetation indices, while the first two methods relied on the definition of reference spectral data measured *in situ* using a spectrometer. The SVM regression models turned out to provide the most accurate estimations at all scales. No evidence for over- or underestimations by the models were observed. Additionally, the estimations of the SVM models were only slightly affected by the degradation of the MODIS sensor. Thus, the time series derived by the new plant coverage product provides a valuable database to investigate recent changes in plant coverage values on the Tibetan Plateau.

The new plant coverage product has been applied in **WP 3** to identify areas where veg-

etation coverage has changed since the year 2000. Specifically, the following hypothesis has been tested:

H 4 On the plateau scale, effects of climate and anthropogenic land-use on degradation status can be separated by comparing the trends in the new plant coverage product to the trends in climate datasets.

The investigated climate data sets were precipitation sums extracted from TRMM data and mean air temperature values from ERA-Interim. The trends in vegetation coverage, precipitation and temperature were compared and revealed plausible patterns. In general, the analysis revealed that vegetation coverage was mainly driven by climate between 2000 and 2013. Large areas in southern Qinghai were identified in which vegetation cover increased due to positive precipitation trends. In contrast, the significant increases in temperature resulted in the decline in vegetation cover in the western and central part of the TAR. This decline was further exacerbated by the increase of livestock numbers in nearly all prefectures in the TAR. In other areas of the TAR in which temperature and precipitation did not change towards a less suitable environment for plant growth, the likewise increasing livestock numbers did not cause a significant reduction in plant coverage. Thus, the proposed comparison of climate and vegetation cover trends was an appropriate method to separate effects of climate and anthropogenic land-use on the degradation of the Tibetan pastures and **H 4** was verified. Since the trends in the plant coverage and the climate data sets were plausible, the new plant coverage product is suitable for future monitoring purposes.

The decline in vegetation coverage in the western and central part of the plateau is in contrast to the results of previous time series analysis on the Tibetan Plateau reporting that trends are dominantly positive (SUN et al., 2013; TIAN et al., 2014; ZHONG et al., 2010). The differences can be explained by several factors. (1) The data sets in the previous studies mostly covered longer time periods than the new plant coverage product presented here. (2) The previous investigations were directly based on vegetation indices without establishing a transfer function by using ground truth data as reference. Since the indices are affected by soil moisture, it is highly probable that the results are distorted at least in the arid parts with low vegetation coverage. (3) The data sets in the previous studies were recorded with different sensors, such as AVHRR[1] and SPOT[2]. Especially

[1] Advanced Very High Resolution Radiometer
[2] Satellite Pour l'Observation de la Terre

the AVHRR sensors are problematic because the sensors of the different generations degraded (e.g., RAO & CHEN, 1999) which causes that the time series of the satellite data may be distorted (GUTMAN, 1999).

The present thesis contributes to a better understanding of the processes and the changes in the degradation status of the pastures on the Tibetan Plateau. Additionally, strong evidences were found that the changes in the degradation status feeds-back with climate. Those interactions have already been studied but were restricted to small scales because area-wide and long term datasets for parameters such as vegetation cover were not available (e.g., CUI et al., 2006; YAMADA & UYEDA, 2006). Since the investigation of the feed-backs was not a primary aim of this thesis, further investigations incorporating additional data sets are necessary to quantify the effects of a decreasing coverage on precipitation amounts, frequencies and intensities across the Tibetan Plateau.

The knowledge about the ecological status of the world's largest high mountain grassland ecosystem is of urgent importance because of the plateau's high influence on the monsoonal system and the high importance of the ecosystem services provided by the vegetation on the Tibetan Plateau. These ecosystem services encompass the protection against soil erosion and the maintenance of the water retention capacity of the soils illustrating that the stability of the investigated grasslands is key to one third of the world's population living at the lower reaches of the large river systems originating on the Tibetan Plateau. Thus, the detected progressive degradation in the central and western part of the TAR is alarming and must be counter-acted by the local political authorities. However, it must be clearly pointed out that the local land-use changes are most likely not the solely reason for the ongoing degradation, because degradation was only detected in areas featuring the coincidence of a less suitable environment under climate change and the land-use change.

The importance of the ecosystem services provided by the vegetation on the Tibetan Plateau underlines the enormous relevance of a transition to a more sustainable usage of the pastures. The development of a pasture degradation monitoring system supports this transition by outlining the areas where pasture degradation is proceeding. Thus, this thesis constituted an important contribution towards the reduction of the threat of degradation.

In future, the plant coverage product developed in this thesis may be used as a valuable database of vegetation cover. A better knowledge about the current status and changes in

vegetation cover are urgently required to simulate processes and interactions between the vegetation, atmosphere and pedosphere on the Tibetan Plateau. This will help to close the knowledge gaps still remaining regarding the influence of the Tibetan Plateau on global climate change.

References

CUI, X., GRAF, H.F., LANGMANN, B., CHEN, W., & HUANG, R. (2006): Climate impacts of anthropogenic land use changes on the Tibetan Plateau. *Global and Planetary Change*, 54, 1-2, 33 – 56.

GUTMAN, G.G. (1999): On the use of long-term global data of land reflectances and vegetation indices derived from the advanced very high resolution radiometer. *Journal of Geophysical Research – Atmospheres*, 104, D6, 6241–6255.

KAUFMANN, H., FÖRSTER, S., WULF, H., SEGL, K., GUANTER, L., BOCHOW, M., HEIDEN, U., MÜLLER, A., HELDENS, W., SCHNEIDERHAN, T., LEITÃO, P., VAN DER LINDEN, S., HOSTERT, P., HILL, J., BUDDENBAUM, H., MAUSER, W., HANK, T., KRASEMANN, H., RÖTTGERS, R., OPPELT, N., & HEIM, B. (2012): Science plan of the environmental mapping and analysis program (EnMAP). Technical Report, Deutsches GeoForschungsZentrum GFZ Potsdam.

RAO, C.R.N. & CHEN, J. (1999): Revised post-launch calibration of the visible and near-infrared channels of the Advanced Very High Resolution Radiometer (AVHRR) on the NOAA-14 spacecraft. *International Journal of Remote Sensing*, 20, 18, 3485–3491.

SUN, J., CHENG, G.W., LI, W.P., SHA, Y.K., & YANG, Y.C. (2013): On the variation of NDVI with the principal climatic elements in the Tibetan Plateau. *Remote Sensing*, 5, 4, 1894–1911.

TIAN, L., ZHANG, Y., & ZHU, J. (2014): Decreased surface albedo driven by denser vegetation on the Tibetan Plateau. *Environmental Research Letters*, 9, 10, 1–11.

YAMADA, H. & UYEDA, H. (2006): Transition of the rainfall characteristics related to the moistening of the land surface over the central Tibetan Plateau during the summer of 1998. *Monthly Weather Review*, 134, 11, 3230–3247.

ZHONG, L., MA, Y., SALAMA, M.S., & SU, Z. (2010): Assessment of vegetation dynamics and their response to variations in precipitation and temperature in the Tibetan Plateau. *Climatic Change*, 103, 3-4, 519–535.

Acknowledgements

This work is the result of the cooperation of many different people. First of all, I would like to thank my supervisor Jörg Bendix and Georg Miehe for their guidance of this work, for their helpful comments and fruitful discussions, but also for handling of German (Jörg) and Chinese (Georg) bureaucracies. Additionally I would like to thank all people in the PaDeMoS project and all my co-authors for their input in the research. I would greatly appreciate if some joint articles would follow in the future.

The field trips to the Tibetan Plateau were only possible because our Tibetan and Chinese colleagues and friends expended a large effort to get all required permissions and to organize the daily life on the plateau. Sorry for my cultural missteps, and thank you for your support and patience. Both field trips would not have been possible without Hanna Meyer who managed the first trip alone and did a lot of work during the second trip. Special thanks go to Yun Wang who could not even been stopped by a broken leg! Thank you for your enormous effort during field measurements!

Special thanks go to my colleagues at the Laboratory for Climatology and Remote Sensing at Philipps-University of Marburg. During this time, they supported me in many situations ranging from little everyday problems to scientific discussions or just coffee breaks in our kitchen. I thank Christoph Reudenbach, Boris Thies, Thomas Nauss, and Frank Rüthrich for many fruitful exchanges and discussions as well as for multiple help in everyday problems in scientific life.

The work was generously supported by the German Federal Ministry of Education and Research. Although, it was not always easy to manage the financial issues, this support was highly appreciated. In this context, I would like to thank Christina Philippi for her effort. Thanks go to the PhD commission to take the time to read through this little book and, thus, contribute to finalize my PhD.

Most of all, however, thank you to my wife Laura, my family and friends for their subsequent patience with the many hours spent in front of the computer. I hope I have not mutated to some sort of weird alien in your eyes. Finally, I would like to thank my sons Jori and Samir for their passive help, although they have seen their father far too rarely in the last time!

Erklärung

Ich erkläre an Eides statt, dass ich meine Dissertation mit dem Titel

”Satellite-based monitoring of pasture degradation on the Tibetan Plateau: A multi-scale approach“

selbstständig ohne unerlaubte Hilfe angefertigt und mich dabei keinerlei anderen als der von mir ausdrücklich bezeichneten Quellen und Hilfen bedient habe.
Die Dissertation wurde in der jetzigen oder einer ähnlichen Form noch bei keiner anderen Hochschule eingereicht und hat noch keinen sonstigen Prüfungszwecken gedient.

Marburg a. d. Lahn, den 18.5.2015

Lukas Lehnert

Diese Seite (134) enthält persönliche Daten (Curriculum Vitae). Sie ist deshalb nicht Bestandteil der Online-Veröffentlichung.

Diese Seite (135) enthält persönliche Daten (Curriculum Vitae). Sie ist deshalb nicht Bestandteil der Online-Veröffentlichung.